(12) INTERNATIONAL APPLICATION PUBLISHED UNDER THE PATENT COOPERATION TREATY (PCT)

(19) World Intellectual Property Organization
International Bureau

(43) International Publication Date
15 December 2005 (15.12.2005)

PCT

(10) International Publication Number
WO 2005/118659 A2

(51) International Patent Classification[7]: C08F 210/00

(21) International Application Number:
PCT/IL2005/000572

(22) International Filing Date: 1 June 2005 (01.06.2005)

(25) Filing Language: English

(26) Publication Language: English

(30) Priority Data:

60/575,369	1 June 2004 (01.06.2004)	US
60/625,971	9 November 2004 (09.11.2004)	US
60/630,561	26 November 2004 (26.11.2004)	US
60/632,236	2 December 2004 (02.12.2004)	US
60/632,515	3 December 2004 (03.12.2004)	US
60/635,630	14 December 2004 (14.12.2004)	US
60/636,088	16 December 2004 (16.12.2004)	US
60/640,215	3 January 2005 (03.01.2005)	US
60/648,385	1 February 2005 (01.02.2005)	US
60/648,690	2 February 2005 (02.02.2005)	US

(71) Applicant *(for all designated States except US)*: **SPECTRUM DYNAMICS (ISRAEL) LTD.** [IL/IL]; 2 HaEtgar Street, Carmel Building, 2nd Floor, 39032 Tirat Hacarmel (IL).

(72) Inventors; and

(75) Inventors/Applicants *(for US only)*: **DICHTERMAN, Eli** [IL/IL]; 8a Vitkin Street, 34756 Haifa (IL). **RAVHON, Ran** [IL/IL]; 60 Weizmann Street, 26350 Kiryat-Motzkin (IL). **NAGLER, Michael** [IL/IL]; 4 Avshalom Haviv Street, 69495 Tel Aviv (IL).

(74) Agent: **G.E. EHRLICH (1995) LTD.**; 11 Menachem Begin Street, 52 521 Ramat Gan (IL).

(81) Designated States *(unless otherwise indicated, for every kind of national protection available)*: AE, AG, AL, AM, AT, AU, AZ, BA, BB, BG, BR, BW, BY, BZ, CA, CH, CN, CO, CR, CU, CZ, DE, DK, DM, DZ, EC, EE, EG, ES, FI, GB, GD, GE, GH, GM, HR, HU, ID, IL, IN, IS, JP, KE, KG, KM, KP, KR, KZ, LC, LK, LR, LS, LT, LU, LV, MA, MD, MG, MK, MN, MW, MX, MZ, NA, NG, NI, NO, NZ, OM, PG, PH, PL, PT, RO, RU, SC, SD, SE, SG, SK, SL, SM, SY, TJ, TM, TN, TR, TT, TZ, UA, UG, US, UZ, VC, VN, YU, ZA, ZM, ZW.

(84) Designated States *(unless otherwise indicated, for every kind of regional protection available)*: ARIPO (BW, GH, GM, KE, LS, MW, MZ, NA, SD, SL, SZ, TZ, UG, ZM, ZW), Eurasian (AM, AZ, BY, KG, KZ, MD, RU, TJ, TM), European (AT, BE, BG, CH, CY, CZ, DE, DK, EE, ES, FI, FR, GB, GR, HU, IE, IS, IT, LT, LU, MC, NL, PL, PT, RO, SE, SI, SK, TR), OAPI (BF, BJ, CF, CG, CI, CM, GA, GN, GQ, GW, ML, MR, NE, SN, TD, TG).

Published:
— *without international search report and to be republished upon receipt of that report*

For two-letter codes and other abbreviations, refer to the "Guidance Notes on Codes and Abbreviations" appearing at the beginning of each regular issue of the PCT Gazette.

(54) Title: METHODS OF VIEW SELECTION FOR RADIOACTIVE EMISSION MEASUREMENTS

(57) Abstract: A method is described for identifying an optimal, or preferred set of views for radioactive–emission measurements of a region of interest within the body. The method is based on a model of the region of interest, and the preferred sets of views are identified for the model, preferably using information theoretic measures. The preferred sets of views may then be applied to the region of interest, in vivo.

WO 2005/118659 A2

METHODS OF VIEW SELECTION FOR RADIOACTIVE EMISSION MEASUREMENTS

FIELD AND BACKGROUND OF THE INVENTION

The present invention relates to selecting optimal views for measuring radiation emitted by an object. More particularly, the present invention relates to selecting the optimal views using a scoring function based on information-theoretic measures. Of particular interest is view selection for medical imaging and/or in conjunction with medical instruments, such as guided minimally invasive surgical instruments.

Radionuclide imaging is one of the most important applications of radioactivity in medicine. Its purpose is to obtain a distribution image of a radioactively labeled substance, e.g., a radiopharmaceutical, within the body following administration thereof to a patient. Radioactive-emission imaging relies on the fact that in general, pathologies, such as malignant tumors, malfunctioning organs, and inflammations, display a level of activity different from that of healthy tissue. Thus, radiopharmaceuticals, which circulate in the blood stream, are picked up by the active pathologies to a different extent than by the surrounding healthy tissue; in consequence, the pathologies are operative as radioactive-emission sources and may be detected by radioactive-emission imaging. It will be appreciated that the pathology may appear as a concentrated source of high radiation, a hot region, as may be associated with a tumor, or as a region of low-level radiation, which is nonetheless above the background level, as may be associated with carcinoma.

A reversed situation is similarly possible. Dead tissue has practically no pick up of radiopharmaceuticals, and is thus operative as a cold region.

Thus radiopharmaceuticals may be used for identifying active pathologies as well as dead tissue.

In the discussion that follows, the term organ target is intended to include pathological features within organs. These pathological features may be expressed, by radioactive-emission imaging, as any one of the following:

i. hot regions, of a radioactive emission intensity higher than the background level;

ii. regions of low-level radioactive emission intensity, which is nonetheless above the background level; and

iii cold regions, of a radioactive emission intensity, lower than the background level.

Examples of radiopharmaceuticals include monoclonal antibodies or other agents, e.g., fibrinogen or fluorodeoxyglucose, tagged with a radioactive isotope, e.g., ^{99M}technetium, ^{67}gallium, ^{201}thallium, ^{111}indium, ^{123}iodine, ^{125}iodine and ^{18}fluorine, which may be administered orally or intravenously. The radiopharmaceuticals are designed to concentrate in the area of a tumor, and the uptake of such radiopharmaceuticals in the active part of a tumor, or other pathologies such as an inflammation, is higher and more rapid than in the tissue that neighbors the tumor. Thereafter, a radiation-emission-measuring-probe, which may be configured for extracorporeal or intracorporeal use, is employed for locating the position of the active area. Another application is the detection of blood clots with radiopharmaceuticals such as ACUTECT from Nycomed Amersham for the detection of newly formed thrombosis in veins, or clots in arteries of the heart or brain, in an emergency or operating room. Yet other applications include radioimaging of myocardial infarct using agents such as radioactive anti-myosin antibodies, radioimaging specific cell types using radioactively tagged molecules (also known as molecular imaging), etc.

The usual preferred emission for such applications is that of gamma rays, which emission is in the energy range of approximately 11-511 KeV. Beta radiation and positrons may also be detected.

Radioactive-emission imaging is performed with a radioactive-emission-measuring detector, such as a room temperature, solid-state CdZnTe (CZT) detector, which is among the more promising that is currently available. It may be configured as a single-pixel or a multi-pixel detector, and may be obtained, for example, from eV Products, a division of II-VI Corporation, Saxonburg Pa., 16056, or from IMARAD IMAGING SYSTEMS LTD., of Rehovot, ISRAEL, 76124, www.imarad.com, or from another source. Alternatively, another solid-state detector such as CdTe, HgI, Si, Ge, or the like, or a combination of a scintillation detector (such as NaI(Tl), LSO,

GSO, CsI, CaF, or the like) and a photomultiplier, or another detector as known, may be used.

Figures 1a – 1i schematically illustrate detecting units 102 and detecting blocks 101 of various geometries and constructions, and radioactive-emission-measuring probes associated with them.

Figure 1a schematically illustrates a detecting unit 102, formed as a single-pixel detector 104, for example, a room-temperature solid-state CdZnTe (CZT) detector, having a diameter D and a thickness τ_d. Both the detector diameter D, or a diameter equivalent in the case of a non-circular detector, and the detector thickness τ_d affect the detecting efficiency. The detector diameter determines the surface area on which radioactive emission impinges; the greater the surface area, the greater the efficiency. The detector thickness affects the stopping power of the detector. High energy gamma rays may go through a thin detector, and the probability of their detection increases with detector thickness. By itself, a single-pixel detector cannot generate an image; rather, all counts are distributed over the surface area of the detector.

Figure 1b schematically illustrates the detecting unit 102 with a collimator 108, formed as a single cell of a diameter D, a length L, and a septa thickness τ, attached to the detector 104. The collimator 108 may be, for example, of lead, tungsten or another material which substantially blocks gamma and beta rays.

The collimator's geometry, and specifically, the ratio of D/L, provides the detecting unit 102 with a collection angle δ analogous to a viewing angle of an optical camera. The collection angle δ limits the radioactive-emission detection to substantially only that radioactive emission, which impinges on the detector 104 after passing through a "corridor" of the collimator 108 (although in practice, some high-energy gamma rays may penetrate the collimator's walls).

Figure 1c schematically illustrates a block 101 of the detecting units 102, with the collimator 108, formed as a multi-cell collimator, of a cell diameter D. The collection angle δ is defined for each of the detecting units 102 in the block, and each of the detecting units 102 forms a pixel in the block 101.

Figure 1d schematically illustrates a radioactive-emission-measuring probe 100 which comprises several detecting units 102, of different geometries and different collection angles δ, within a housing 107.

Figures 1e – 1i schematically illustrate the block 101, formed as a combination of a scintillation detector (such as NaI(Tl), LSO, GSO, CsI, CaF, or the like), a collimator grid, and photomultipliers.

As seen in Figure 1e, the block 101, having proximal and distal ends 109 and 111, respectively, vis a vis an operator (not shown), is formed of the scintillation detector 104, of a single pixel, and the collimators 108, to create the detecting units 102. A plurality of photomultipliers 103 is associated with the single pixel scintillation detector 104, and with proper algorithms, as known, their output can provide a two dimensional image of the scintillations in the single pixel scintillation detector 104. In essence, this is an Anger camera, as known.

The distal view 111 of the collimator grid is seen in Figure 1f.

Two optional proximal views 109 of the photomultipliers 103 are seen in Figures 1g and 1h, as a square grid arrangement, and as an arrangement of tubes.

An Anger camera 117, of the block 101 in the housing 107 is seen in Figure 1i.

In each of the cases of Figures 1a – 1i, the geometry of the collimator 108 determines the collection angle δ, wherein with no collimator, the collection angle δ, is essentially a solid angle of 4π steradians. Thus, the collimator's geometry affects both the detection efficiency and the image resolution, which are defined as follows:

i. The detection efficiency is the ratio of measured radiation to emitted radiation; and

ii. The image resolution is the capability of making distinguishable closely adjacent radioactive-emission organ targets, or the capability to accurately determine the size and shape of individual radioactive-emission organ targets.

Naturally, it is desired to optimize both the detection efficiency and the image resolution. Yet, they are inversely related to each other. The detection efficiency increases with increasing collimator's collection angle, and the image resolution decreases with increasing collimator's collection angle. For example, when the ratio of D/L is 1/2, the collection angle δ is substantially 2.5 steradians, so the cell views

incident radiation within the confinement of about a 2.5-steradian sector. However, when the ratio of D/L is 1/12, the collection angle δ is substantially 0.31 steradians, so the cell views incident radiation within the confinement of about a 0.31-steradian sector.

Once the emission data is obtained, the data is processed to reconstruct the intensity distribution within the measured volume. The reconstruction process is generally complex, due to the large quantity of data which must be processed in order to obtain an accurate reconstruction. The following prior art statistical model may be used to perform reconstruction.

We assume an intensity distribution, I, defined over an input space U, where U comprises a set of basic elements (*e.g.*, pixels in two dimensional spaces, voxels in three dimensional spaces), and $I(u)$ is the intensity of a given basic element $u \in U$. A detecting unit positioned on a radiation-emission-measuring-probe takes a series of measurements $\mathbf{y}=(y_t)_{t=1}^{T}$ from different positions and orientations around the volume U. The geometrical and physical properties of the detecting unit, together with its position and orientation in a given measurement t, determine the detection probability $\phi_t(u)$ of a photon emitted from location u. Thus the effective intensity of location u as viewed by the detecting unit during measurement t is $\phi_t(u)I(u)$.

The random count $X_t(u)$ of photons that are emitted from location u and detected in measurement t is modeled by a Poisson process with mean $\phi_t(u)I(u)$. The total count of photons detected in measurement t is $Y_t = \Sigma_{u\in U} X_t(u)$, and the reconstruction problem is to reconstruct the intensities $(I(u))_{u\in U}$ from the measurements $(y_t)_{t=1}^{T}$.

The 2-D Radon transform is a mathematical relationship which may be used to reconstruct the emission intensities of volume U when the set of measurements $(y_t)_{t=1}^{T}$ is unconstrained. The Radon transform is not statistical and does not take into account the Poissonian nature of the counts. In addition, it models the views as line projections. The Radon transform maps the spatial domain (x,y) to the Radon domain (p,ϕ). For a fixed projection angle, the Radon transform is simply a projection of the object. A technique known in the art as filtered back-projection (FBP) uses a back-

projection operator and the inverse of the Radon transform to reconstruct the intensity distribution in volume U from measurements $(y_t)_{t=1}^{T}$.

The basic, idealized problem solved by the FBP approach is to reconstruct an image from its Radon transform. The Radon transform, when properly defined, has a well-defined inverse. However, in order to invert the transform one needs measured data spanning 180°. In many medical imaging situations, the positioning of the detecting unit relative to the emitting object is constrained, so that complete measured data is not available. Reconstruction based on filtered back-projection is therefore of limited use for medical imaging. Maximum likelihood (ML) and Maximum A Posteriori (MAP) estimation methods, which address the statistical nature of the counts, have been found to provide better image reconstructions than FBP.

Limited-angle tomography is a reconstruction technique in the related art which reconstructs an image from projections acquired over a limited range of angular directions. The success of the reconstruction process depends upon the extent of the angular range acquired compared with the angular range of the missing projections. Any reconstruction from a limited range of projections potentially results in spatial distortions (artifacts) in the image. Limited angle techniques can be applied for both the Radon transform and the statistical models, but better results are generally achieved within the statistical framework. While it is known that the severity of the artifacts increases with the increasing angular range of the missing projections, limited-angle tomography does not provide information on which projections should be used in order to most effectively reconstruct the image.

Maximum likelihood (ML) estimation is a widely used method in the related art for reconstructing an image from a constrained set of measurements. A parameterization of the generative model described above is obtained by assigning an intensity $I(u)$ to every voxel in U. The likelihood of the observed data $\mathbf{y} = (y_t)_t$, given the set of parameters $\mathbf{I} = \{I(u) : u \in U\}$ is:

$$\begin{aligned} L(\mathbf{y}|\mathbf{I}) = \ln P(\mathbf{y}|\mathbf{I}) &= \ln \prod_t P(y_t|\mathbf{I}) = \sum_t \ln P\left(\sum_u x_t(u)\,|\,\mathbf{I}\right) \\ &= \sum_t \ln \mathrm{Poisson}\left(y_t \mid \sum_u \phi_t(u) I(u)\right) \\ &= \sum_t \left\{-\sum_u \phi_t(u) I(u) + y_t \ln \sum_u \phi_t(u) I(u) - \ln(y_t!)\right\} \end{aligned} \quad (1)$$

Note that the lower and upper bound of an indexing variable (such as voxels u and time index t) are omitted in the following description, when they are clear from the context.

There is currently no analytic way to solve Eqn. 1 for the maximum of the likelihood function. However, optimization methods that find local maxima of the likelihood are known. One such method is the Expectation-Maximization (EM) process.

Since the data generated by the model is only partially observable by our measurements, a basic ingredient of the Expectation-Maximization formalism is to define a set of random variables that completely define the data generated by the model. In the current case, since $Y_t = \Sigma_u X_t(u)$, the set of variables $\{X_u(t) : u \in U;\ t = 1, \ldots, T\}$ is such a set; the generated data is $\mathbf{x} = (\mathbf{x}_t)_t$, where $\mathbf{x}_t = (x_t(u))_u$, and the observed data $\mathbf{y}$ is completely determined by $\mathbf{x}$. The main tool in the EM formalism is the complete data likelihood:

$$\begin{aligned} \ln P(\mathbf{x}|I) &= \ln \prod_t P(\mathbf{x}_t|I) = \sum_t \ln \prod_u \mathrm{Poisson}(x_t(u)\,|\,\phi_t(u) I(u)) \\ &= \sum_t \sum_u \{-\phi_t(u) I(u) + x_t(u) \ln(\phi_t(u) I(u)) + \ln(x_t(u)!)\} \end{aligned} \quad (2)$$

Since the likelihood depends on the complete data, which is only partially observable, we take its expectation with respect to the space of the unobserved data, given the current set of hypothesized parameters (i.e. the current estimator). The result is a function $Q(\mathbf{I}|\mathbf{I}')$ which assigns likelihood to sets $\mathbf{I}$ of model parameters, given the current set $\mathbf{I}'$, and given the observed data $\mathbf{y}$:

$$\begin{aligned} Q(\mathbf{I}|\mathbf{I}') &= E[\ln P(\mathbf{x}|\mathbf{I})\,|\,\mathbf{y};\mathbf{I}'] \\ &= \sum_t \sum_u \{-\phi_t(u) I(u) + E[x_t(u)|y_t;\mathbf{I}'] \ln(\phi_t(u) I(u)) + C\} \end{aligned} \quad (3)$$

where C is a term which is independent of the intensities $\mathbf{I}$. The function $Q(I|I')$ is maximized by the following new estimates:

$$I(u) = \frac{1}{\sum_t \phi_t(u)} \sum_t E[x_t(u) \,|\, y_t; \mathbf{I}'] \quad ; \quad \forall\, u \in U. \tag{4}$$

The expectation in Equation 4 is obtained as follows:

$$\begin{aligned} & P_{X_t(u)}(x_t(u)|y_t;\mathbf{I}') = \frac{P_{Y_t}(y_t|x_t(u);\mathbf{I}')\; P_{X_t(u)}(x_t(u)|\mathbf{I}')}{P_{Y_t}(y_t|\mathbf{I}')} \\ = \; & \frac{\text{Poisson}(y_t - x_t(u)|\sum_{v\neq u}\phi_t(v)I'(v))\;\text{Poisson}(x_t(u)\,|\,\phi_t(u)I'(u))}{\text{Poisson}(y_t\,|\,\sum_v \phi_t(v)I(v))} \\ = \; & \text{Binomial}(x_t(u)\,|\,\frac{\phi_t(u)I'(u)}{\sum_v \phi_t(v)I'(v)};\, y_t) \end{aligned} \tag{5}$$

It follows that $E[x_t(u)|y_t; I'] = y_t \frac{\phi_t(u)I'(u)}{\sum_v \phi_t(v)I'(v)}$, and hence the EM iteration is:

$$I(u) = \frac{1}{\sum_t \phi_t(u)} \sum_t y_t \frac{\phi_t(u)I'(u)}{\sum_v \phi_t(v)I'(v)} \tag{6}$$

It is provable that each EM iteration improves the likelihood. Thus, given a random starting estimator, the EM algorithm iterates the above improvement step until it converges to a local maximum of the likelihood. Several random starts increase the chance of finding a globally good estimator.

It is usually desired to maximize the expected posterior probability (given a proper prior) rather than the expected likelihood. In that case we assume a prior probability on the intensities $P(\mathbf{I}) = \prod_u P(I(u))$. A proper conjugate prior for the Poisson distribution is the Gamma distribution:

$$P(I(u)) = \text{Gamma}(I(u)\,|\,\alpha_u;\beta_u) = \frac{\beta_u^{\alpha_u+1}}{\Gamma(\alpha_u+1)} I(u)^{\alpha_u} e^{-\beta_u I(u)} \tag{7}$$

Now the maximization is done on $Q(\mathbf{I}|\mathbf{I}') = E[lnP(\mathbf{x}|I)p(I)\,|\mathbf{y};\, I']$. Plugging the Gamma prior into Q, and solving for $I(u)$, we get the following EM iteration for the maximum posterior estimation:

$$I(u) \;=\; \frac{\alpha_u + \sum_t E[x_t(u)|y_t;\mathbf{I}']}{\beta_u + \sum \phi_t(u)} \tag{8}$$

$$= \frac{1}{\beta_u + \sum_t \phi_t(u)} \left[\alpha_u + \sum_t y_t \frac{\phi_t(u) I'(u)}{\sum_v \phi_t(v) I'(v)} \right] \quad (9)$$

The EM update step can be formulated in matrix notation as follows. Let Φ be the matrix of the projections $[\phi_t(u)]_{t,u}$, and let $\mathbf{I}, \mathbf{I}', \mathbf{y}, \alpha$ and β be represented as column vectors. Equation 8 can be written in vector and matrix notations as:

$$\mathbf{I} = \frac{\alpha + \mathbf{I}' \cdot \left(\Phi^T \frac{\mathbf{y}}{\Phi \mathbf{I}'} \right)}{\beta + \Phi^T \mathbf{1}} \quad (10)$$

where the explicit multiplication and division denote element-wise operations, and where $\mathbf{1}$ is a vector (of the appropriate length) consisting solely of 1's.

Limited computational resources (*i.e.*, when the entire projection matrix Φ cannot be kept in memory) may require breaking the update computation according to a partition of Φ into a set of sub-matrices (Φ_i). In that case the intensities can be updated gradually (using only one sub-matrix at each step) according to the following computation:

$$\mathbf{I} = \frac{\alpha + \mathbf{I}' \cdot \sum_i \Phi_i^T \frac{\mathbf{y}_i}{\Phi_i \mathbf{I}'}}{\beta + \sum_i \Phi_i^T \mathbf{1}} \quad (11)$$

where $\mathbf{y}_i$ is the vector of observations that are obtained using the views of Φ_i.

In order to achieve a reconstructed image which is adequate for medical diagnostic and treatment purposes, a high-resolution image of the tested object must be obtained. When high-resolution detecting units are used, their efficiency is relatively low, and the detecting units must remain at each position for a relatively long time in order to achieve a high probability of detection. Since during medical testing, measurements are generally performed at many locations as the detecting unit is moved relative to the observed organ, the testing procedure generally requires a long time and is physically and emotionally difficult for the patient. Additionally, reconstruction is based upon a large quantity of data, and is a lengthy and computationally complex process.

SUMMARY OF THE INVENTION

A method is described for identifying an optimal, or preferred set of views for radioactive–emission measurements of a region of interest within the body. The method is based on a model of the region of interest, and the preferred sets of views

are identified for the model, preferably using information theoretic measures. The preferred sets of views may then be applied to the region of interest, in vivo.

The present invention successfully addresses the shortcomings of the presently known configurations by providing methods for identifying optimal, or preferred sets of views for radioactive–emission measurements of a region of interest within the body. The methods are based on models of the region of interest, and the preferred sets of views are identified for the models, preferably using information theoretic measures. The preferred sets of views may then be applied to the region of interest, in vivo.

Unless otherwise defined, all technical and scientific terms used herein have the same meaning as commonly understood by one of ordinary skill in the art to which this invention belongs. Although methods and materials similar or equivalent to those described herein can be used in the practice or testing of the present invention, suitable methods and materials are described below. In case of conflict, the patent specification, including definitions, will control. In addition, the materials, methods, and examples are illustrative only and not intended to be limiting.

Implementation of the method and system of the present invention involves performing or completing selected tasks or steps manually, automatically, or a combination thereof. Moreover, according to actual instrumentation and equipment of preferred embodiments of the method and system of the present invention, several selected steps could be implemented by hardware or by software on any operating system of any firmware or a combination thereof. For example, as hardware, selected steps of the invention could be implemented as a chip or a circuit. As software, selected steps of the invention could be implemented as a plurality of software instructions being executed by a computer using any suitable operating system. In any case, selected steps of the method and system of the invention could be described as being performed by a data processor, such as a computing platform for executing a plurality of instructions.

BRIEF DESCRIPTION OF THE DRAWINGS

The invention is herein described, by way of example only, with reference to the accompanying drawings. With specific reference now to the drawings in detail, it

is stressed that the particulars shown are by way of example and for purposes of illustrative discussion of the preferred embodiments of the present invention only, and are presented in the cause of providing what is believed to be the most useful and readily understood description of the principles and conceptual aspects of the invention. In this regard, no attempt is made to show structural details of the invention in more detail than is necessary for a fundamental understanding of the invention, the description taken with the drawings making apparent to those skilled in the art how the several forms of the invention may be embodied in practice.

In the drawings:

Figs. 1a-1i show detecting units and blocks of various geometries and constructions and radioactive-emission-measuring probes, associated with them.

Figs. 1j and 1k present the principles of modeling, for obtaining an optimal set of views, in accordance with the present invention;

Figs. 1l and 1m pictorially illustrate a view and viewing parameters associated with it, in accordance with definitions of the present invention.

Fig. 2 is a simplified flowchart of a method for selecting a set of optimal views of a volume to be imaged, according to a first preferred embodiment of the present invention.

Fig. 3 shows an example of a volume with two views.

Fig. 4 illustrates the concept of uniform coverage of a volume.

Fig. 5 is a simplified flowchart of a method for selecting a set of optimal views of a volume to be imaged, according to a second preferred embodiment of the present invention.

Fig. 6 shows four models of a prostate emittance model.

Figs. 7a-7f show emittance models of a given volume to illustrate view selection using the separability criterion.

Figs. 7g-7j show emittance models of a given volume to illustrate view selection using a weighted-combination criterion.

Fig. 8 is a simplified flowchart of an iterative method for selecting a set of views, according to a preferred embodiment of the present invention.

Fig. 9 is a simplified flowchart of a single iteration of a view selection method, according to a preferred embodiment of the present invention.

Fig. 10 is a simplified flowchart of a method for selecting a set of optimal views of a volume to be imaged, according to a third preferred embodiment of the present invention.

Fig. 11 is a simplified block diagram of a set selector for selecting a set of optimal views of a volume to be imaged, according to a first preferred embodiment of the present invention.

Fig. 12 is a simplified block diagram of a set selector for selecting a set of optimal views of a volume to be imaged, according to a second preferred embodiment of the present invention.

Figs. 13-18 illustrate view set selection results for the uniformity criterion.

Figs. 19-24 illustrate view set selection results for the separability criterion.

Figs. 25-32 illustrate view set selection results for the reliability criterion, based on the Fisher information measure.

Fig. 33 illustrates view set selection results for the reliability criterion, based on minimizing the inverse mean of the Fisher information measure.

DESCRIPTION OF THE PREFERRED EMBODIMENTS

The present invention is of methods for identifying optimal, or preferred sets of views for radioactive–emission measurements of a region of interest within the body. The methods are based on models of the region of interest, and the preferred sets of views are identified for the models, preferably using information theoretic measures. The preferred sets of views may then be applied to the region of interest, in vivo. The principles and operation of the methods for optimizing radioactive-emission measurements, according to the present invention, may be better understood with reference to the drawings and accompanying descriptions.

Before explaining at least one embodiment of the invention in detail, it is to be understood that the invention is not limited in its application to the details of construction and the arrangement of the components set forth in the following description or illustrated in the drawings. The invention is capable of other embodiments or of being practiced or carried out in various ways. Also, it is to be understood that the phraseology and terminology employed herein is for the purpose of description and should not be regarded as limiting.

Referring now to the drawings, Figures 1j and 1k present the principles of modeling, for obtaining an optimal set of views, in accordance with the present invention.

Figure 1j schematically illustrates a body section 120, having a region of interest (ROI) 130. The region of interest 130 may be associated with an organ 140, with a specific radioactive-emission-density distribution, possibly suggestive of a pathological feature 150, termed herein an organ target 150. Additionally, there may be certain physical viewing constraints, associated with the region of interest 130.

We thus consider the following problem: how can we best identify an optimal and permissible set of views for radioactive-emission measurements of the region of interest 130, for reconstructing a three-dimensional image of it?

In accordance with the present invention, our approach is delineated by the following process:

i. modeling the region of interest 130, as a model 160 of a volume U, possibly with one or several modeled organ targets HS, within anatomical constraints AC, as seen in Figure 1k;

ii. obtaining an optimal and permissible set of views for the modeled volume U of Figure 1k; and

iii. applying the optimal set of views to the in-vivo region of interest 130 and the organ 140 of Figure 1j.

It will be appreciated that the model 160 of the region of interest 130 may be based on general medical information of the organ 140 and common pathological features associated with it. Additionally, the model may be based on information related to a specific patient, such as age, sex, weight, and body type. Furthermore, a structural image, such as by ultrasound or MRI, may be used for providing information about the size and location of the organ 140 in relation to the body section 120, for generating the model 160.

The present application concentrates on the second step of the process, namely, obtaining the optimal and permissible set of views for the volume U of the model 160.

Referring now to the drawings, Figures 1l and 1m pictorially illustrate a view and viewing parameters associated with it, in accordance with definitions of the present invention.

Seen in Figure 1l is a volume U, subdivided into voxels u. The volume U is defined in a six-degree coordinate system (x;y;z;ω;θ;σ) and has a point of origin P0(x0; y0; z0; ω0; θ0; σ0). A detecting unit 102 is positioned at a location and orientation P1(x1; y1; z1; ω1; θ1; σ1). The detecting unit 102 has a detector 104 of a specific detector material of a thickness τ_d, and a collimator 108 of a diameter D and a length L, so as to define a collection angle δ. The location, orientation, and collection angle parameters determine a three-dimensional sector S, which is the portion of the volume U that is within the detector unit's field of view. The probability of detection of a given voxel outside of sector S is negligible, since a photon emitted from the given voxel outside of sector S will have a very low probability of reaching detector 104 through collimator 108.

Figure 1m schematically illustrates the emission rate of the volume U, as a function of time, given that a radioactive material of a specific half-life has been administered at a time T0.

A view may thus be defined as a group of nonzero probabilities of detecting a radioactive emission associated with all the voxels that form sector S (Figure 1l).

A view is sometimes referred to as a projection, and the two terms are synonymous. Furthermore, a view defined over the sector S can be naturally extended to be defined over the group of all voxels in the volume U, by simply associating a zero probability with every voxel outside the sector S. This enables applying mathematical operations over the entire volume U.

The viewing parameters, which are the factors affecting the detection of radioactive emissions, are as follows:

i. **location and orientation parameters:**

a location and an orientation in a six-dimensional space, P1(x1; y1; z1; ω1; θ1; σ1), with respect to the origin P0(x0; y0; z0; ω0; θ0; σ0) of the volume U, in which the detecting unit 102 is positioned;

ii. **detector-unit parameters:**

- the detector unit geometry (e.g. length L, diameter D, and/or collection angle δ), which together with the location and orientation parameters, P1(x1; y1; z1; ω1; θ1; σ1) with respect to the origin P0(x0; y0; z0; ω0; θ0; σ0) define the sector S;
- the septa thickness τ, which affects the probability that a photon that enters the collimator will reach the detector as well as crosstalk effects (which occur when a photon which entered a neighboring cell penetrates the collimator and reaches the detector), hence, the detector efficiency
- the detector material, which affects the detector efficiency; and
- the detector thickness τ_d, which affects the detector's stopping power, hence, its efficiency;

iii. **attenuation parameters:**

attenuation properties of all the voxels within the sector S, as they affect the probabilities that radioactive emissions from a specific voxel within the sector S will reach the detector, wherein different voxels within the sector S may have different attenuation properties, since several types of tissue may be involved;

iv. **time parameters:**

since the radiopharmaceutical decays with a specific half-life, the time t_1 since administration, and the duration of the measurement Δt_1, affect the number of emissions that occur during the radioactive-emission measurement.

v. **radiopharmaceutical parameters:**

The half-life $t_{1/2}$, of the radiopharmaceutical, the types of radioactive emission, whether gamma or beta, and the energies of the radioactive emission affect the probability of detection.

Some of these viewing parameters are fixed for a particular situation. Specifically, the tissue attenuation parameters are given. Additionally, the time t_1 since administration of the radiopharmaceutical is generally governed by the blood pool radioactivity, since it is generally necessary to wait until the blood pool

radioactivity dies out for low-level detection to be possible. For the remaining viewing parameters, optimization may be carried out.

To recapitulate the problem describe above, an intensity distribution I , in terms of radioactive emissions per seconds, is defined over the volume U, forming our input space. U comprises a set of basic elements u (*e.g.*, pixels in two dimensional spaces, voxels in three dimensional spaces), and $I(u)$ is the intensity in a given basic element $u \in U$. An inverse (or reconstruction) problem arises when one cannot sample directly from I, but can sample from a given set of views $\mathbf{\Phi}$. A projection $\varphi \in \mathbf{\Phi}$ is defined by the set of probabilities $\{\varphi(u) : u \in U\}$, where $\varphi(u)$ is the probability of detecting a radioactive emission from a voxel u, as defined by viewing parameters, such as the physical and geometrical properties of the detecting unit, as well as the attenuation parameters of the viewed volume U, and the time parameters. A measurement is obtained by choosing a view $\varphi \in \mathbf{\Phi}$, and then sampling according to the viewing parameters.

In the following analysis, I is the intensity of a radioactive substance, and the viewing parameters include the geometrical properties of a collimated detecting unit and the detecting unit's position and orientation with respect to volume U. The number of radioactive emissions counted by the detecting unit within a time interval is a Poisson distribution, where $\varphi(u)$ is the detection probability of a photon emitted from voxel $u \in U$ and the mean of the distribution is the weighted sum $\Sigma_{u \in U} \varphi(u) I(u)$.

The projection set is thus defined by a matrix $\mathbf{\Phi}$, whose rows are the projections of the chosen views. I is a vector of densities (specified per each element in U), and ΦI is a vector of respective effective intensity levels for the views in the set. A vector of measurements $\mathbf{y}$ is obtained by a random sample from each view (according to the associated Poisson distribution). As discussed above, there are various known reconstruction methods that provide estimators for I given the projections $\mathbf{\Phi}$ and the measurements $\mathbf{y}$.

We consider here the following problem: Assume that there is a large pool of candidate views to choose from, but due to time restrictions or other restrictions, we are limited to a specific number of views N. Which are the best N projections in terms of the quality of the reconstruction? It is further assumed that the pool of projections may be constrained, and hence general sampling theorems (*e.g.*, Radon Transform)

cannot be applied. For instance, we consider a scenario in emission tomography where the detecting unit can be located on top of one face of a given volume but not on the others. In such cases, prior-art methods do not clearly establish what is the best scanning scheme, in order to provide the best reconstruction of the radioactive intensity distribution of the volume.

The following embodiments are of a method for selecting a set of optimal views of a volume to be imaged, and are not confined to a specific reconstruction algorithm. View selection is preferably based on information theoretic measures that quantify the quality of the data fed to the reconstruction algorithm.

Reference is now made to Fig. 2, which is a simplified flowchart of a method for selecting a set of optimal views of a volume to be imaged, according to a first preferred embodiment of the present invention. In step 200, a volume is provided, and is preferably represented as a collection of voxels. In step 210, a collection of views of the volume is provided. Each view reflects a possible data collection option, from which the goal is to select a set of views which together provide the desired image reconstruction quality. Each view is associated with one or more viewing parameters, such as the location and orientation of the detecting unit with respect to the volume.

The viewing parameters preferably further contain at least one of the following detecting unit characteristics: detector material, detector thickness, collimator length, diameter, septa thickness, and collection angle. When the viewing parameters include detecting unit characteristics, such as those discussed above, the view may be said to incorporate a model of a detecting unit.

In the preferred embodiment, the viewing parameters include a detection duration parameter, which corresponds to the duration of the measurement is performed (at the associated location, orientation, etc.). Increasing the detection duration generally improves the probability of the detection for those voxels in the detecting unit's collection angle.

Preferably, the viewing parameters include a type of radiopharmaceutical. The type of radiopharmaceutical determines the type of radioactivity being detected, and consequently the probability of detection.

Preferably, the viewing parameters include a time of detection, t_D, relative to an initial time t_0. As discussed above, in conjunction with Figure 1m, during radionuclide imaging a radiopharmaceutical is administered to a patient, and after a suitable interval, to allow the radiopharmaceutical to disperse throughout the body, measurements are taken. Since the radiopharmaceutical decays at a specific rate after administration, depending on its half-life, the length of time between when the radiopharmaceutical is administered and the time of measurement affects the radioactive emission detection of the given view.

The view set is preferably tailored to correspond to the actual limitations and constraints likely to be encountered when collecting data for a given object. For example, in medical applications the detecting unit can generally view the body structure only from certain distances and orientations, which are determined by the patient's anatomy and the structure of the probe. The view set may therefore be designed to contain views having only those viewing parameter values consistent with attainable distances and orientations. The view set may also be designed to contain views having only those viewing parameter values suitable for a given measurement scenario, for example having identical values for the type of radiopharmaceutical and time since administration.

Preferably, the collection of views represents a quantized continuum of views. The view collection thus reflects the detection probability distribution for a detecting unit making periodic measurements while moving along a trajectory.

Reference is now made to Fig. 3, which shows a non-limiting example of a volume 300 with two views, V_1 and V_2. Volume 300 divided into twenty-seven cube-shaped voxels (labeled 1-27). Each view reflects a number of viewing parameters, in the case shown a location (in the XYZ coordinate system), orientation (ω, θ and σ) and collection angle δ. The viewing parameters determine which voxels in volume 300 are within a detecting unit's collection angle, and generally affect the probability of detection for each voxel. The probability of detection may be affected by additional factors, including the attenuation coefficients within the volume.

During data collection, the probability of detection for each voxel is dependent on the parameters outlined above. In the preferred embodiment, a respective projection is calculated for each view, giving the view's detection probability

distribution (i.e. the detection probability for each voxel of the volume). For a given view, the associated projection will have significant detection probabilities only for those voxels within the sector defined by the detecting unit's collection angle and location and orientation, as illustrated in conjunction with Figure 11.

The detection probability distribution for each view, that is the group of probabilities for each voxel, for a given view, is calculated according to techniques known in the art for determining the detection probability of a radioactive emission from a given voxel, under the constraints specified by the viewing parameters, for example, based on computer simulations of the geometry and the other viewing parameters, delineated hereinabove.

Generally, more distant voxels will have a lower probability of detection than closer voxels along the same line of sight. The volume attenuation coefficient may be constant or may vary over the volume. Thus, different sets of views may be produced for a single sector, by defining volumes with differing attenuation coefficients. For example, bone tissue and muscle tissue have different attenuations. Anatomical knowledge of the body structure being imaged may be used to develop a model of the volume U with a non-uniform attenuation that reflects the expected attenuation of the given body structure.

Referring again to Fig. 2, in step 220 a scoring function is provided. The scoring function rates the information that is obtainable from the volume using any set of views (containing at least one view) taken from the collection of views. Several examples of scoring functions based on information-theoretic measures are discussed in detail below. Preferably, the scoring function is a function of the detection probability distribution, as given by the projections. Several preferred embodiments of the scoring function, are discussed in detail below.

In step 225, sets of views are formed from the collection of views. A score is then calculated for each of the sets.

In step 230, the scores calculated in step 225 are used to select one of the formed sets of views . A given scoring function may be used to select a set in a number of ways. In a first preferred embodiment, a required number of views is specified, and the highest scoring set with the specified number of views is selected. In a second preferred embodiment, the user may specify a minimal score which is

known to provide satisfactory information quality, and select the smallest set which provides the specified score. However given a large collection of views the required number of calculations may be prohibitive. A third preferred embodiment used to reduce the computational burden is the greedy algorithm embodiment described for Figs. 8-9 below.

Since each view is associated with known values of the viewing parameter(s), selecting a view effectively specifies known viewing parameter values. The selected set of views thus defines a set of viewing parameter values, which may be used to collect data which yields a high-quality reconstruction of the emission distribution of the volume.

As discussed above, the scoring function is a measure of the quality of information which may be gathered for the volume using the given set of views. In a first preferred embodiment, the scoring function implements a uniformity criterion, to ensure uniform coverage of the volume. It is often desired to obtain a uniform reconstruction quality among a given set of voxels $W \subseteq U$, where W is the set of voxels for which it is desired to obtain uniform detection. Note that by selecting the appropriate W, the uniformity criterion is applied to all or a portion of the body. The uniformity criterion ensures that the spread of the total influence of each element on the set of measurements is as uniform as possible. The uniformity criterion depends only on the collection of views $\mathbf{\Phi}$ and requires no assumptions on the distribution I.

For a set $\mathbf{\Phi}$ of projections, the total influence of an element, u, is given by $\Sigma_{\varphi \in \Phi} \varphi(u)$. Normalizing these values to $P_{\mathbf{\Phi}}(u)$, such that $\sum_{u \in W} P_{\Phi}(u) = 1$, a probability measure is obtained for which the entropy $H(\Phi)$ can serve as a uniformity measure:

$$H(\Phi) = -\sum_{u \in W} \mathrm{P}_{\Phi} \log \mathrm{P}_{\Phi}(u) \qquad (12)$$

The selected set Φ^* is the set (containing the required number of views) that satisfies:

$$\Phi^* = \arg\max_{\Phi} H(\Phi) \qquad (13)$$

Reference is now made to Fig. 4, which illustrates the concept of uniform coverage of a volume. Volume 400 consists of twenty-seven cube-shaped voxels, including voxels 410 and 420. **A, B, C** and **D** are three views of volume 400, showing the detector position and orientation for each view. For the uniformity criterion, it is desired that the overall influence of voxels 410 and 420 be approximately equal.

Assume that the probabilities of detection are as follows:

View	Voxel 410	Voxel 420
A	0.6	0
B	0.2	0.5
C	0	0.3
D	0	0.1

Consider two possible sets of views: set {**A, B, C**} and set {**B, C, D**}. For set {**A, B, C**}, the total contribution of voxel 410 is 0.8 (0.6+0.2+0) and of voxel 420 is 0.8 (0+0.5+0.3). Normalizing these values for set {**A, B, C**} gives a probability set of [0.5,0.5]. For set {**B, C, D**}, the total contribution of voxel 410 is 0.2 (0.2+0+0) and of voxel 420 is 0.9 (0.5+0.3+0.1). Normalizing these values for set for set {**B, C, D**} gives a probability set of [0.18,0.82]. Thus:

$$H(\{\mathbf{A, B, C}\}) = -(0.5 * \log_2 0.5 + 0.5 * \log_2 0.5) = -(-0.5 - 0.5) = 1$$

$$H(\{\mathbf{B, C, D}\}) = -(0.18 * \log_2 0.18 + 0.82 * \log_2 0.82) = -(-0.44 - 0.07) = 0.51$$

Set {**A, B, C**} is thus seen to provide a more uniform coverage of volume 400 than set {**B, C, D**}.

In the above, the scoring function is defined independently of the emission intensity of the volume. However, scoring functions may be defined which calculate the score for a given set in relation to one or more emittance models. An emittance model is a representation of a specific radioactive-emission intensity distribution within the volume U, so as to model organ targets, such as hot regions, of a radioactive emission intensity, higher than the background level, regions of low-level

radioactive emission intensity, which is nonetheless above the background level, and cold regions, of a radioactive emission intensity, lower than the background level. Given an object or class of objects, emittance models may be devised to reflect expected or typical emission patterns for the given object. The information quality given by a set of views may thus be measured in relation to expected emitted intensities from the volume.

Reference is now made to Fig. 5, which is a simplified flowchart of a method for selecting a set of optimal views of a volume to be imaged, according to a second preferred embodiment of the present invention. A volume is provided in step 500 and a collection of views is provided in step 510, essentially as described above. The current method differs from the method of Fig. 2 by the addition of step 515, in which a set of one or more emittance models is provided. An emittance model specifies the radiative intensity of each voxel in the volume. As discussed above, some of the viewing parameters affect the radiative intensity of the voxels in the volume, for example the type of radiopharmaceutical and the time since administration of the radiopharmaceutical. Therefore, the emittance models provided in step 515 preferably correspond to the relevant viewing parameters.

Once the emittance models are provided, a scoring function is provided in step 520. Sets of views are formed in step 525, and each of the formed sets is scored with the scoring function. In step 530, a set of views is selected from the collection of views based on the calculated scores.

Developing an emittance model for a particular object involves analyzing known information about the object to determine expected emission patterns of the object. In the preferred embodiment, the volume corresponds to a body structure. Preferably the body structure is one of: a prostate, a heart, a brain, a breast, a uterus, an ovary, a liver, a kidney, a stomach, a colon, a small intestine, an oral cavity, a throat, a gland, a lymph node, the skin, another body organ, a limb, a bone, another part of the body, and a whole body. In order to develop a model of a particular body structure, for example a prostate, many factors may be considered. Physical aspects, such as the size and shape of the prostate and the position of the prostate within the torso may be considered, as well as medical knowledge regarding typical emissions

from healthy and diseased prostates. Additional information may concern variations between individuals, such as age, weight, percentage of body fat, and the like.

Reference is now made to Fig. 6, which shows four models of a prostate emittance model. Three views are given for each of the emittance models shown. Each of the views is a maximum intensity projection (MIP) along a different one of the three axes. For example, in an X-Y projection the intensity of a given point is taken as the maximum intensity for that point along a line parallel to the z-axis. Thus the volume in effect becomes "transparent", and the maximum intensity regions are shown clearly. Variations in emission levels are indicated by differences in shading. The emittance model is shaped as an ellipsoid, the typical shape of a prostate. Since a diseased prostate is generally characterized by one or more hot regions, each of the emittance models shown has a number of high-emittance portions (two hot regions in Models A-C and three hot regions in Model D). Each high-emittance area is an ellipsoid, with a size of approximately 1 cubic centimeter. The intensity of the modeled organ targets varies randomly from two to eight times brighter than the surrounding volume.

In the preferred embodiment, one or more of the emittance models contains at least one high-emittance portion (i.e. hot region). A prostate containing a tumor, for example, may be modeled as an ellipsoid volume with one or more high-emittance portions. A high-emittance portion is characterized by an intensity that is greater than the background intensity by a factor of at least $(1+\alpha)$, where α is a parameter specified by the user. In practice, a hotspot is usually detectable only if the radiation levels within the hotspot are higher than the background level by a factor of 1.5-2. α is therefore typically defined between 0.5-1. However, the detectability of a hotspot rises as the radioactive intensity of the body rises, raising the photon count. Thus, a lower value of α may be used when high-intensity emittance models are used.

In the preferred embodiment, one or more of the emittance models contains at least one low-emittance portion. A low-emittance portion is characterized by an intensity that is lower than the background intensity by a factor of at least $(1+\beta)$, where β is a parameter specified by the user. In heart imaging, for example, the locations of interest are low-emittance portions of the structure, indicating non-

functional tissues. A diseased heart may therefore be modeled as a heart-shaped volume with low-emittance portions.

Note that an emittance model need not contain high- or low- emittance portions, but may have a uniform intensity or a slowly varying intensity. Following are two more embodiments of scoring functions, both of which include considerations of the emission pattern of the volume, in light of the emittance models provided in step 515.

Following are a number of preferred embodiments of scoring functions which score view sets in relation to one or more emittance models.

In a second preferred embodiment, the scoring function implements a separability criterion. Separability is a measure of the extent to which the measurements that are obtained from each pair of models can be distinguished from one another.

The concept of separability is illustrated in Figs. 7a-7c, each of which shows an emittance model of a given volume 700. Each of the emittance models contains two high-emittance portions (hot regions), 710 and 720, which are located in respectively different locations in each of the models. It can be seen that the hot regions in emittance models 7b and 7c are in similar portions of the volume, as opposed to the hot regions in model 7a. It may therefore be difficult to distinguish between reconstructions of emittance models 7b and 7c. The separability criterion ensures that the selected set includes views which provide reconstructions which distinguish between emittance models 7b and 7c.

Letting $\boldsymbol{I}$ be the emittance model set, a measure for the dissimilarity of any two given densities in $\boldsymbol{I}$ is defined. Since most state-of-the-art estimating algorithm are aimed at finding ML estimators, in the current example the scoring function is based on the likelihood function. The likelihood of an estimator of I, given a set of Poissonian measurements $\mathbf{y}$ is:

$$\mathcal{L}(I) = \sum_t \left\{ -\sum_u \phi_t(u) I(u) + y_t \ln \sum_u \phi_t(u) I(u) - \ln(y_t!) \right\} \qquad (14)$$

For separability, it is desired that this measure be different for each $I \in \boldsymbol{I}$. Since the measure is a random variable that depends on the actual measurements, all possible pairings of emittance models should be examined to ensure that the resulting distributions are separable. A scoring function that captures this separability is given by the square of the difference between the means of the distributions normalized by the sum of their variances:

$$\text{SEPARABILITY}_{\Phi}(I_1, I_2) = \frac{\left|\mathbf{E}\boldsymbol{\mathcal{L}}(I_1) - \mathbf{E}\boldsymbol{\mathcal{L}}(I_2)\right|^2}{\mathbf{Var}\boldsymbol{\mathcal{L}}(I_1) + \mathbf{Var}\boldsymbol{\mathcal{L}}(I_2)} \qquad (15)$$

The expectations and variances in Equation 15 are taken over random measurements y, sampled from the true intensity I_1 (note that the measure is not symmetric).

Since the true (unknown) intensity can be any $I \in \boldsymbol{I}$, a projection set Φ^* that maximizes the worst-case separability is desired. That is:

$$\Phi^* = \arg\max_{\Phi} \min_{I_1, I_2 \in \boldsymbol{I}} \text{SEPARABILITY}_{\Phi}(I_1, I_2) \qquad (16)$$

Scoring for separability is based on the minimum separability obtained with a given set of views for all of the possible pairings of emittance models from the set of emittance models, thereby enabling defining a desired resolution in more than one direction, or in more than one portion of the volume. All of the emittance models are modeled on a substantially identical volume. The emittance models preferably differ from one another in the modeled organ targets, where the modeled organ targets are separated by a difference of at least the required resolution (where the displacement which produces the required resolution is denoted delta herein). Substantially identical sets of views are formed from the collection of views, and each of the formed sets is scored with respect to each of the pairs. One of the sets of views is selected, based on the minimum or average score for the plurality of pairs.

For example, assume the set of emittance models contains the three models 7a-7c. A separability score is calculated for a given formed set of views by applying

Equation 15 to all three pairs 7a/7b, 7a/7c, and 7b/7c. The lowest of the three calculated values is taken as the separability score for the formed set. Once a separability score has been calculated in such manner for each of the formed sets of views, the view set having the highest separability is selected.

The separability criterion may be used to ensure that a required resolution is obtained in all or a portion of the body. In a preferred embodiment, view set selection for separability is performed utilizing a set of emittance models consisting of one pair of emittance models having substantially identical volumes but with different modeled organ targets. The modeled organ targets are separated by a delta in a given direction so as to define a required resolution in that direction and portion of the volume U. Substantially identical sets of views are formed from the collection of views, and scored with respect to the pair of emittance models, using a scoring function based on the separability criterion, and one of the sets of views is selected based on the separability scores. The selected set is thus the set which provides the optimum resolution in the given direction and in the vicinity of the modeled organ targets.

A similar approach may be used to ensure resolution in more than one direction and/or portion of the volume U. Consider for example, a pair of models of substantially identical volumes, as follows: The model of Figure 7d, which schematically illustrates the volume U, having the modeled organ target HS, whose center is at a location $(x;y;z)_{HS}$, and the model of Figure 7e, which schematically illustrates the volume U, having the modeled organ target HS', whose center is at a location $(x;y;z)_{HS'}$. Fig. 7e also shows modeled organ target HS of Fig. 7d superimposed over the present emittance model to illustrate that HS' is somewhat displaced from HS, along the x-axis, and the displacement, is denoted as delta1 in the present example. The displacement delta may be measured, for example, in mm.

An optimal set of views, from the standpoint of separability, is that which will best distinguish between the model of Figure 7d and that of Figure 7e. Thus, a score, in terms of separability is given for the pair of models, and relates to a resolution as defined by the difference between the models of the pair. In the present example, the difference is delta1 along the x-axis, around the locations of HS and HS', so the score given by the information theoretic measure of separability will relate specifically to a

resolution as defined by delta1 along the x-axis, around the locations of HS and HS'. Other portions of the volume U and other directions may have different resolutions.

For example, consider the model of Figure 7f, which schematically illustrates the volume U, having the modeled organ target HS", whose center is at a location $(x;y;z)_{HS"}$, and shows HS of Fig. 7d and HS' of Fig. 7e superimposed over the present emittance model. HS" is displaced from HS, along the z-axis, a displacement delta2. and additionally, HS" is displaced from HS', along the x- and z- axes, a displacement delta3.

Scores, in terms of separability, may be given to all the paring combinations, that is the models of Figures 7d – 7e, relating to delta1; the models of Figures 7d –7f, relating to delta2, and the models of Figures 7e – 7f, relating to delta3. An optimal set of views may be selected based on its minimum or average scores for all the pairing combinations; for example, the optimal set may be that whose average score for all the pairing combinations is the highest. Alternatively, a weighted average may be applied.

In an additional preferred embodiment, the scoring function implements a reliability criterion, which is a measure of how reliably the intensity distribution of a given object may be reconstructed from the sampled views. Since the input to the reconstructed algorithm is a random sample, the output estimator is also random. A desired property of this output is that it be reliable in the sense that similar estimators for different projected samples (i.e. different sets of measurements) of the same input intensity are obtained with high confidence.

The Fisher Information, $F_\Phi(I)$ is a measure, known in the art, which is used to evaluate the expected curvature of the likelihood of a model I (taken over measurements sampled from the model I). The Fisher Information is defined as:

$$F_\Phi(I) = -\mathrm{E}\nabla^2 \mathcal{L}(I) \qquad (17)$$

The derivatives are taken with respect to the parameters of the intensity I, and the expectation is taken with respect to the random counts. Intuitively, a sharper curvature means that a maximum-likelihood estimation algorithm is more likely to produce a low-variance estimator. Indeed, this property is captured by the Cramer-Rao lower bound, which states that the inverse of the Fisher Information is a lower

bound for the variance of any unbiased estimator, where an estimator f of the intensity I is unbiased if $\mathbf{E}f(\mathrm{y}) = I$.

The Fisher information provides a value, $F_\Phi(I)_{u,v}$, for each pair of voxels u and v. To provide a single measure for the reliability of the estimator, the average level, worst case, or other reasonable measure may be taken over the voxels. In the current example, the scoring function is based on the average Fisher information. Starting with a set of emittance models to be used by the estimating algorithm to provide a reliable estimator, the average of the above measure is maximized over the entire set, defining the selected set Φ^* as:

$$\Phi^* = \arg\max_\phi \sum_{I \in \boldsymbol{I}} \sum_{u \in U} \left[F_\Phi(I)\right]_{u,u} \qquad (18)$$

Alternately, a set may be chosen to minimize the inverse of the Fisher information, by selecting for:

$$\Phi^* = \arg\min_\phi \sum_{I \in \boldsymbol{I}} \sum_{u \in U} \left[F_\Phi(I)^{-1}\right]_{u,u} \qquad (19)$$

Since inverting $F_\Phi(I)$ may be computationally expensive, the $\left[F_\Phi(I)^{-1}\right]_{u,u}$ term in Equation 19 may be replaced with $1/[F_\Phi(I)]_{u,u}$ (thus neglecting the off-diagonal elements of the Fisher Information matrix $F_\Phi(I)$). Note that Equations 18 and 19 are not mathematically equivalent, and may therefore yield different selected sets.

In the preferred embodiment, scoring is performed using the reliability criterion, and two or more emittance models are provided, having substantially identical volumes, but different modeled organ targets. Substantially identical sets of views are formed for all the emittance models, and each set is scored for reliability. One of the sets of views is then selected based on the average score for all the of the emittance models.

In a fourth preferred embodiment, a weighted combination of several information theoretic measures is used. For example, a plurality of models may be provided, all having substantially identical dimensions and volumes, as follows:

i. a first model, free of radioactive emission sources, as seen in Figure 7g, for scoring sets of views in terms of uniformity;

ii. a pair of models with slightly different distributions of radioactive emission sources, as seen in Figures 7h and 7i, for scoring sets of views in terms of separability;

iii. a model with a given distribution of radioactive emission sources, as seen in any one of Figures 7h, 7i or 7j, for scoring sets of views in terms of reliability.

Identical sets of views may be applied to all the models, and each view may be scored in terms of uniformity, separability, and reliability. An optimal set of views may be selected based on a summation of the three scores, or based on a weighted average of the three scores, where the relative weight given to each criterion reflects the relative importance of each measure per the given application.

The scoring function is preferably defined in accordance with one of the following: worst case effectiveness for the given view over the volume, average effectiveness for the given view over the volume, worst case effectiveness for the given view over the set of emittance models and average effectiveness for the given view over the set of emittance models.

As discussed above, selecting the best set of size N from amongst a large set of candidate projections is computationally complex. Since the size of the collection of views and of the required set may be large, a brute force scheme might not be computationally feasible.

In an additional preferred embodiment, a so-called "greedy algorithm" is used to incrementally construct larger and larger sets, until a set containing the required number of views is obtained. The algorithm starts with an initial set, and in each iteration adds the view that yields the maximum improvement of the set score (hence the name "greedy").

In theoretical terms, assume $\rho(\cdot)$ is the quality measure we are using for the view selection, and assume without loss of generality that we are trying to maximize this measure. We gradually build a set W of projections as follows. We start with an empty set $W = \varnothing$, and at every stage choose the projection that maximizes the quality measure when added to the current set:

$$W \leftarrow \arg\max_{W'} \{\rho(W') \mid W' = W \cup \{\phi\}, \phi \in \Phi\} \quad (21)$$

In other words, during a given iteration, a respective score is calculated for a combination of the previous set with each of the views which is not a member of the current set. The current set is then expanded by adding the view which yielded the highest respective score, and the expanded current set serves as the input to the following iteration. Thus the number of times the scoring function is calculated per iteration drops from iteration to iteration. For a large initial collection of views, the greedy algorithm reduces the total number of computations required for set selection.

Reference is now made to Fig. 8, which is a simplified flowchart of an iterative "greedy" method for selecting a set of views, according to a preferred embodiment of the present invention. In step 800 an initial set of views is established from the collection of views. In the preferred embodiment, the initial set is an empty set. In step 810 the view set is incrementally increased by a single view during each iteration, until a set containing the required number of views has been selected.

Reference is now made to Fig. 9, which is a simplified flowchart of a single iteration of the view selection method of Fig. 8, according to a preferred embodiment of the present invention. The method of Fig. 9 expands the current set of views by a single view. The method begins with a current set of views, which is the initial set (step 800 above) for the first iteration, or the set formed at the end of the previous iteration (step 920 below) for all subsequent iterations. In step 900, a respective expanded set is formed for each view not yet in the current set of views. A given view's expanded set contains all the views of the current set as well as the given view. In step 910, a respective score is calculated for each of the expanded sets using the scoring function. Finally, in step 920, the current set is equated to the highest-scoring expanded set by adding the appropriate view to the current set. The newly formed current set serves as an input to the subsequent iteration, until the desired number of views is attained.

Following is a further preferred embodiment of a view selection method, in which multiple view sets are first formed from one or more scoring functions, and then a final selection is made of one of the resulting sets.

Reference is now made to Fig. 10, which is a simplified flowchart of a method for selecting a set of optimal views of a volume to be imaged, according to a third preferred embodiment of the present invention. In step 1000, a volume to be imaged is provided. The volume preferably corresponds to a body structure. In step 1010, a collection of views for performing radiation detection of a volume is provided. Each of the views is associated with at least one viewing parameter. Preferably the viewing parameters consist of at least one the following: detector location, detector orientation, viewing angle, material, thickness, collimator length, septa thickness, cell size, detection duration, time of detection, and a type of radiopharmaceutical.

In step 1020 at least one scoring function is provided. Each scoring functions is for scoring sets of views, essentially as described above. As discussed above, a single scoring function may be used to select several sets of views, where each set of views contains a different number of views.

In step 1030, multiple sets of views are formed from the collection of views, using the scoring function(s) provided in step 1020. In a first preferred embodiment, each of the sets is formed using a different one of the scoring functions. In an alternate preferred embodiment, one or more of the scoring functions are used to form more than one set of views, where sets formed with the same scoring function have differing numbers of views.

In step 1040, a selected set of views is obtained from the sets formed in step 1030. Knowledge about the conditions under which a particular set of measurements will be taken may be used to determine the optimal final set of views for a given data collection scenario.

In a first preferred embodiment, the final set of views is obtained by choosing one of the sets formed in step 1030 using a set selection criterion. For example, a respective set is formed in step 1030 for each of the uniformity, separability, and reliability criteria independently. A set selection criterion which calculates an overall performance rating for a given set taking all three criteria into account is defined, and the formed set with the highest overall rating is selected as the final set.

In another preferred embodiment, the selected set of views is obtained by merging the sets formed in step 1030 according to the relative importance of the respective scoring function used to form each set.

In the preferred embodiment, the method further consists of providing at least one emittance model representing the radioactive-emission density distribution of the volume, and scoring with at least one of the scoring functions of step 1020 is performed in relation to the emittance models. Preferably the emittance model(s) represent a body structure.

As discussed above, since each view is associated with one or more parameters, the selected set yields a group of optimal parameter values for performing effective detection of the intensity distribution of a volume. For example, if each view is associated with a view location parameter the selected set defines a set of locations for collecting emission data from an object, in order to provide a high-quality reconstruction of the intensity distribution of the object.

Reference is now made to Fig. 11, which is a simplified block diagram of a set selector for selecting a set of optimal views of a volume to be imaged, according to a first preferred embodiment of the present invention. Set selector 1100 consists of volume provider 1110, view provider 1120, scoring function provider 1130, and set selector 1140. Volume provider 1110 provides the volume to be imaged. View provider 1120 provides a collection of views of the volume to be imaged, where each of the views is associated with at least one viewing parameter. Scoring function provider 1130 provides a scoring function, which can score any set of view(s) from the collection with a score that rates information obtained from the volume by the set. Set selector 1140 utilizes the volume, views, and scoring functions to select a set from the collection.

Preferably, set selector 1100 further contains projection calculator 1150 which calculates a detection probability distribution for each of the views, in accordance with the respective viewing parameters and a volume attenuation coefficient.

Reference is now made to Fig. 12, which is a simplified block diagram of a set selector for selecting a set of optimal views of a volume to be imaged, according to a second preferred embodiment of the present invention. Set selector 1200 consists of volume provider 1210, view provider 1220, scoring functions provider 1230, sets former 1240, and set chooser 1260. Volume provider 1210 provides the volume to be imaged. View provider 1220 provides a collection of views of the volume to be imaged, where each of the views is associated with at least one viewing parameter.

Scoring functions provider 1230 provides one or more scoring functions. Each of the scoring functions can be used to calculate a score for any set of view(s) from the collection. The calculated score rates the information obtained from the volume by the given set. Sets former 1240 uses the various scoring functions to form multiple sets of views from the collection of view, as discussed above for Fig. 10. Set obtainer 1260 obtains a final set of views from the sets of views formed by sets former 1240.

Preferably, set selector 1200 further contains projection calculator 1250 which calculates a detection probability distribution for each of the views, in accordance with the respective viewing parameters and a volume attenuation coefficient.

The abovedescribed set selection methods may each be embodied as a computer program stored on a computer-readable storage medium. In a first preferred embodiment, the computer-readable storage medium contains a set of instructions for selecting a set of optimal views of a volume to be imaged, consisting of the following routines. A volume provision routine provides the volume to be imaged. A view provision routine provides a collection of views of the volume to be imaged, each of the views being associated with at least one viewing parameter. A scoring function provision routine provides a scoring function, by which any set of at least one view from the collection is scorable with a score that rates information obtained from the volume by the set. The set formation routine forms sets of views from the collection of views, and scores them using the scoring function. The set selection routine selects a set of views from the collection of views, based on the scoring function.

In a second preferred embodiment, the computer-readable storage medium contains a set of instructions for selecting a set of optimal views of a volume to be imaged, consisting of the following routines. A volume provision routine provides the volume to be imaged. A view provision routine provides a collection of views of the volume to be imaged, each of the views being associated with at least one viewing parameter. A scoring functions provision routine provides at least one scoring function. Each of the scoring functions is usable to calculate a score for any set of at least one view taken from the collection of views. The score rates information obtained from the volume by the set of views. A sets formation routine selects multiple sets of the views using the scoring function(s), and a set obtaining routine obtains a final set of views from the sets formed by the sets formation routine.

It is expected that during the life of this patent many relevant detection probes, detector types, radiation-based detection systems and algorithms will be developed and the scope of the corresponding terms are intended to include all such new technologies *a priori*.

As used herein the term "about" refers to ± 10 %.

Additional objects, advantages, and novel features of the present invention will become apparent to one ordinarily skilled in the art upon examination of the following examples, which are not intended to be limiting. Additionally, each of the various embodiments and aspects of the present invention as delineated hereinabove and as claimed in the claims section below finds experimental support in the following examples.

EXAMPLES

Reference is now made to the following examples, which together with the above descriptions, illustrate the invention in a non-limiting fashion.

Figs. 13-18 illustrate view set selection results for the uniformity criterion. The selected views are chosen from a collection of views using an entropy-based scoring function. The specified viewing parameters are the detector location and the detector type (having a given detector size, D, and collimator length, L). Each view is defined for one of three detector types, large (D=10, L=25), medium (D=5, L=12.5) or small (D=2.5, L=6.25).

Fig. 13 shows a selected set of 500 views. The location of each view in the XY surface is shown, along with the associated detector type. As expected, the selected views are distributed relatively evenly over the XY surface and over the three detector types shown.

Figs. 14a-14c show the resulting coverage provided by the selected views, from the top, side, and front aspects of the volume respectively. Even coverage is indicated by an even hue in the figure. Uniform coverage is well obtained for the side and front aspects, but is less successfully obtained for the top aspect.

Fig. 15 illustrates the distribution of the detector types as a function of the number of views in the set. The large detectors, with their high sensitivity but low resolution, predominate only for small selected sets. As the size of the selected set

increases the number of small detectors increases, improving the coverage of the collected data.

Figs. 16-18 show the value of the entropy measure, used for the uniformity criterion, for each of the detector types, as the number of views increases. For sets including up to 400 views, the large detector gives the highest entropy level (i.e. enables the most uniform coverage). However, for selected sets containing more than 400 views the highest entropy value is obtained with the small detector. This is in accordance with Fig. 15, which shows an increasing proportion of small detector views as the size of the selected set increases.

Figs. 19-24 illustrate view set selection results for the separability criterion. The viewing parameters include detector location, detector orientation, and one of three detector types, large (D=10, L=25), medium (D=5, L=12.5) or small (D=2.5, L=6.25).

Figs. 19-21 show selected sets containing 100 views having a single detector type, for large, medium, and small detectors respectively. Each view shows the detector location in the XY surface and the detector orientation (arrow), as seen from above where the shorter the arrow is the more downward it is pointing. The figures show that the selected set for the large detectors contains views which are mostly in the center of the XY surface and pointing directly in to the volume, whereas the selected set for the small detectors has the detectors located around the periphery of the volume and oriented at an angle towards the center of the volume.

Figs 22-24 show a selected set containing 1000 views selected for the separability criterion. The selected set includes views of all three detector types. The selected set contains 55 large-detector views (Fig. 22), 370 medium-detector views (Fig. 23), and 575 small-detector views. Similarly to Figs. 19-21, as the detectors decrease in size they are physically more dispersed over the XY surface.

Figs. 25-32 illustrate view set selection results for the reliability criterion, based on the Fisher information measure. The specified viewing parameters are the location (on the XY surface) and the detector type. Each view is defined for one of four detector types, large (D=10, L=25), medium (D=5, L=12.5), small (D=2.5, L=6.25), and extra-focused (D=5, L=25).

Figs. 25-29 show selected sets based on the Fisher information measure, containing 100, 200, 500, 1000, and 2000 views respectively. As can be seen, for a small number of views the detectors are distributed around the periphery of the volume. As the number of views in the selected set increases, the detector move towards the center of the XY surface. In generally the selected sets with a greater number of views contain a higher proportion of small detector views than do the selected sets with fewer views. In particular, it is seen in Fig. 29 that the large detectors are concentrated in the center of the XY surface, while the smaller detectors are dispersed around the circumference.

Fig. 30 shows the detector coverage of a volume for selected sets containing 500, 1000, and 2000 views. The coverage is shown from the XY, YZ, and XZ aspects of the volume. It is seen from the figure that for a small number of views, the views are clustered around the exterior of the volume. As the number of views increases, an increasingly uniform distribution of views is achieved.

Figs. 31-32 show the number of detectors selected for each of the four detector types, as the total number of selected views is increased. The selected set is constrained to have no more than 3400 views of a single detector type. It can be seen that the detectors are selected in order of size, as the total number of selected views increases. It is only after the number of the large detector views nears 3400 that the number of medium detector views begins to increase significantly, and so forth. The Fisher information measure is thus seen to select for larger-sized detectors, in order to ensure high-reliability reconstructions from the collected data.

Figs. 33 illustrates view set selection results for the reliability criterion, based on minimizing the inverse mean of the Fisher information measure. In accordance with the Cramer-Rao lower bound, the inverse of the Fisher Information is a lower bound for the variance of the intensity *I*.

Fig. 33 shows the behavior of the Fisher inverse mean for the three detector types, large (D=10, L=25), medium (D=5, L=12.5), and small (D=2.5, L=6.25). The number of collimators is normalized for the collimator size, so that an effective detector number of 1600 is achieved with 100 large detectors, 400 medium detectors, or with 1600 small detectors. The Fisher inverse mean of the medium and small detectors is relatively close, with the large detector having a greater mean value.

Since our aim is to minimize the score, it is seen that the smaller detectors are more efficient in providing a low-variance estimation.

By enabling high-quality reconstruction based on data collected from a limited collection of views, the abovedescribed view set selection techniques present a way to resolve the current conflict between the relatively large-pixel detectors needed for measurement speed and data processing considerations, with the small-pixel detectors needed until now to obtain a high-resolution reconstruction. The data obtained using the selected set of views enables a high-resolution reconstruction from a smaller number of measurements. Additionally, reconstructing the intensity distribution from a smaller quantity of collected data simplifies the computational process. The abovedescribed embodiments are particularly suitable for medical imaging purposes, where a high-resolution image is needed and it is desired to minimize the difficulties of the patient undergoing the diagnostic testing or treatment.

Radioactive emission imaging, in accordance with the present invention may be performed with a radioactive-emission-measuring detector, such as a room temperature, solid-state CdZnTe (CZT) detector. It may be configured as a single-pixel or a multi-pixel detector, and may be obtained, for example, from eV Products, a division of II-VI Corporation, Saxonburg Pa., 16056, or from IMARAD IMAGING SYSTEMS LTD., of Rehovot, ISRAEL, 76124, www.imarad.com, or from another source. Alternatively, another solid-state detector such as CdTe, HgI, Si, Ge, or the like, or a combination of a scintillation detector (such as NaI(Tl), LSO, GSO, CsI, CaF, or the like) and a photomultiplier, or another detector as known, may be used.

It is appreciated that certain features of the invention, which are, for clarity, described in the context of separate embodiments, may also be provided in combination in a single embodiment. Conversely, various features of the invention, which are, for brevity, described in the context of a single embodiment, may also be provided separately or in any suitable subcombination.

Although the invention has been described in conjunction with specific embodiments thereof, it is evident that many alternatives, modifications and variations will be apparent to those skilled in the art. Accordingly, it is intended to embrace all

such alternatives, modifications and variations that fall within the spirit and broad scope of the appended claims. All publications, patents and patent applications mentioned in this specification are herein incorporated in their entirety by reference into the specification, to the same extent as if each individual publication, patent or patent application was specifically and individually indicated to be incorporated herein by reference. In addition, citation or identification of any reference in this application shall not be construed as an admission that such reference is available as prior art to the present invention.

WHAT IS CLAIMED IS:

1. A method for selecting a set of optimal views of a volume to be imaged, comprising:

providing said volume to be imaged;

providing a collection of views of said volume to be imaged;

providing a scoring function, by which any set of at least one view from said collection is scorable with a score that rates information obtained from said volume by said set;

forming sets of views and scoring them, by said scoring function; and

selecting a set of views from said collection, based on said scoring function.

2. The method of claim 1, wherein each of said views is associated with viewing parameters comprising a detector location and orientation.

3. The method of claim 1, wherein each of said views is associated with viewing parameters selected from the group consisting of: detector material, detector thickness, septa thickness, and collection angle.

4. The method of claim 1, wherein each of said views is associated with viewing parameters selected from the group consisting: of measurement duration, time elapsed from the administration of the pharmaceutical to the measurement, radiopharmaceutical half life, radioactive emission type, and radioactive emission energy.

5. The method of claim 4, further comprising calculating for each of said views a respective detection probability distribution of said volume for each of said views, in accordance with respective viewing parameters and a volume attenuation coefficient.

6. The method of claim 5, wherein said volume attenuation coefficient varies over said volume.

7. The method of claim 1, wherein said selecting is to obtain a minimal-size set which attains a predefined score.

8. The method of claim 1, wherein said selecting is to obtain a highest scoring set having a predefined number of views.

9. The method of claim 1, wherein said collection of views comprises a quantized continuum of views.

10. The method of claim 1, wherein said scoring function comprises an information-theoretic entropy measure, for ensuring uniform coverage of said volume.

11. The method of claim 1, wherein said scoring function comprises a worst-case effectiveness for said given view over said volume.

12. The method of claim 1, wherein said scoring function comprises an average effectiveness for said given view over said volume.

13. The method of claim 1, further comprising providing at least one emittance model, wherein an emittance model comprises a representation of a radioactive-emission density distribution of said volume.

14. The method of claim 13, wherein said providing at least one emittance model includes modeling a radioactive-emission density distribution to form at least one modeled organ target.

15. The method of claim 13, wherein said scoring function comprises an information-theoretic Fisher information measure, for ensuring reliable reconstruction of a radioactive-emission density distribution.

16. The method of claim 13, wherein:

said providing at least one emittance model comprises providing a plurality of emittance models of substantially identical volumes, but different modeled organ targets.

the forming sets of views from the collection of views and scoring them, comprises forming substantially identical sets of views for all the models and scoring the sets with respect to each model, based on the information theoretic measure of reliability; and

the selecting one of the sets of views, based on its score, comprises selecting based on the average score for the plurality of models.

17. The method of claim 13, wherein said scoring function comprises an information-theoretic likelihood measure, for ensuring separable reconstructions of said emittance models.

18. The method of claim 13, wherein:

said providing at least one emittance model comprises providing a pair of models of substantially identical volumes, but different modeled organ targets, wherein the difference between the modeled organ targets is defined by at least one delta;

the scoring function is based on an information theoretic measure of separability;

the forming the sets of views from the collection of views and scoring them, comprises forming substantially identical sets of views for the pair of models and scoring the sets with respect to the pair; and

the selecting one of the sets of views, based on its score, comprises selecting based on the score for the pair.

19. The method of claim 13, wherein:

said providing at least one emittance model comprises providing a plurality of pairs of models of substantially identical volumes, but different modeled organ targets, wherein the difference between the modeled organ targets for each pair is defined by at least one delta;

the scoring function is based on an information theoretic measure of separability;

the forming the sets of views from the collection of views and scoring them, comprises forming substantially identical sets of views for the plurality of pairs of models and scoring the sets with respect to each of the pairs; and

the selecting one of the sets of views, based on its score, comprises selecting based on an average score for the plurality of pairs.

20. The method of claim 13, wherein:

the modeling the body-structure comprises providing at least one model of no radiation emission density distribution and at least two models of different radiation emission density distributions, so as to form different modeled organ targets for those two models; and

the providing the scoring function comprises providing a scoring function as a combination of uniformity, separability and reliability.

21. The method of claim 13, wherein said scoring function comprises a worst-case effectiveness for said given view over said set of emittance models.

22. The method of claim 13, wherein said scoring function comprises an average effectiveness for said given view over said set of emittance models.

23. The method of claim 13, wherein said set of emittance models comprises a single emittance model.

24. The method of claim 13, wherein said at least one emittance model corresponds to a body structure.

25. The method of claim 24, wherein said body structure comprises one of a group of body structures comprising: a prostate, a heart, a brain, a breast, a uterus, an ovary, a liver, a kidney, a stomach, a colon, a small intestine, an oral cavity, a throat, a

gland, a lymph node, the skin, another body organ, a limb, a bone, another part of the body, and a whole body.

26. The method of claim 1, wherein said selecting comprises:

initially establishing a current set of views from said collection of views; and

iteratively expanding said current set until a predefined number of views are obtained, wherein a set expansion iteration comprises:

forming a respective expanded set for each view not in said current set, wherein an expanded set comprises said current set and a respective view;

calculating a respective score for each of said expanded sets using said scoring function; and

equating said current set equal to a highest-scoring expanded set.

27. The method of claim 26, wherein said initially established current set is an empty set.

28. A method for selecting a set of optimal views of a volume to be imaged, comprising:

providing said volume to be imaged;

providing a collection of views of said volume to be imaged;

providing at least one scoring function, wherein a scoring function is for scoring any set of at least one view from said collection is scorable with a score that rates information obtained from said volume by said set;

using said scoring functions to form a plurality of selected sets of said views; and

obtaining a final set of views from said formed sets.

29. A set selector for selecting a set of optimal views of a volume to be imaged, comprising:

a volume provider, for providing said volume to be imaged;

a view provider, for providing a collection of views of said volume to be imaged;

a scoring function provider, for providing a scoring function, by which any set of at least one view from said collection is scorable with a score that rates information obtained from said volume by said set; and

a set selector associated with said volume provider, said view provider, and said scoring function provider, for selecting a set from said collection, based on said scoring function.

30. A set selector for selecting a set of optimal views of a volume to be imaged, comprising:

a volume provider, for providing said volume to be imaged;

a view provider, for providing a collection of views for performing radiation detection of said volume;

a scoring functions provider, for providing at least one scoring function, wherein a scoring function is for scoring any set of at least one view from said collection is scorable with a score that rates information obtained from said volume by said set;

a sets former associated with said view provider, for using said scoring functions to select a plurality of sets; and

a set obtainer associated with said set former, for obtaining a final set of views from said formed sets.

31. A computer-readable storage medium containing a set of instructions for selecting a set of optimal views of a volume to be imaged, the set of instructions comprising:

a volume provision routine for providing said volume to be imaged;

a view provision routine for providing a collection of views of said volume to be imaged;

a scoring function provision routine for providing a scoring function, by which any set of at least one view from said collection is scorable with a score that rates information obtained from said volume by said set;

a set formation routine, for forming sets of views and scoring them, by said scoring function; and

a set selection routine selecting a set from said collection, based on said scoring function.

32. A computer-readable storage medium containing a set of instructions for selecting a set of optimal views of a volume to be imaged, the set of instructions comprising:

a volume provision routine for providing said volume to be imaged;

a view provision routine for providing a collection of views of said volume to be imaged;

a scoring functions provision routine for providing at least one scoring function, wherein any set of at least one view from said collection is scorable by any of said scoring functions with a score that rates information obtained from said volume by said set;

a sets formation routine for selecting a plurality of sets of said views using at least one scoring function; and

a set obtaining routine for obtaining a final set of views from said formed sets.

33. A method for selecting a set of optimal views of a volume to be imaged, comprising:

providing said volume to be imaged;

providing a collection of views of said volume to be imaged;

providing an evaluator, by which any set of at least one view from said collection is evaluated so as to rate information obtained from said volume by said set;

forming sets of views and performing an evaluation on them, by said evaluator; and

selecting a set of views from said collection, based on said evaluation.

34. A method for selecting a set of optimal views of a volume to be imaged, comprising:

providing said volume to be imaged;

providing a collection of views of said volume to be imaged;

providing at least one evaluator, wherein an evaluator is for scoring any set of at least one view from said collection is evaluated so as to rate information obtained from said volume by said set;

using said evaluators to form a plurality of selected sets of said views; and

obtaining a final set of views from said formed sets.

35. A set selector for selecting a set of optimal views of a volume to be imaged, comprising:

a volume provider, for providing said volume to be imaged;

a view provider, for providing a collection of views of said volume to be imaged;

an evaluator provider, for providing an evaluator, by which any set of at least one view from said collection is evaluated so as to rate information obtained from said volume by said set; and

a set selector associated with said volume provider, said view provider, and said evaluator provider, for selecting a set from said collection, based on said evaluator.

36. A set selector for selecting a set of optimal views of a volume to be imaged, comprising:

a volume provider, for providing said volume to be imaged;

a view provider, for providing a collection of views for performing radiation detection of said volume;

an evaluators provider, for providing at least one scoring function, wherein an evaluator is for scoring any set of at least one view from said collection is evaluated so as to rate information obtained from said volume by said set;

a sets former associated with said view provider, for using said evaluators to select a plurality of sets; and

a set obtainer associated with said set former, for obtaining a final set of views from said formed sets.

37. A computer system, configured for selecting a set of optimal views of a volume to be imaged, comprising:

providing said volume to be imaged;

providing a collection of views of said volume to be imaged;

providing a scoring function, by which any set of at least one view from said collection is scorable with a score that rates information obtained from said volume by said set;

forming sets of views and scoring them, by said scoring function; and

selecting a set of views from said collection, based on said scoring function.

38. A computer system, configured for selecting a set of optimal views of a volume to be imaged, comprising:

providing said volume to be imaged;

providing a collection of views of said volume to be imaged;

providing at least one scoring function, wherein a scoring function is for scoring any set of at least one view from said collection is scorable with a score that rates information obtained from said volume by said set;

using said scoring functions to form a plurality of selected sets of said views; and

obtaining a final set of views from said formed sets.

39. A computer system, configured for selecting a set of optimal views of a volume to be imaged, comprising:

providing said volume to be imaged;

providing a collection of views of said volume to be imaged;

providing an evaluator, by which any set of at least one view from said collection is evaluated so as to rate information obtained from said volume by said set;

forming sets of views and performing an evaluation on them, by said evaluator; and

selecting a set of views from said collection, based on said evaluation.

40. A computer system, configured for selecting a set of optimal views of a volume to be imaged, comprising:

providing said volume to be imaged;

providing a collection of views of said volume to be imaged;

providing at least one evaluator, wherein an evaluator is for scoring any set of at least one view from said collection is evaluated so as to rate information obtained from said volume by said set;

using said evaluators to form a plurality of selected sets of said views; and

obtaining a final set of views from said formed sets.

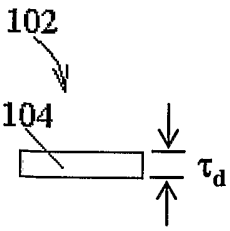

Figure 1a

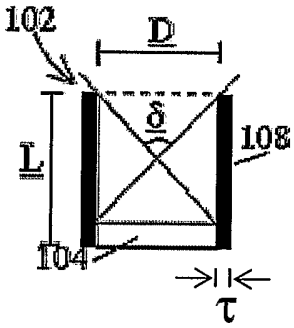

Figure 1b

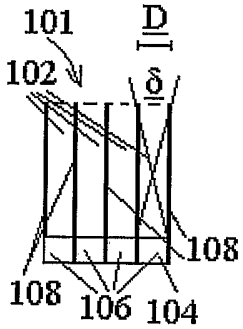

Figure 1c

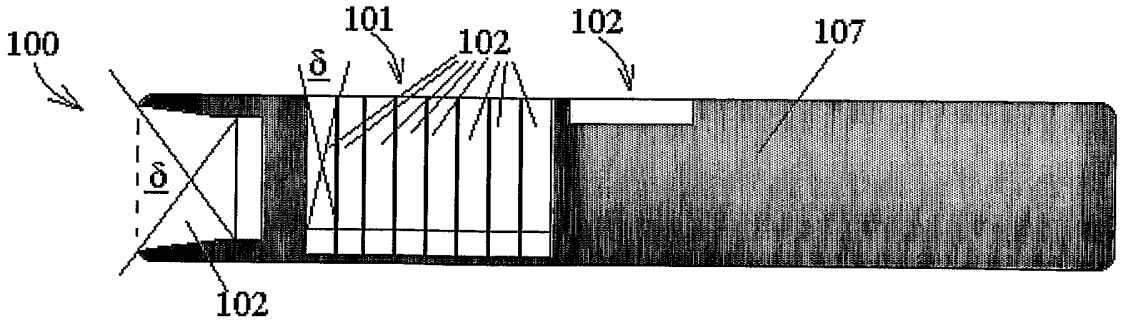

Figure 1d

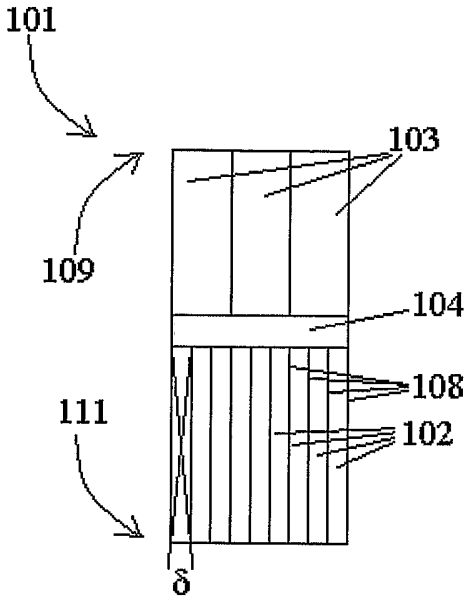

Figure 1e

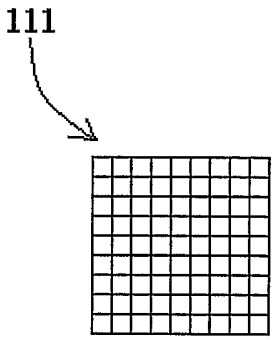

Figure 1f

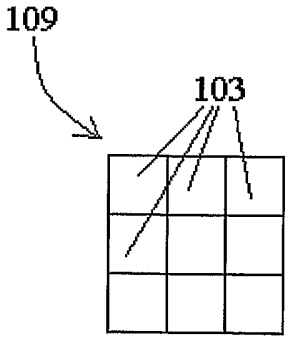

Figure 1g

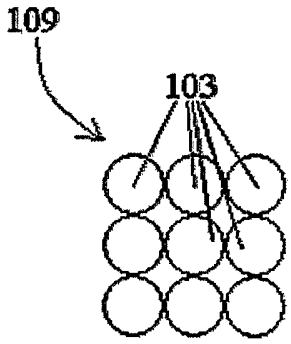

Figure 1h

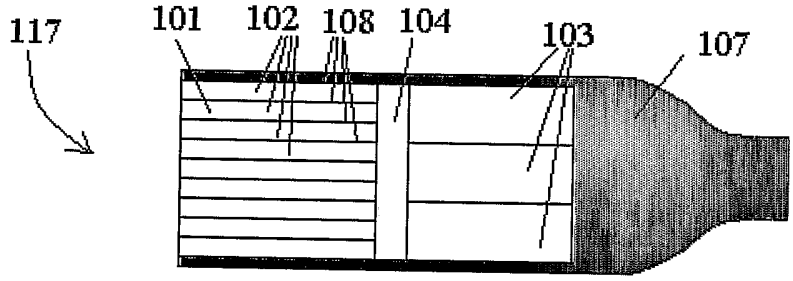

Figure 1i

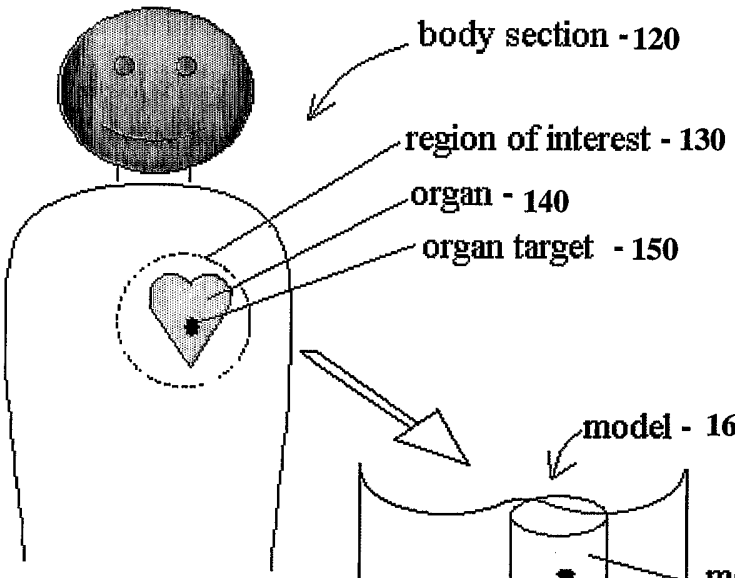

Figure 1j

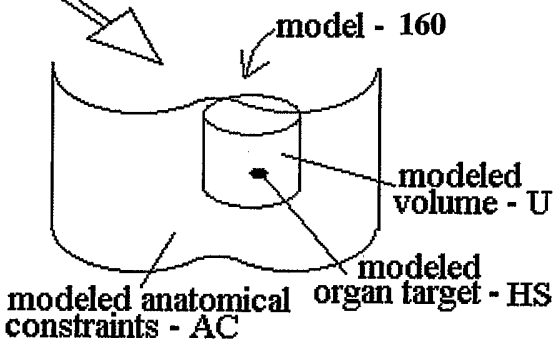

Figure 1k

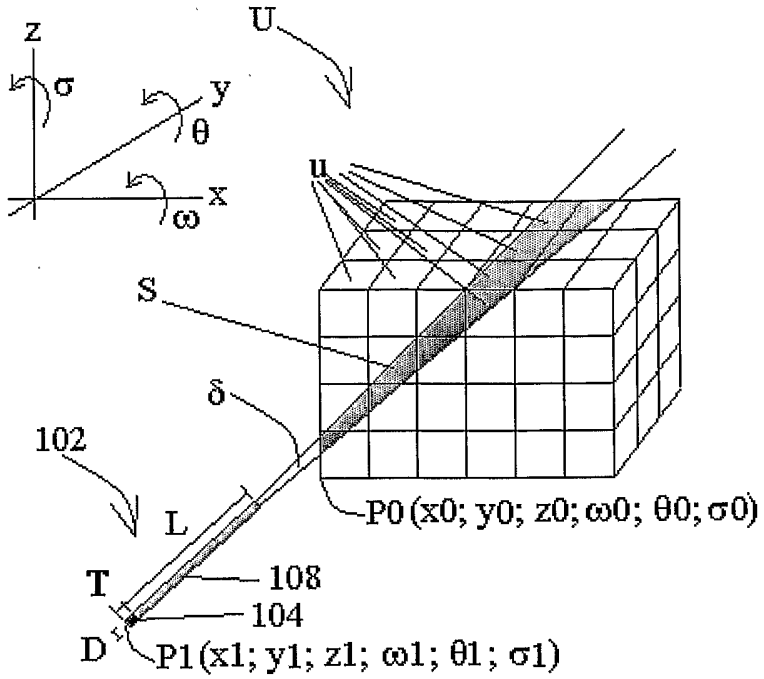

Figure 1l

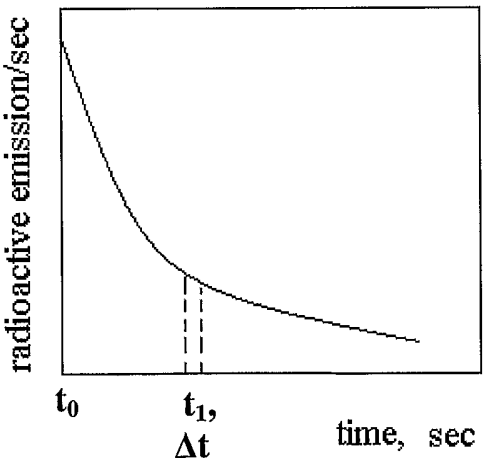

Figure 1m

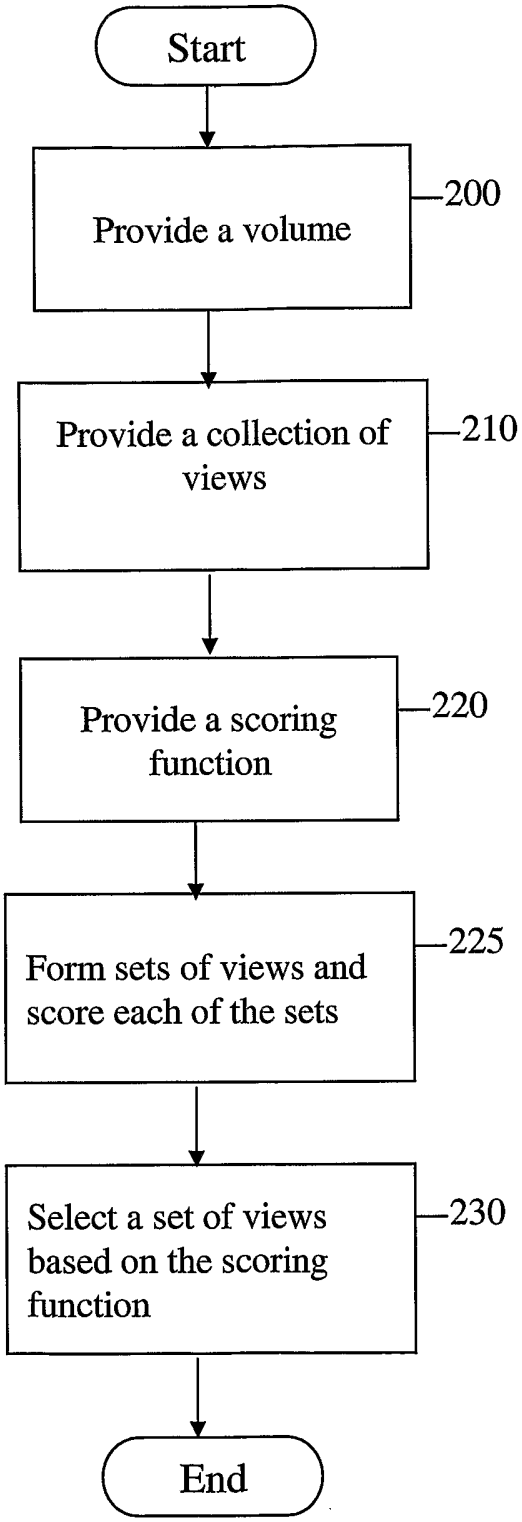
Start
Provide a volume
200
Provide a collection of views
210
Provide a scoring function
220
Form sets of views and score each of the sets
225
Select a set of views based on the scoring function
230
End

Figure 2

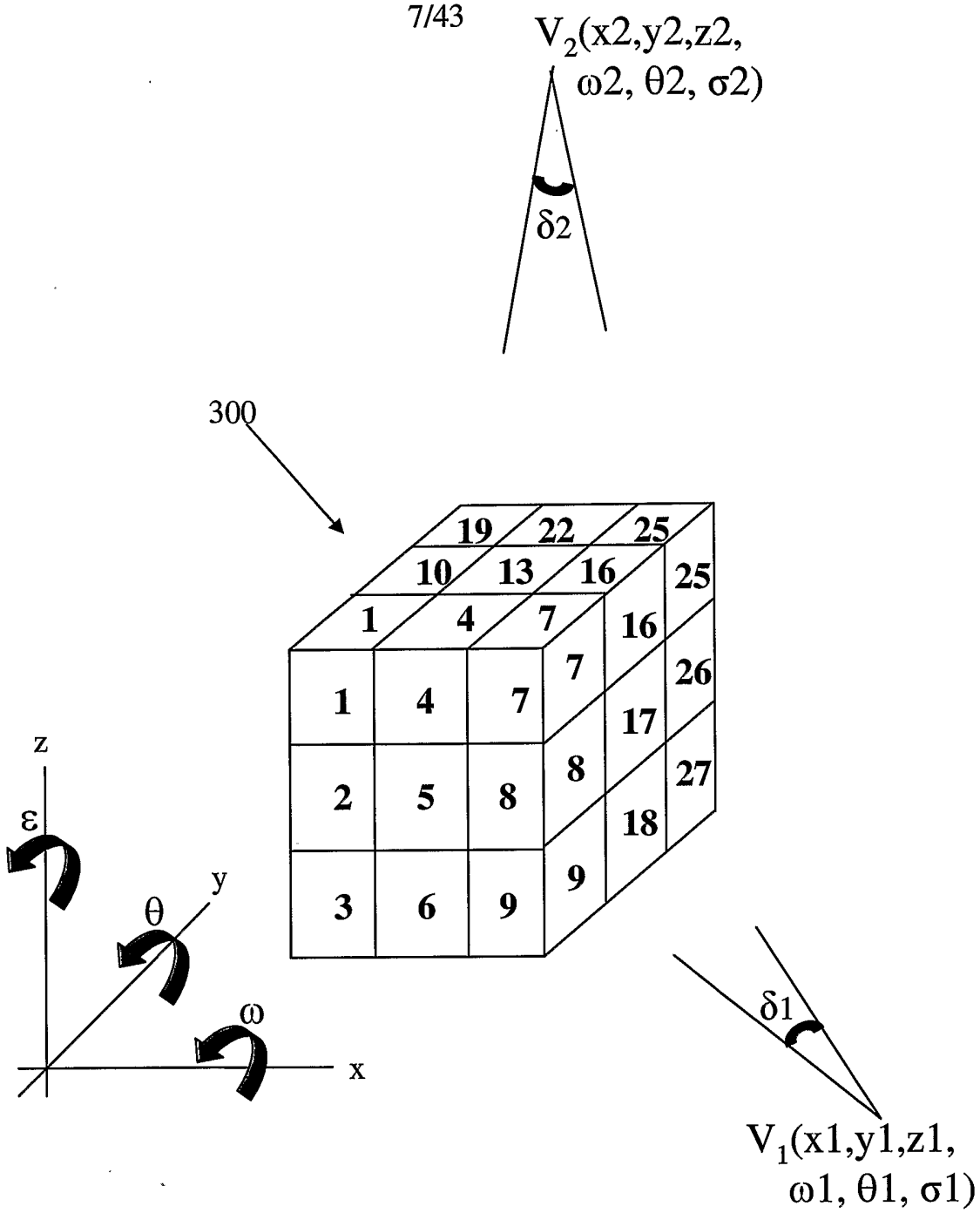
V2(x2,y2,z2,
ω2, θ2, σ2)
δ2
300
19 22 25
10 13 16 25
1 4 7 16
7 26
1 4 7 17
8 27
2 5 8 18
9
3 6 9
z
ε
y
θ
ω
x
δ1
V1(x1,y1,z1,
ω1, θ1, σ1)

Figure 3

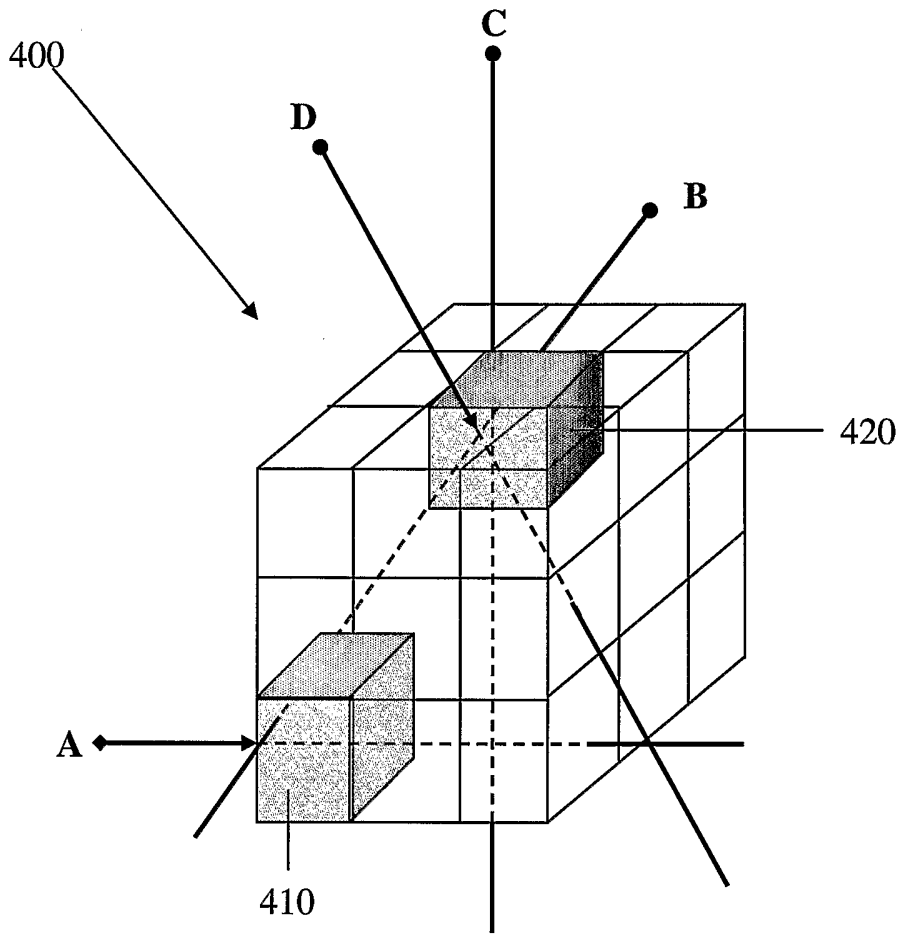

Figure 4

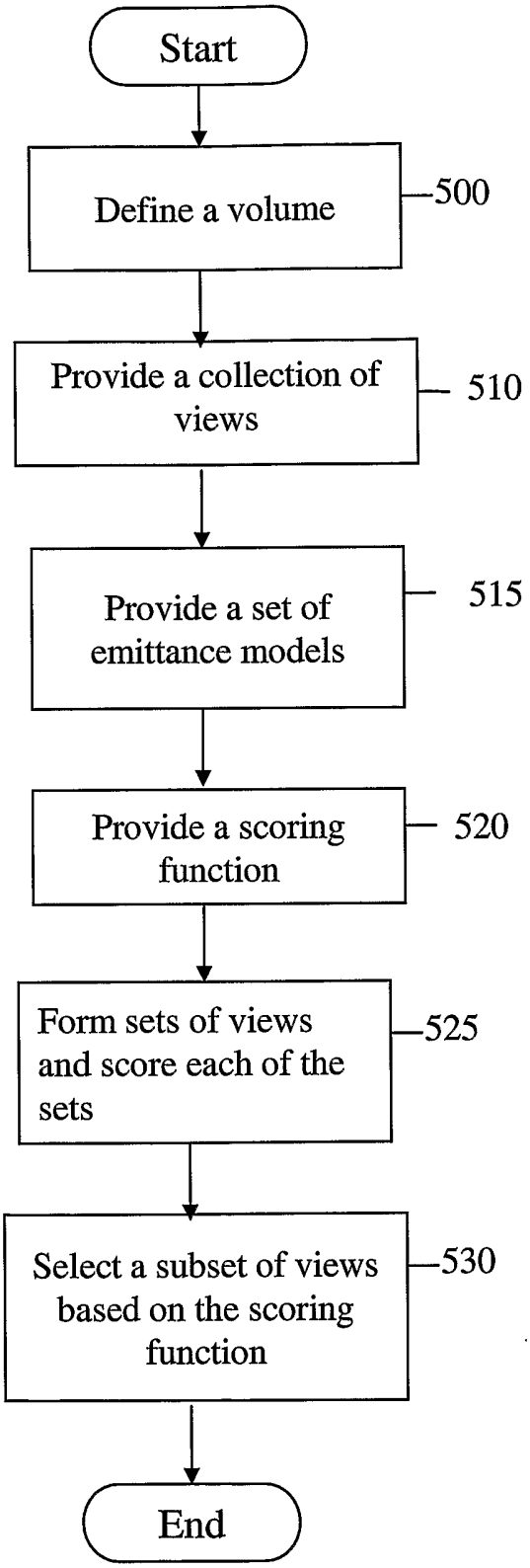
Start
Define a volume
500
Provide a collection of views
510
Provide a set of emittance models
515
Provide a scoring function
520
Form sets of views and score each of the sets
525
Select a subset of views based on the scoring function
530
End

Figure 5

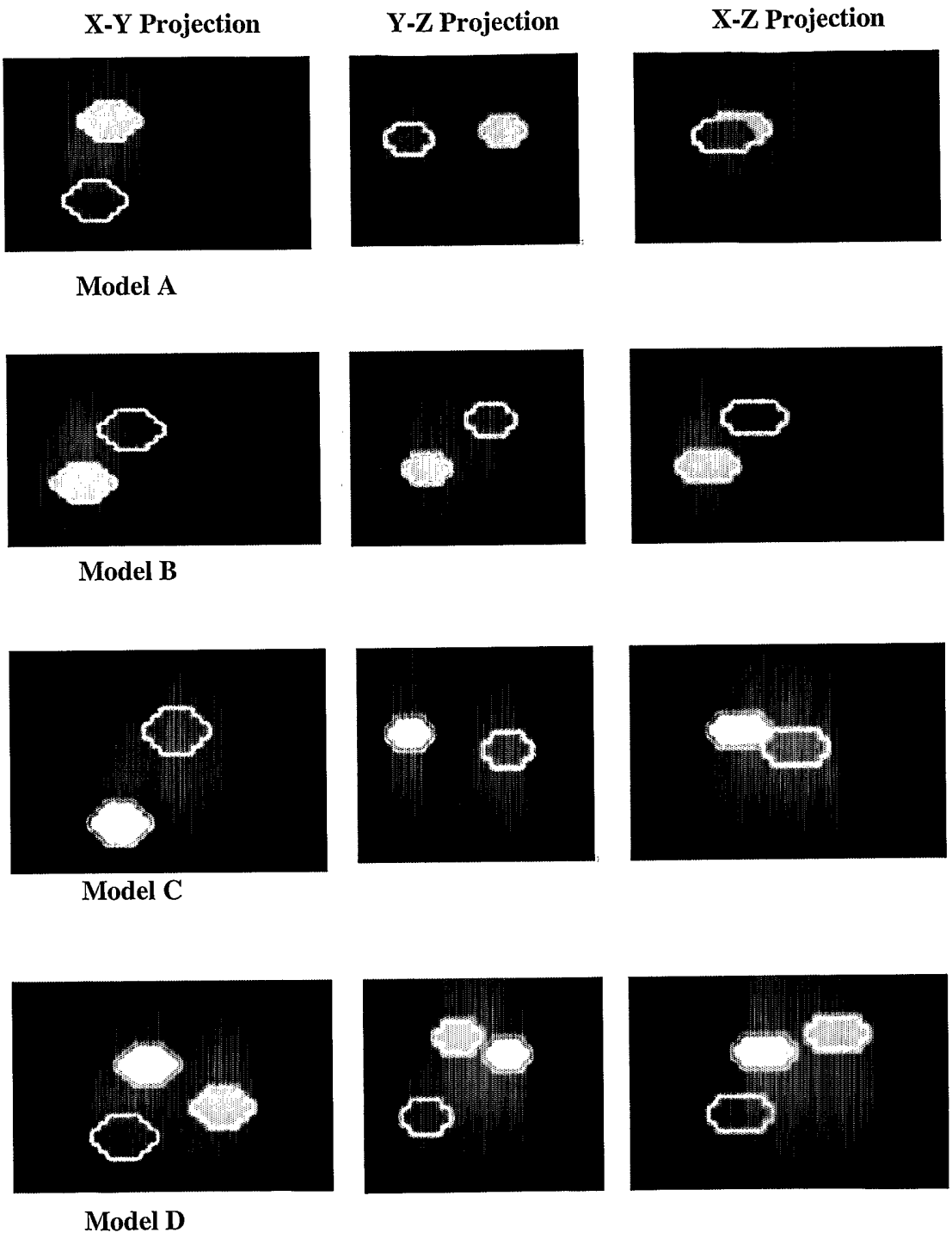
X-Y Projection
Y-Z Projection
X-Z Projection
Model A
Model B
Model C
Model D

Figure 6

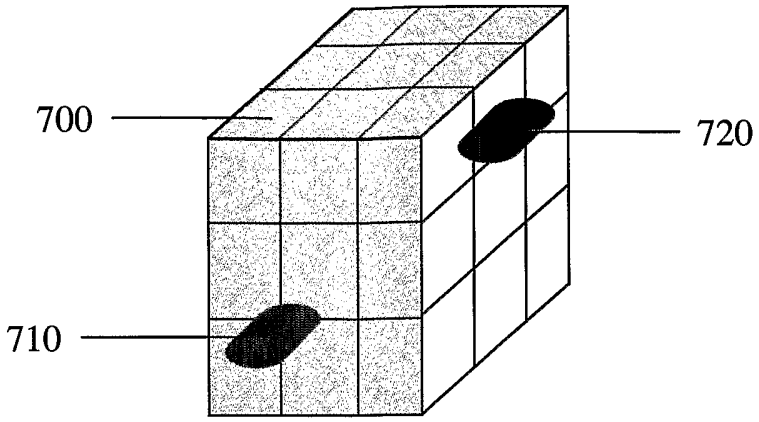

Figure 7a

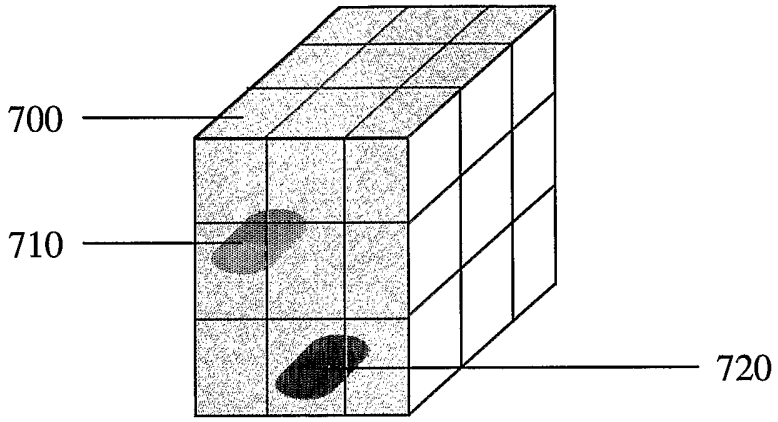

Figure 7b

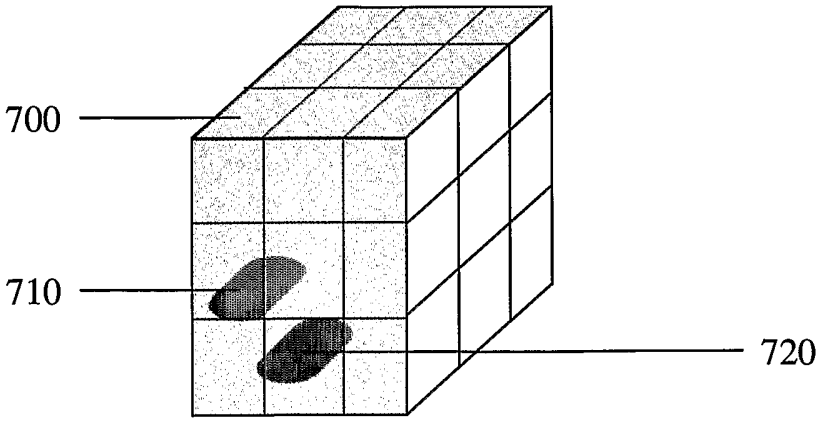

Figure 7c

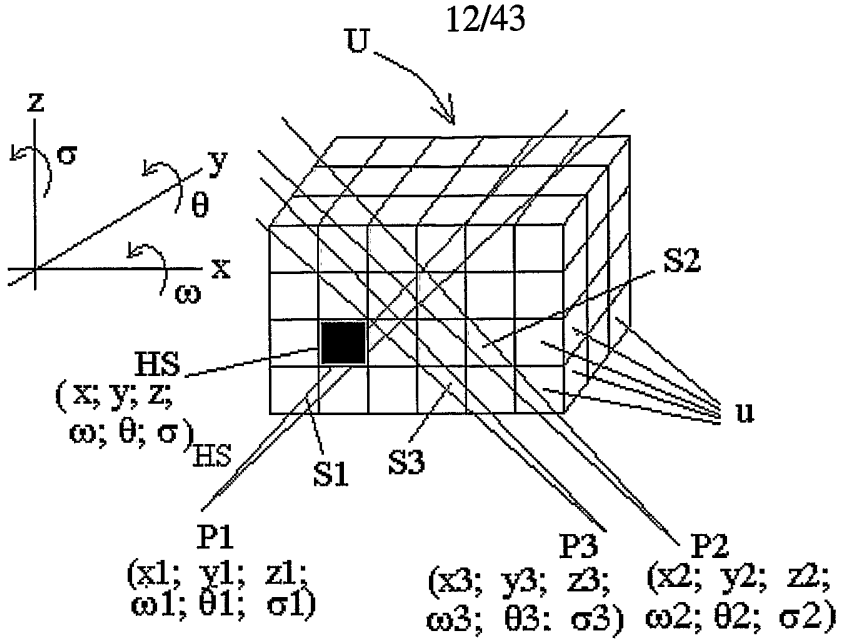

Figure 7d

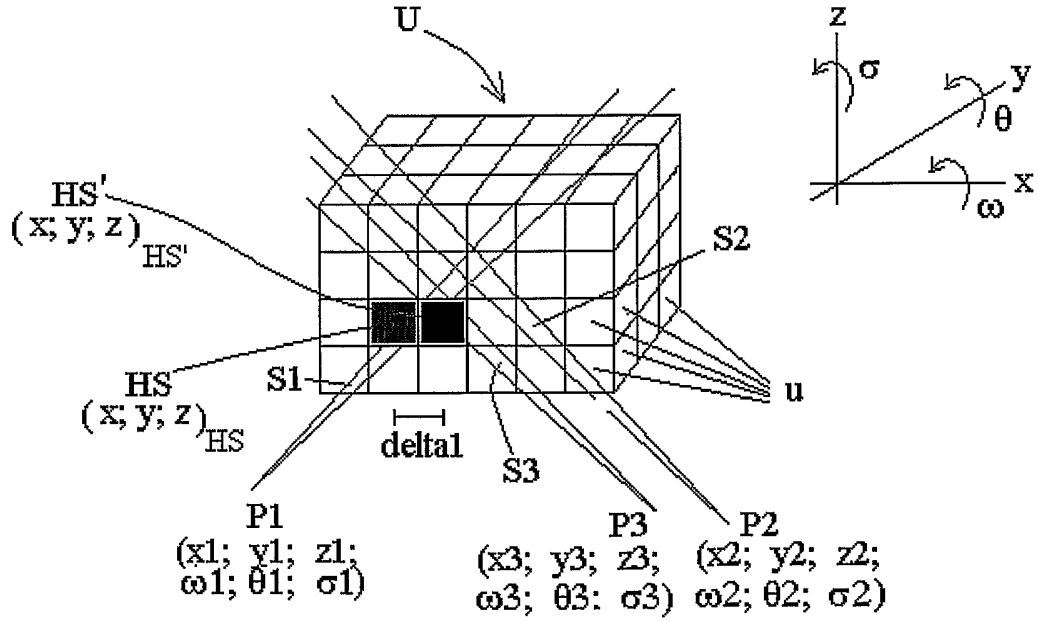

Figure 7e

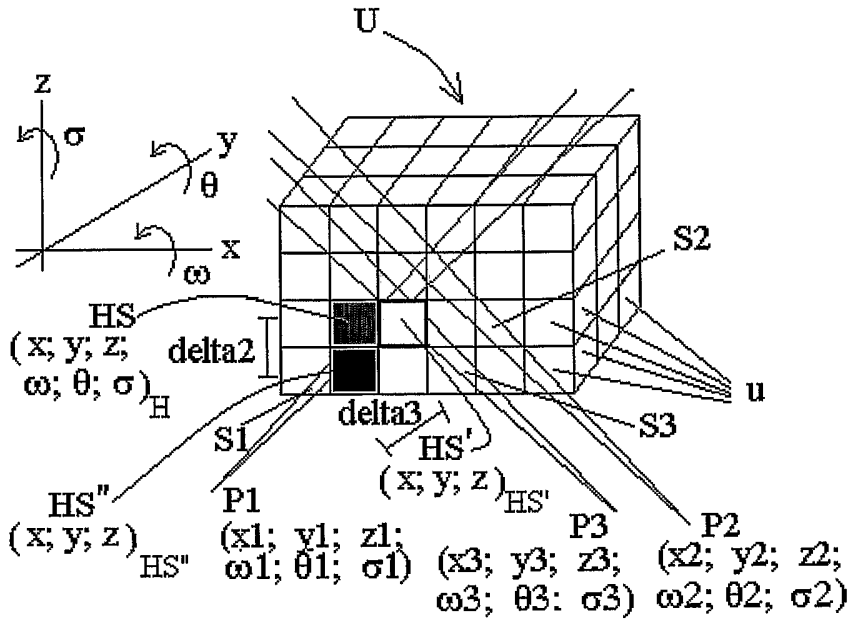
U
z
σ
y
θ
x
ω
HS
(x; y; z;
ω; θ; σ)H
delta2
S2
u
delta3
S1
HS'
(x; y; z)HS'
S3
HS"
(x; y; z)HS"
P1
(x1; y1; z1;
ω1; θ1; σ1)
P3
(x3; y3; z3;
ω3; θ3: σ3)
P2
(x2; y2; z2;
ω2; θ2; σ2)

Figure 7f

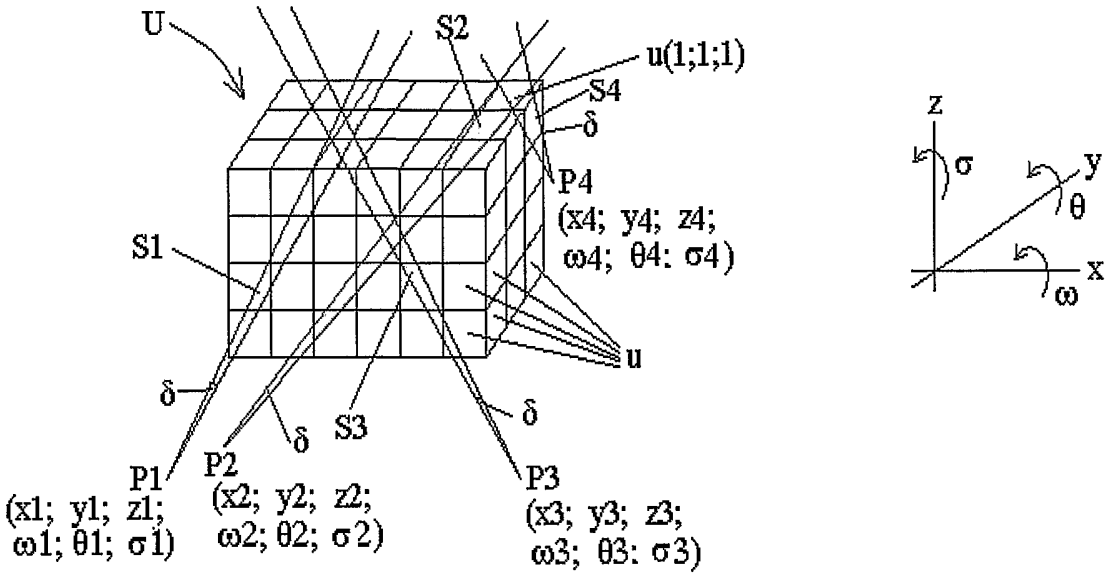
U
S2
u(1;1;1)
S4
δ
P4
(x4; y4; z4;
ω4; θ4: σ4)
S1
u
δ
δ
S3
δ
P1
(x1; y1; z1;
ω1; θ1; σ1)
P2
(x2; y2; z2;
ω2; θ2; σ2)
P3
(x3; y3; z3;
ω3; θ3: σ3)
z
σ
y
θ
x
ω

Figure 7g

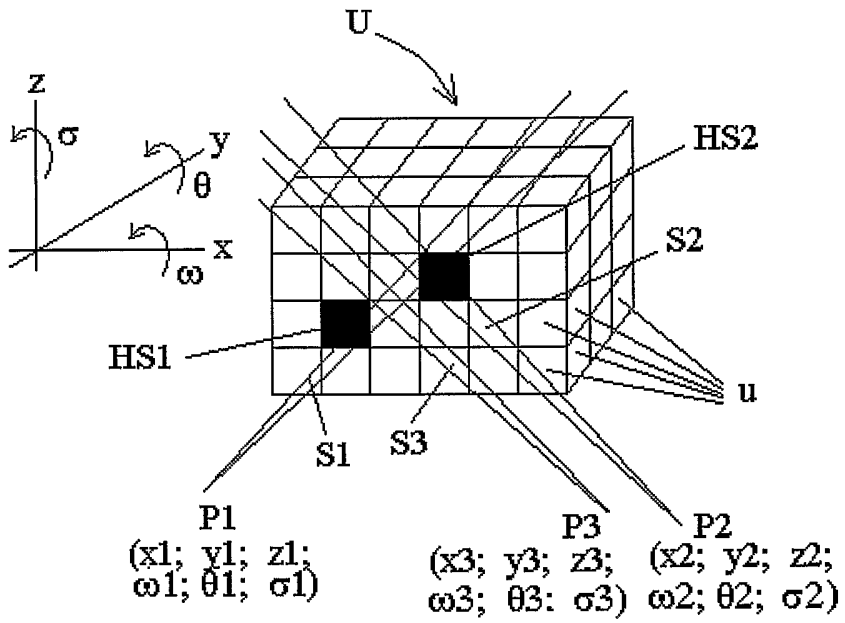
U
z
σ
y
θ
x
ω
HS2
S2
HS1
u
S1
S3
P1
(x1; y1; z1;
ω1; θ1; σ1)
P3
(x3; y3; z3;
ω3; θ3: σ3)
P2
(x2; y2; z2;
ω2; θ2; σ2)

Figure 7h

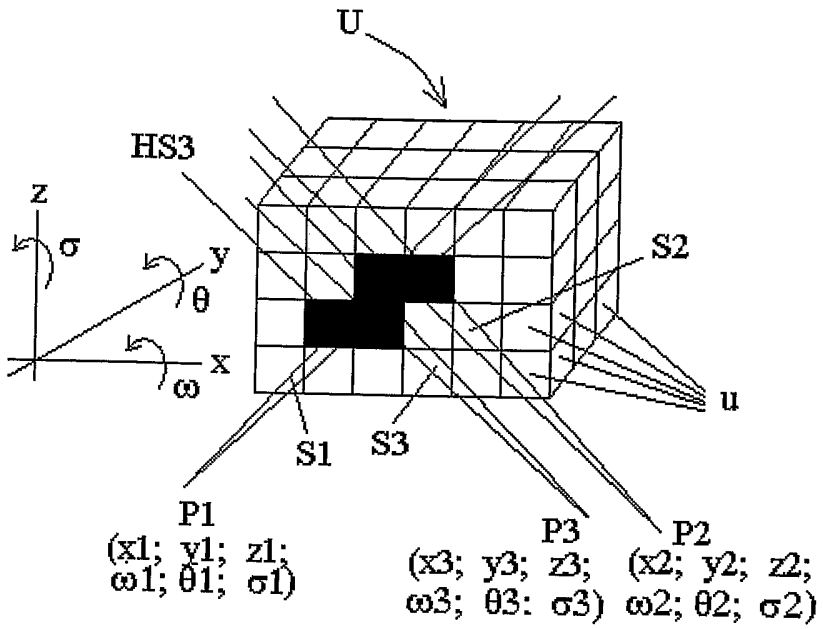
U
HS3
z
σ
y
θ
x
ω
S2
u
S1
S3
P1
(x1; y1; z1;
ω1; θ1; σ1)
P3
(x3; y3; z3;
ω3; θ3: σ3)
P2
(x2; y2; z2;
ω2; θ2; σ2)

Figure 7i

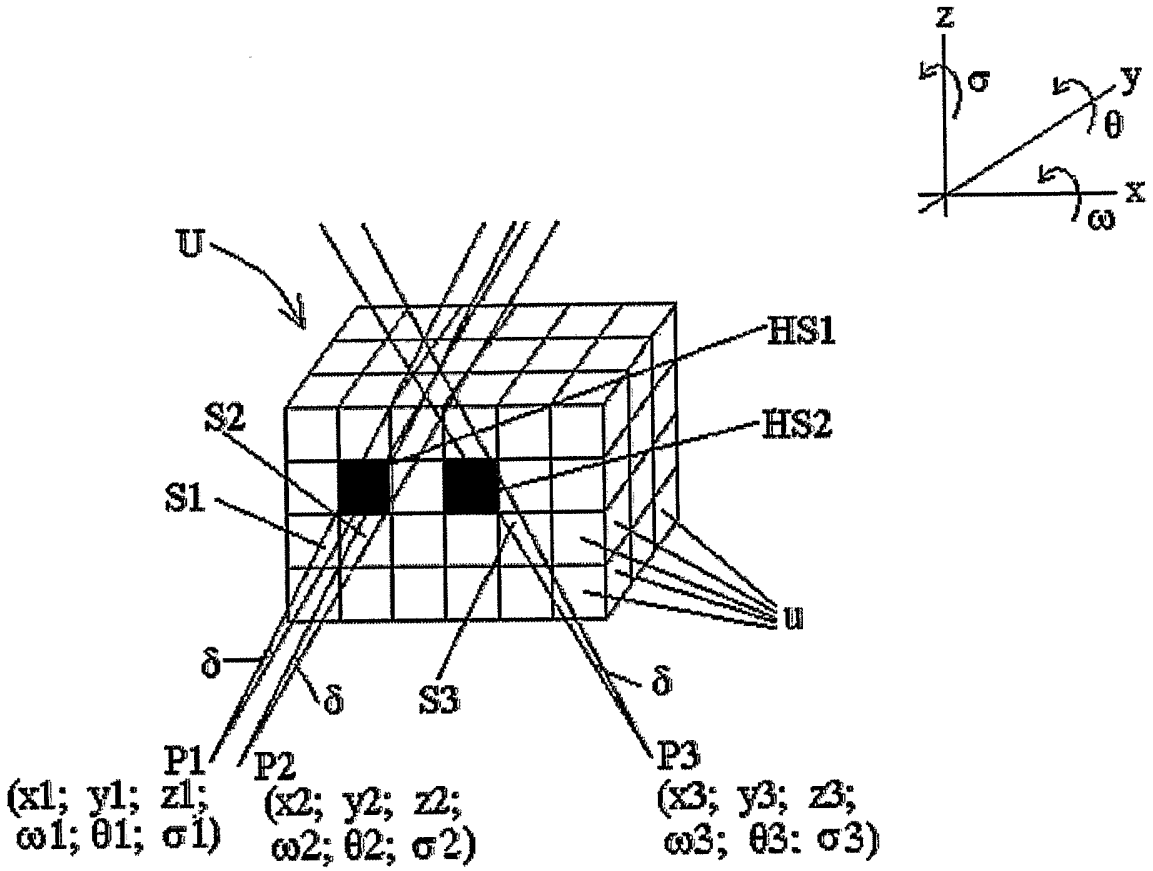
z
σ
y
θ
x
ω
U
HS1
HS2
S2
S1
u
δ
δ
S3
δ
P1
P2
P3
(x1; y1; z1;
ω1; θ1; σ1)
(x2; y2; z2;
ω2; θ2; σ2)
(x3; y3; z3;
ω3; θ3: σ3)

Figure 7j

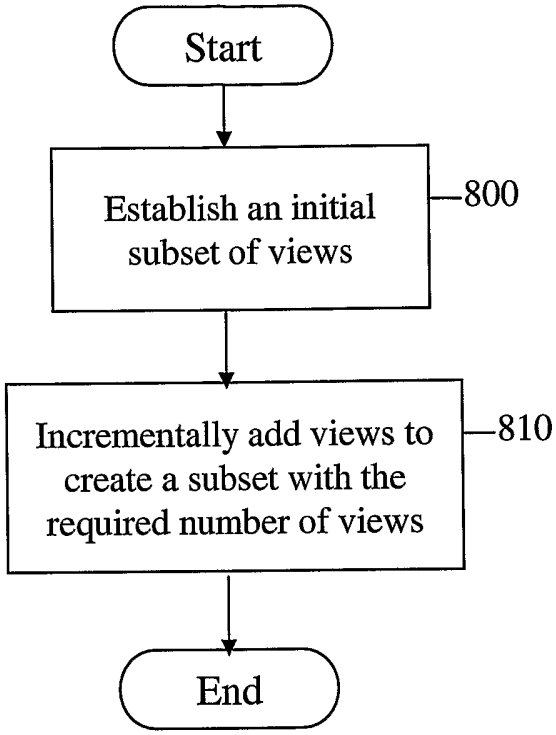
Start
Establish an initial subset of views
800
Incrementally add views to create a subset with the required number of views
810
End

Figure 8

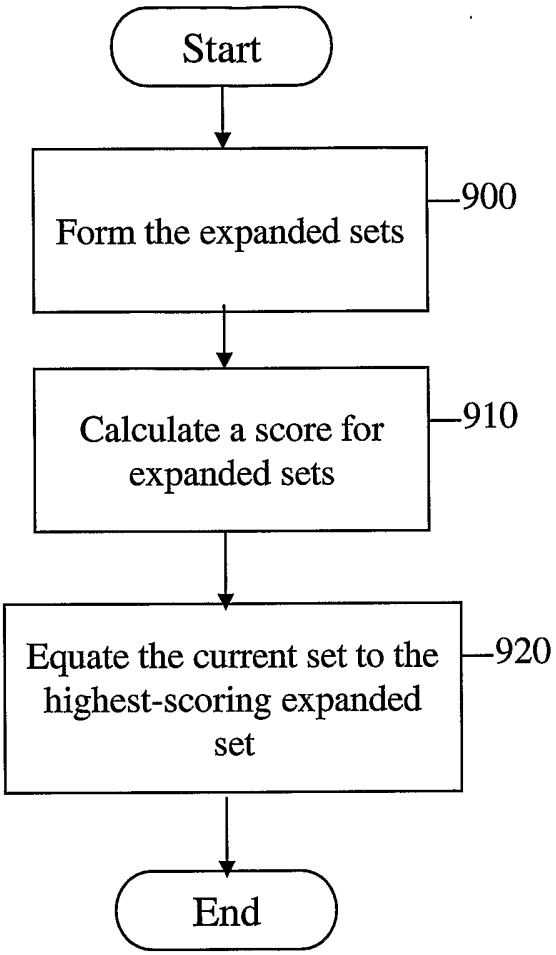
Start
Form the expanded sets
900
Calculate a score for expanded sets
910
Equate the current set to the highest-scoring expanded set
920
End

Figure 9

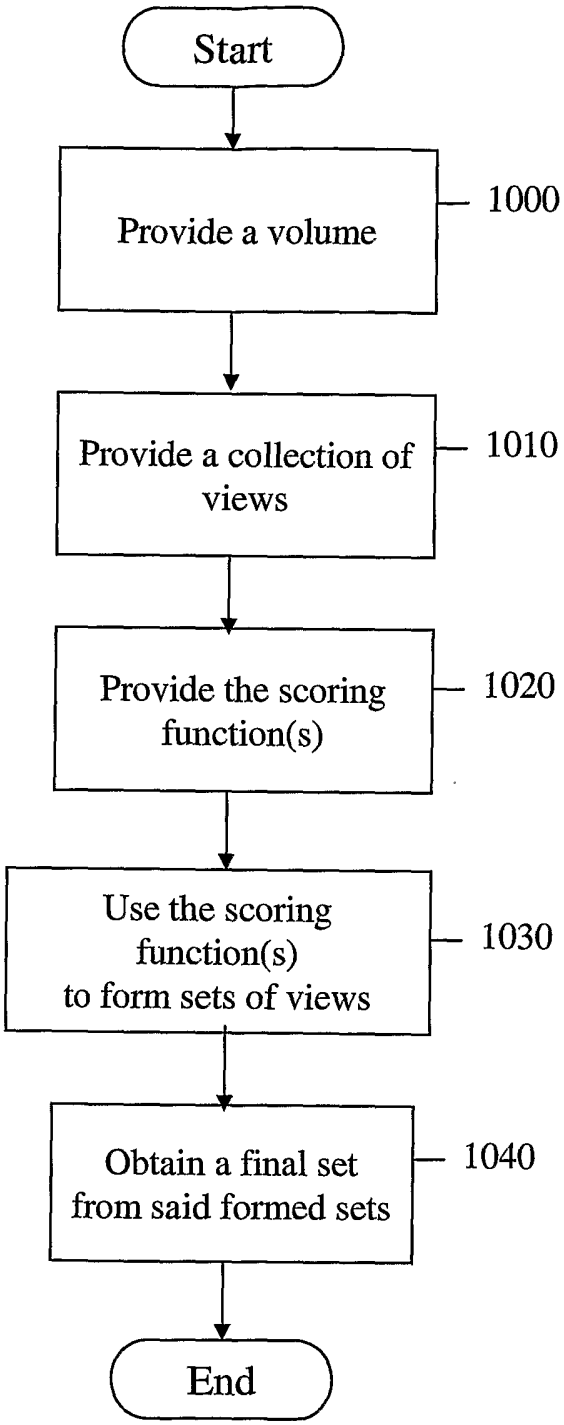
Start
Provide a volume
1000
Provide a collection of views
1010
Provide the scoring function(s)
1020
Use the scoring function(s) to form sets of views
1030
Obtain a final set from said formed sets
1040
End

Figure 10

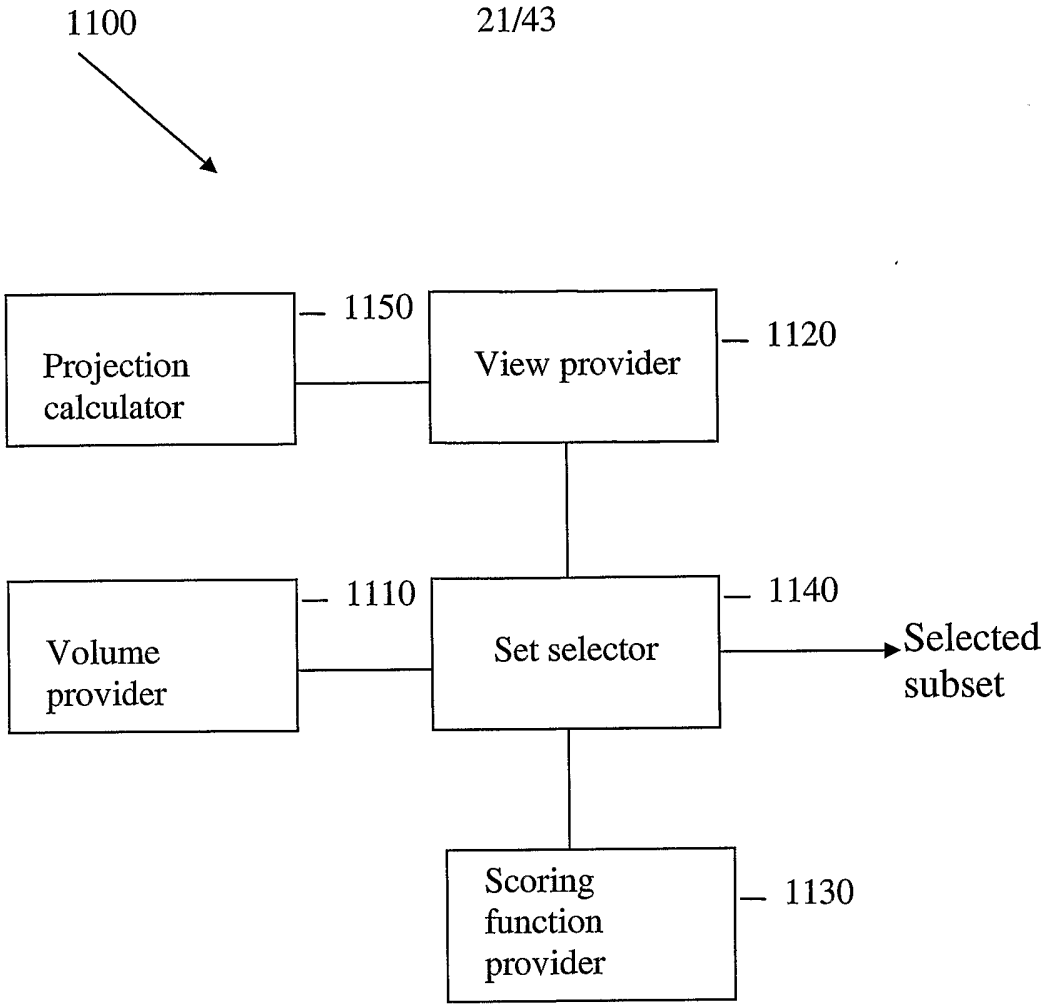
1100
Projection calculator
1150
View provider
1120
Volume provider
1110
Set selector
1140
Selected subset
Scoring function provider
1130

Figure 11

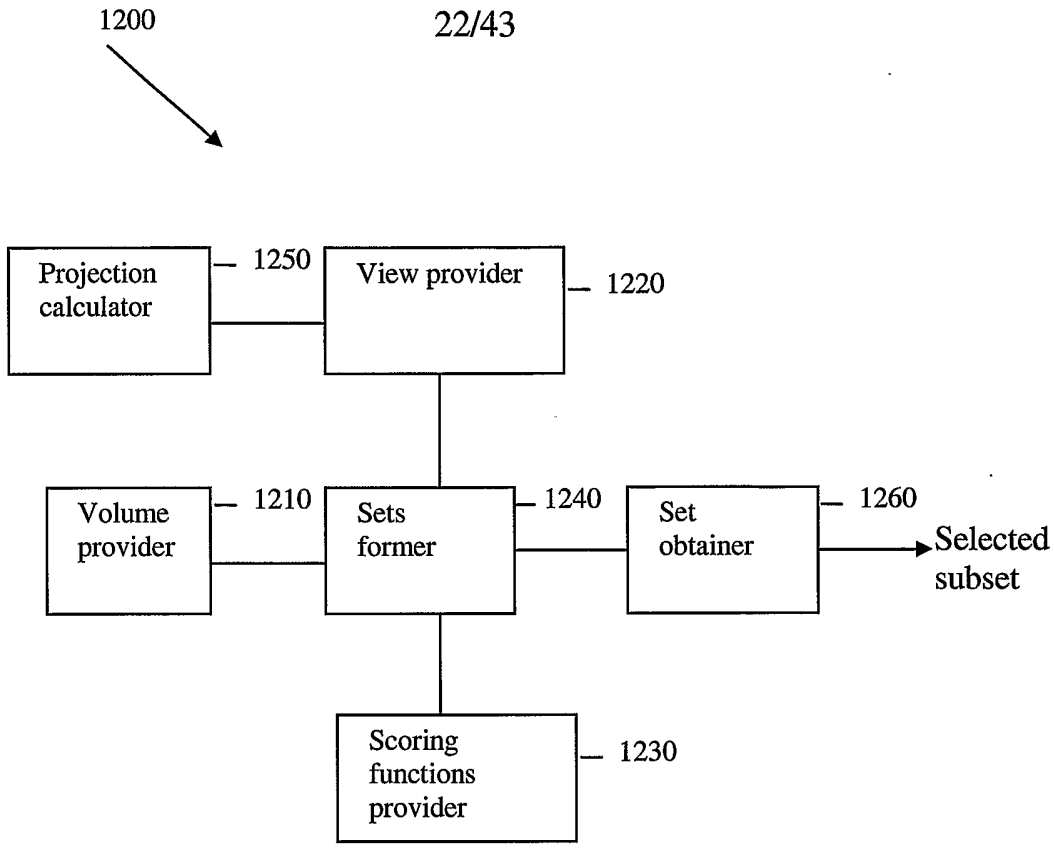
1200
Projection calculator
1250
View provider
1220
Volume provider
1210
Sets former
1240
Set obtainer
1260
Selected subset
Scoring functions provider
1230

Figure 12

Figure 13

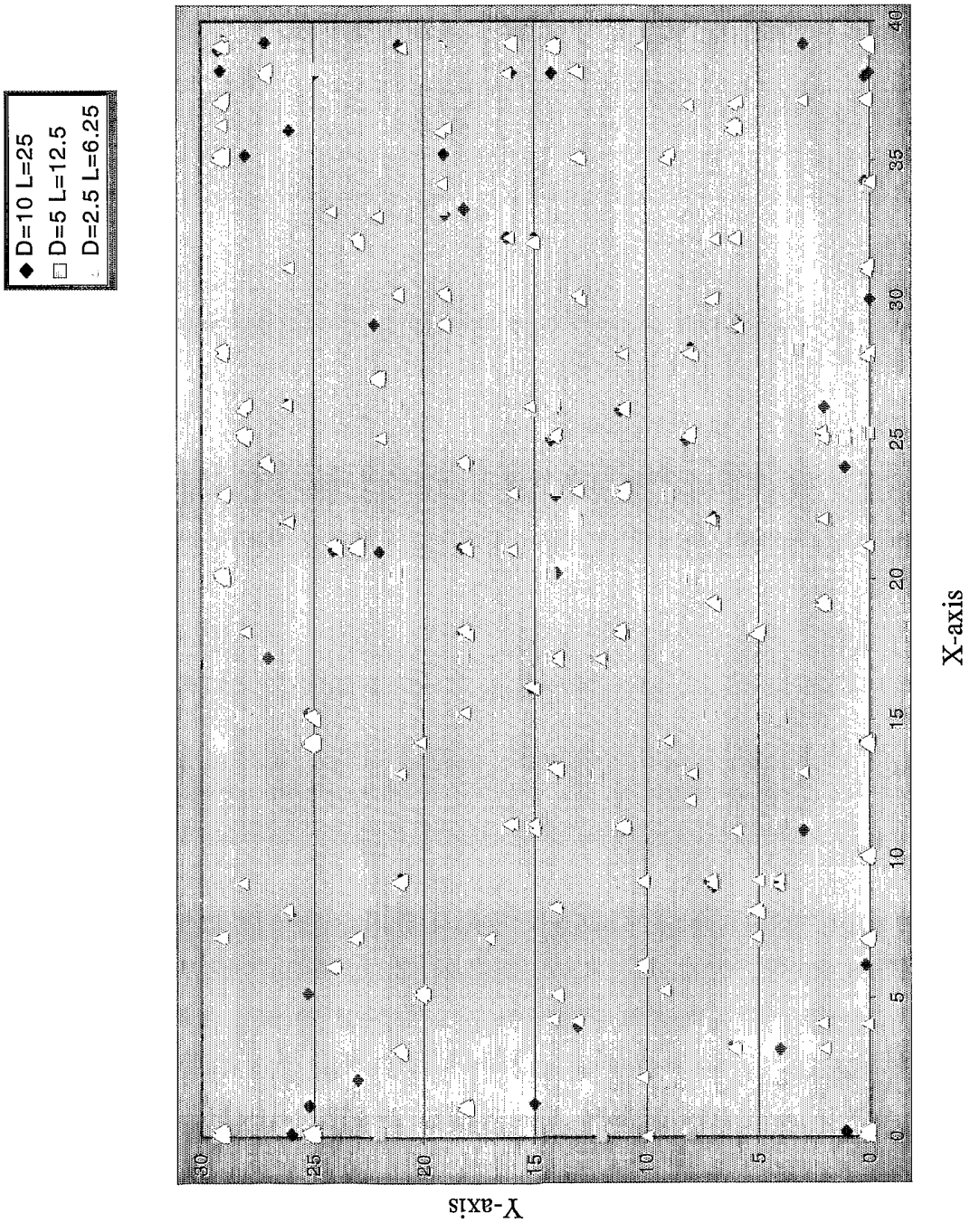

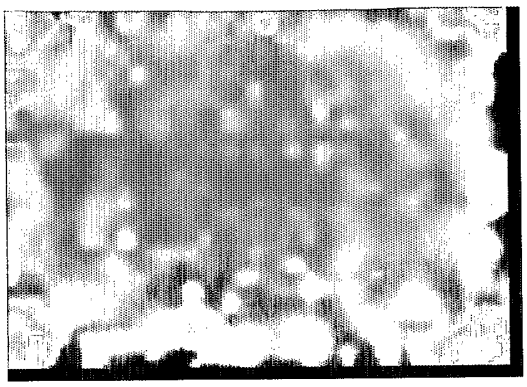

Top

Figure 14a

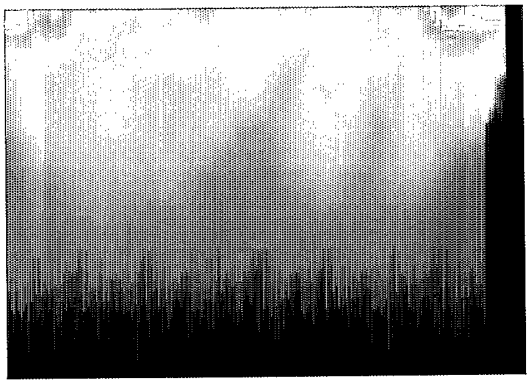

Side

Figure 14b

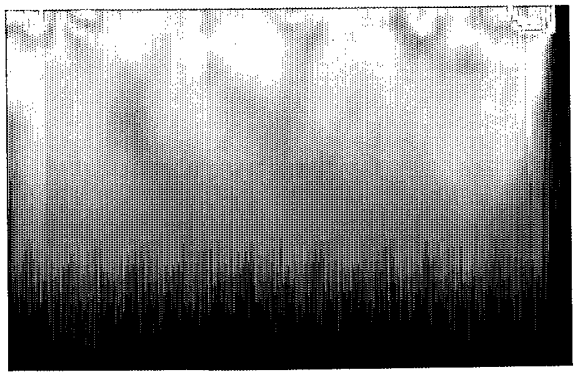

Front

Figure 14c

Figure 15

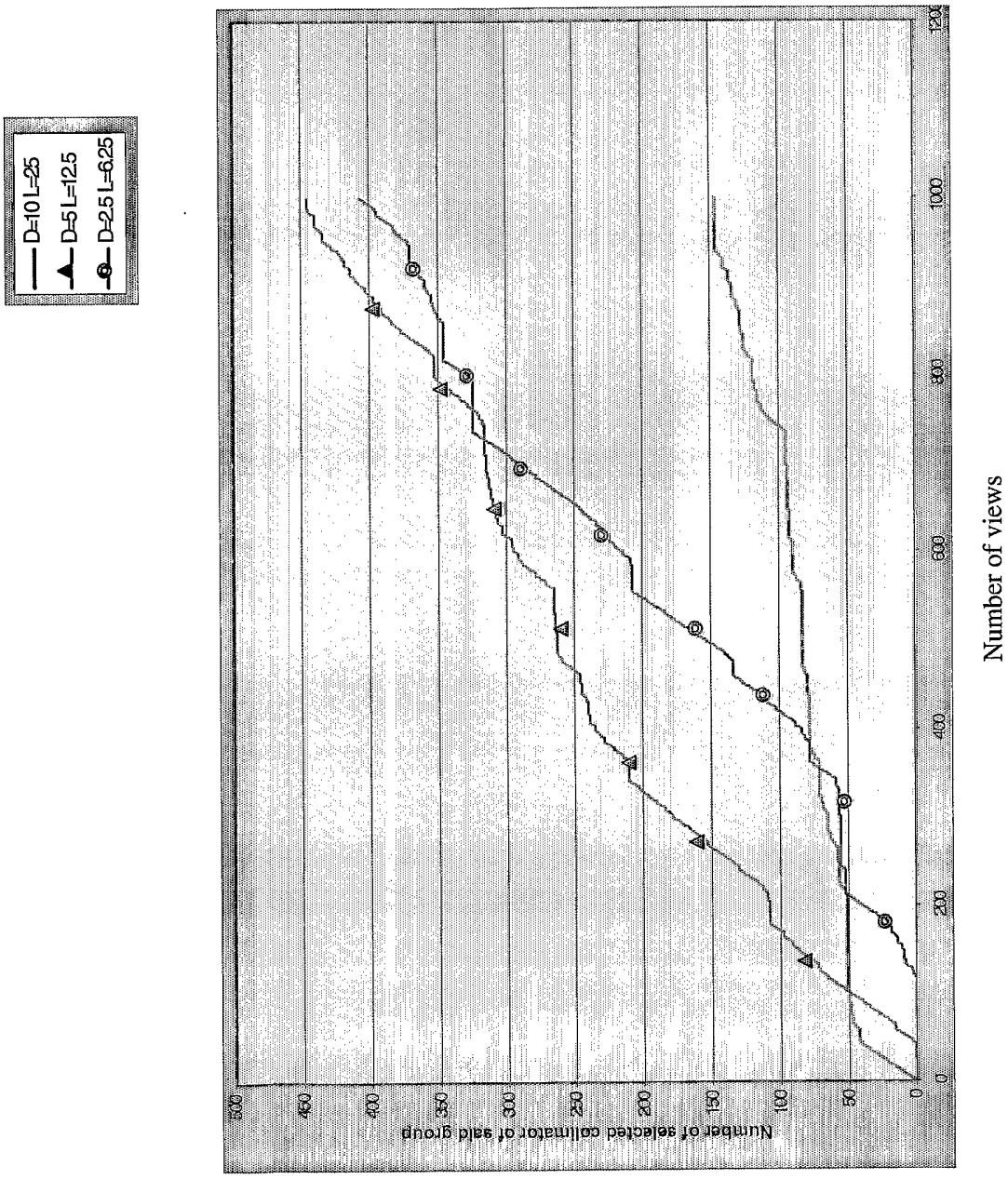
D=10 L=25
D=5 L=12.5
D=2.5 L=6.25
Number of selected collimator of said group
Number of views
0
50
100
150
200
250
300
350
400
450
500
0
200
400
600
800
1000
1200

Figure 16

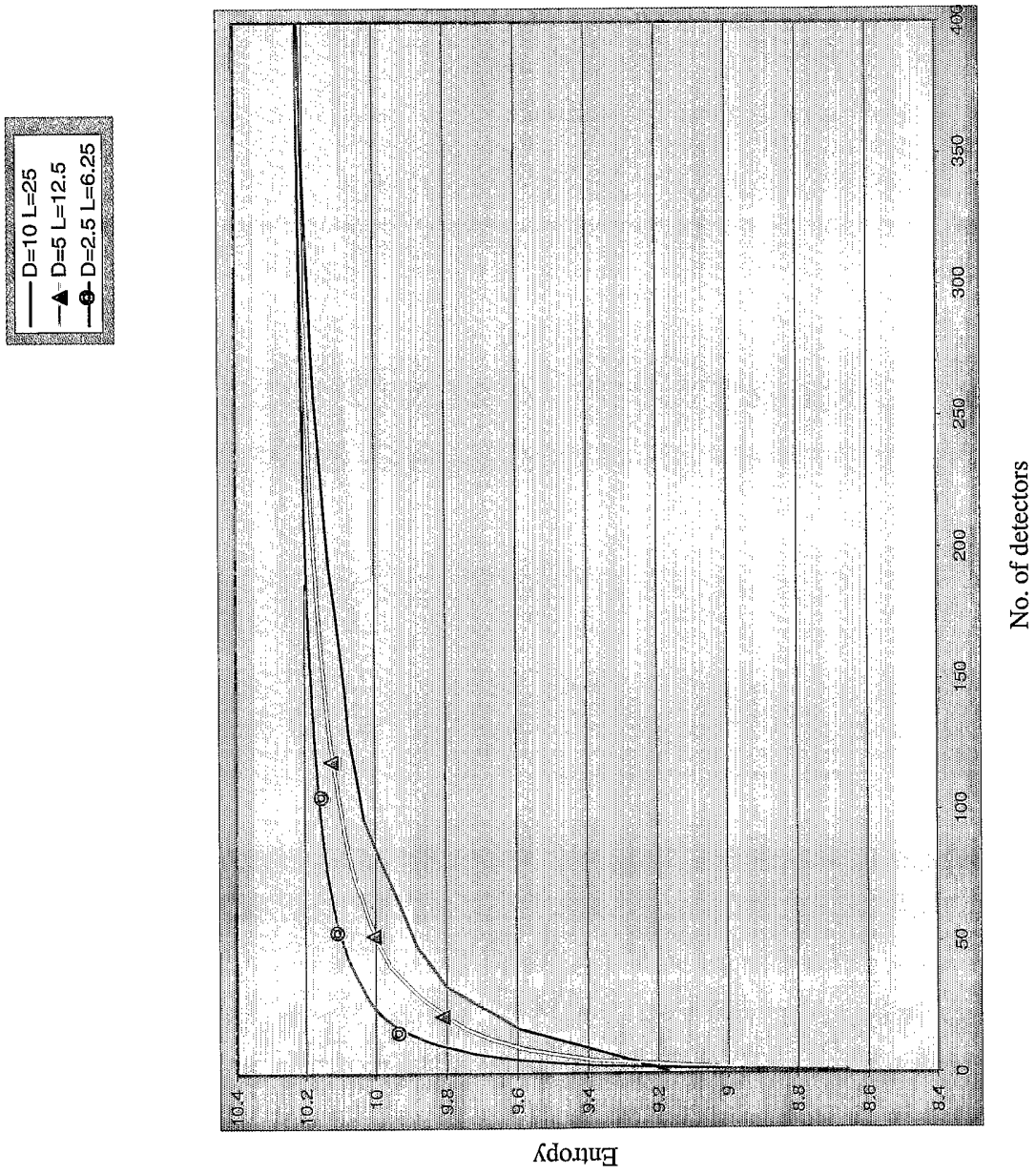
D=10 L=25
D=5 L=12.5
D=2.5 L=6.25
Entropy
10.4
10.2
10
9.8
9.6
9.4
9.2
9
8.8
8.6
8.4
0
50
100
150
200
250
300
350
400
No. of detectors

Figure 17

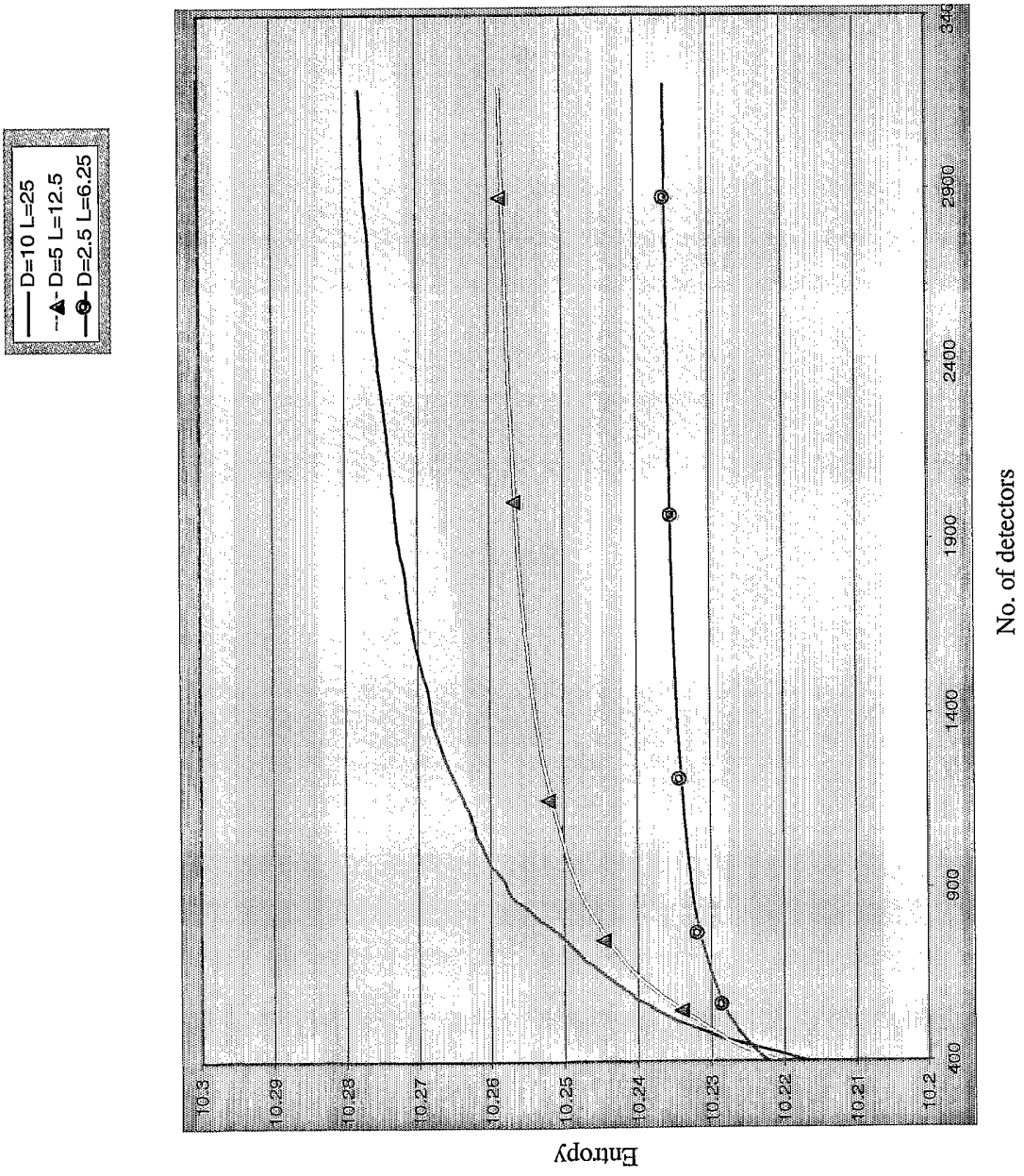
D=10 L=25
D=5 L=12.5
D=2.5 L=6.25
Entropy
10.3
10.29
10.28
10.27
10.26
10.25
10.24
10.23
10.22
10.21
10.2
400
900
1400
1900
2400
2900
No. of detectors

Figure 18

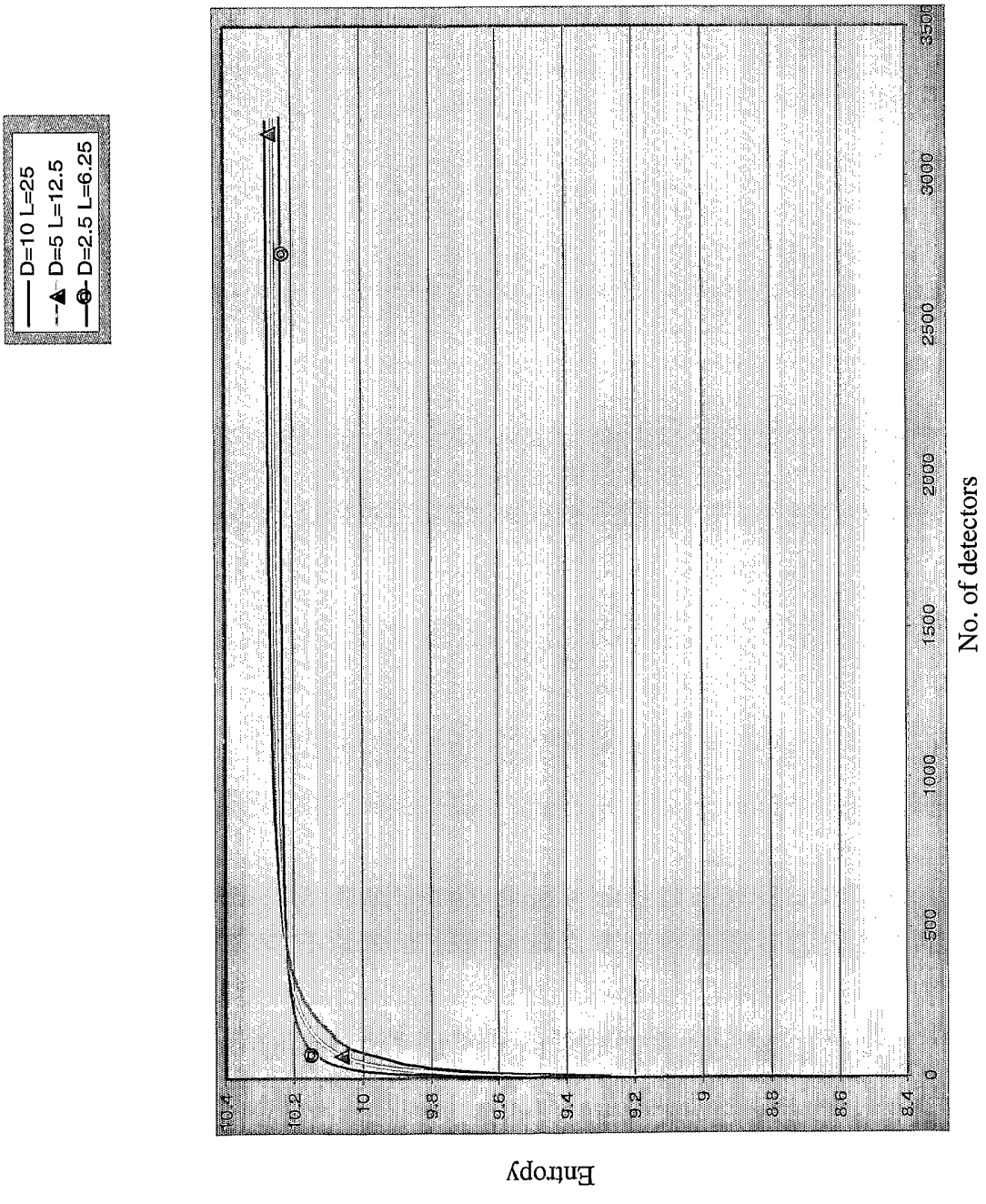
D=10 L=25
D=5 L=12.5
D=2.5 L=6.25
Entropy
10.4
10.2
10
9.8
9.6
9.4
9.2
9
8.8
8.6
8.4
0
500
1000
1500
2000
2500
3000
3500
No. of detectors

Figure 19

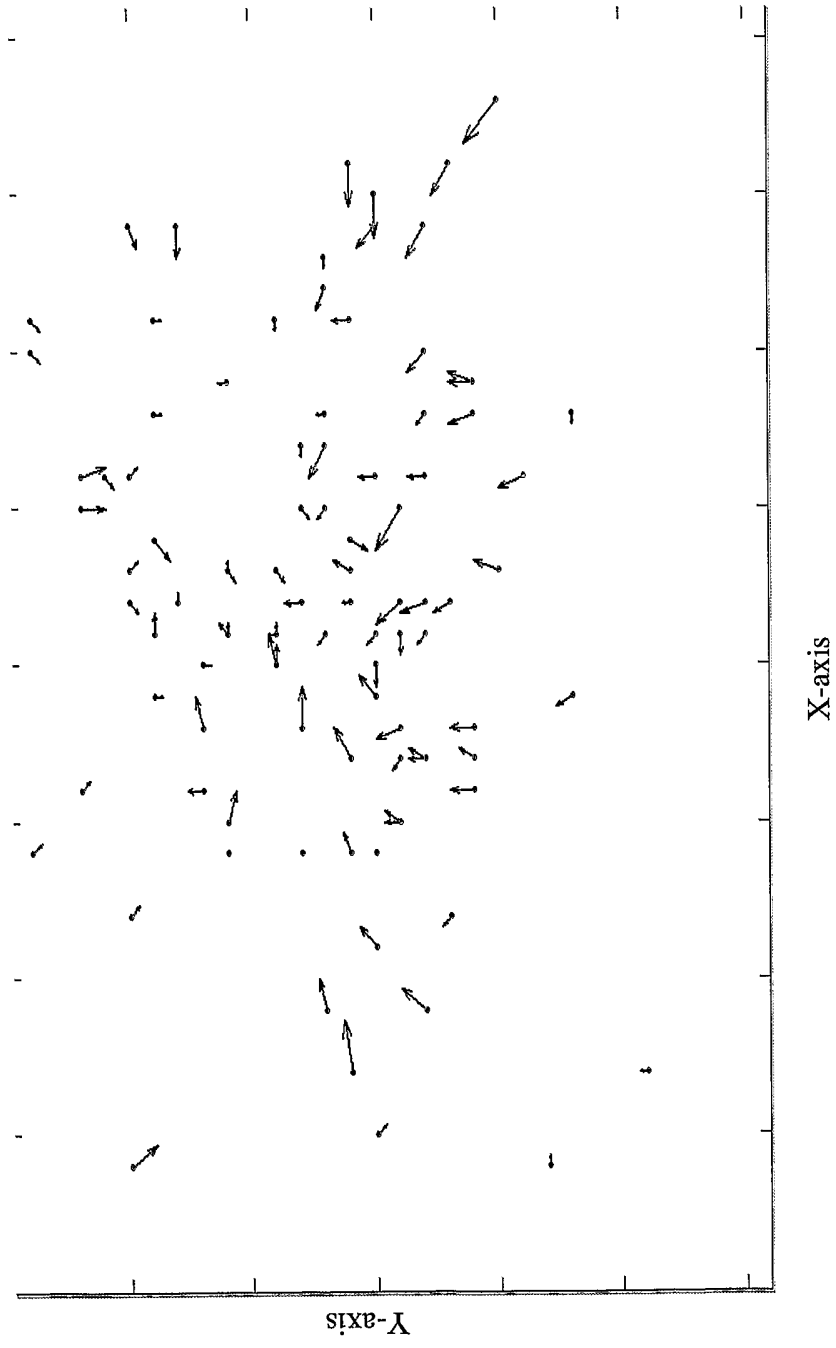

Figure 20

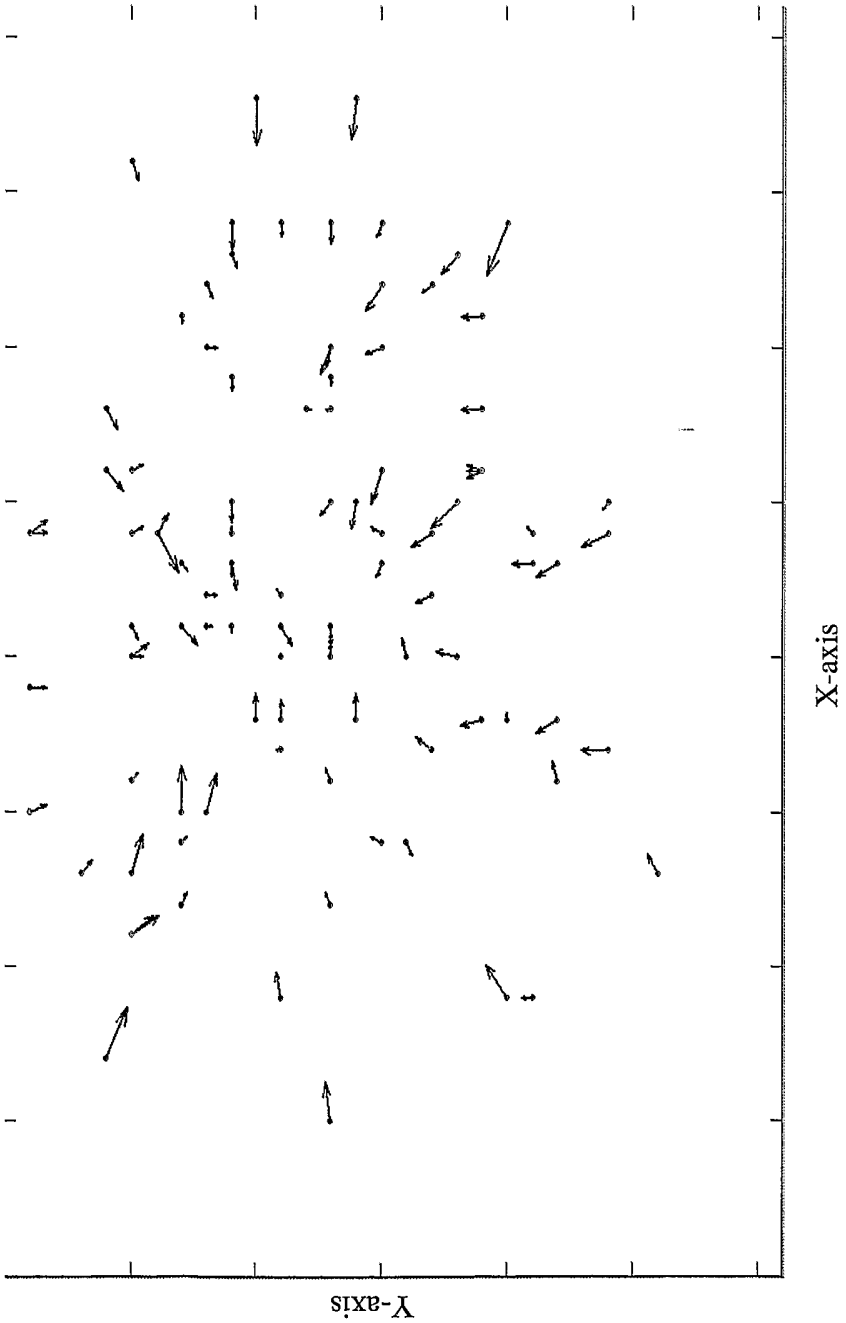

Figure 21

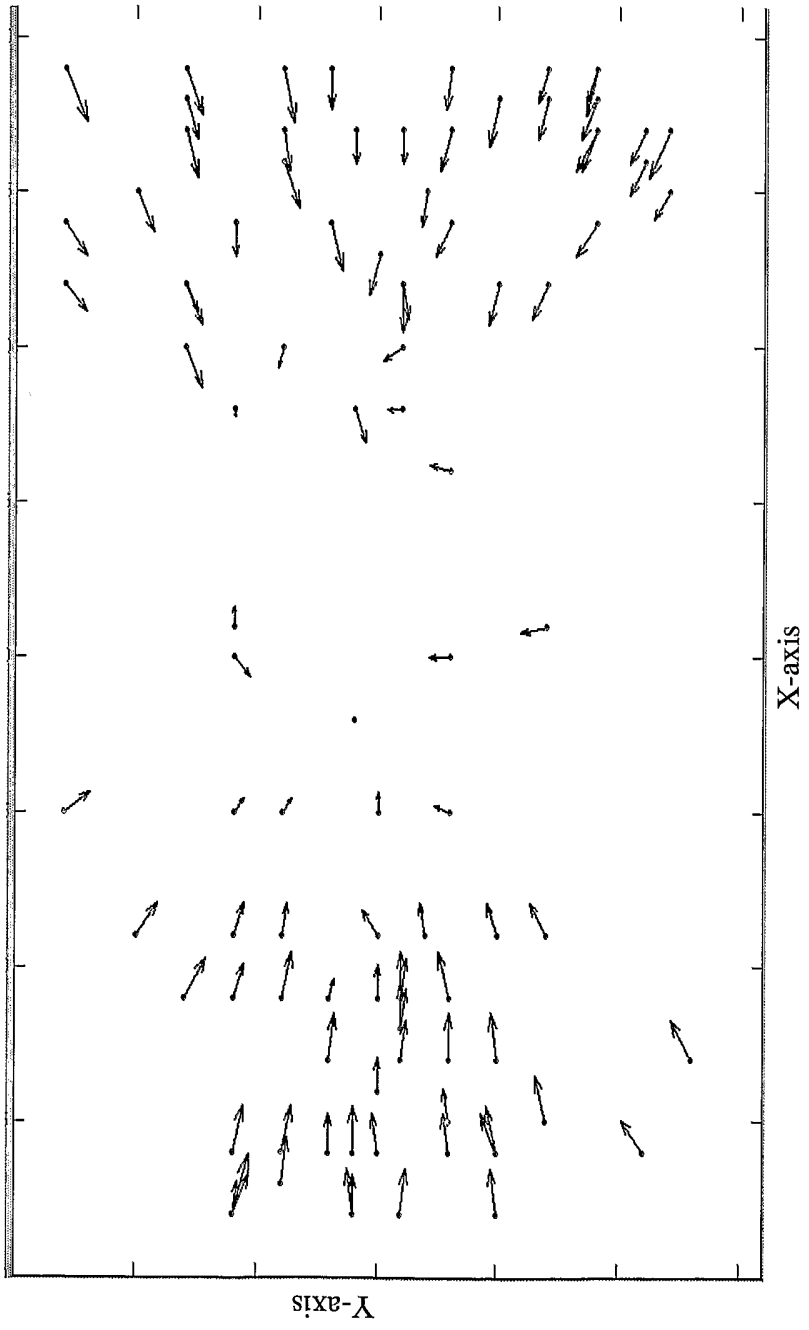

Figure 22

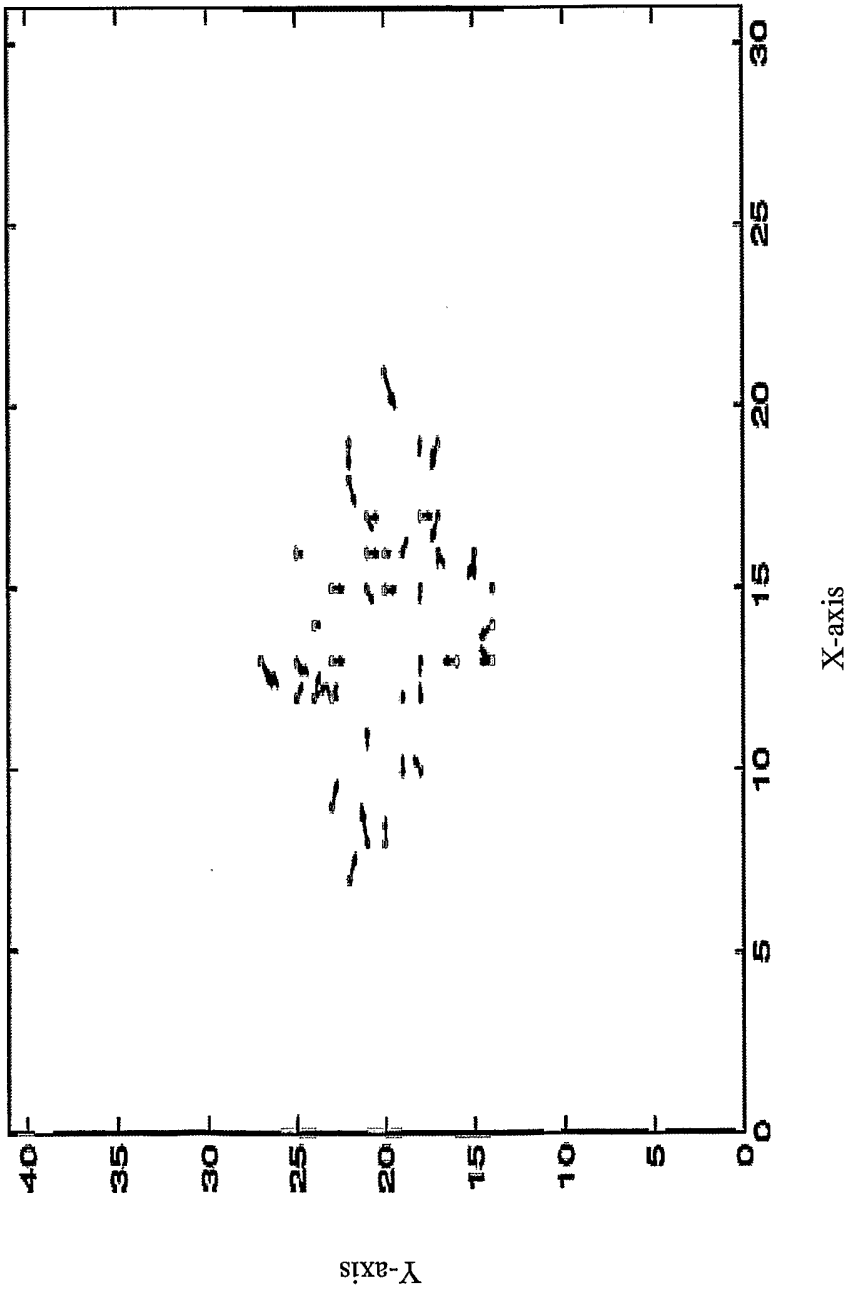

Figure 23

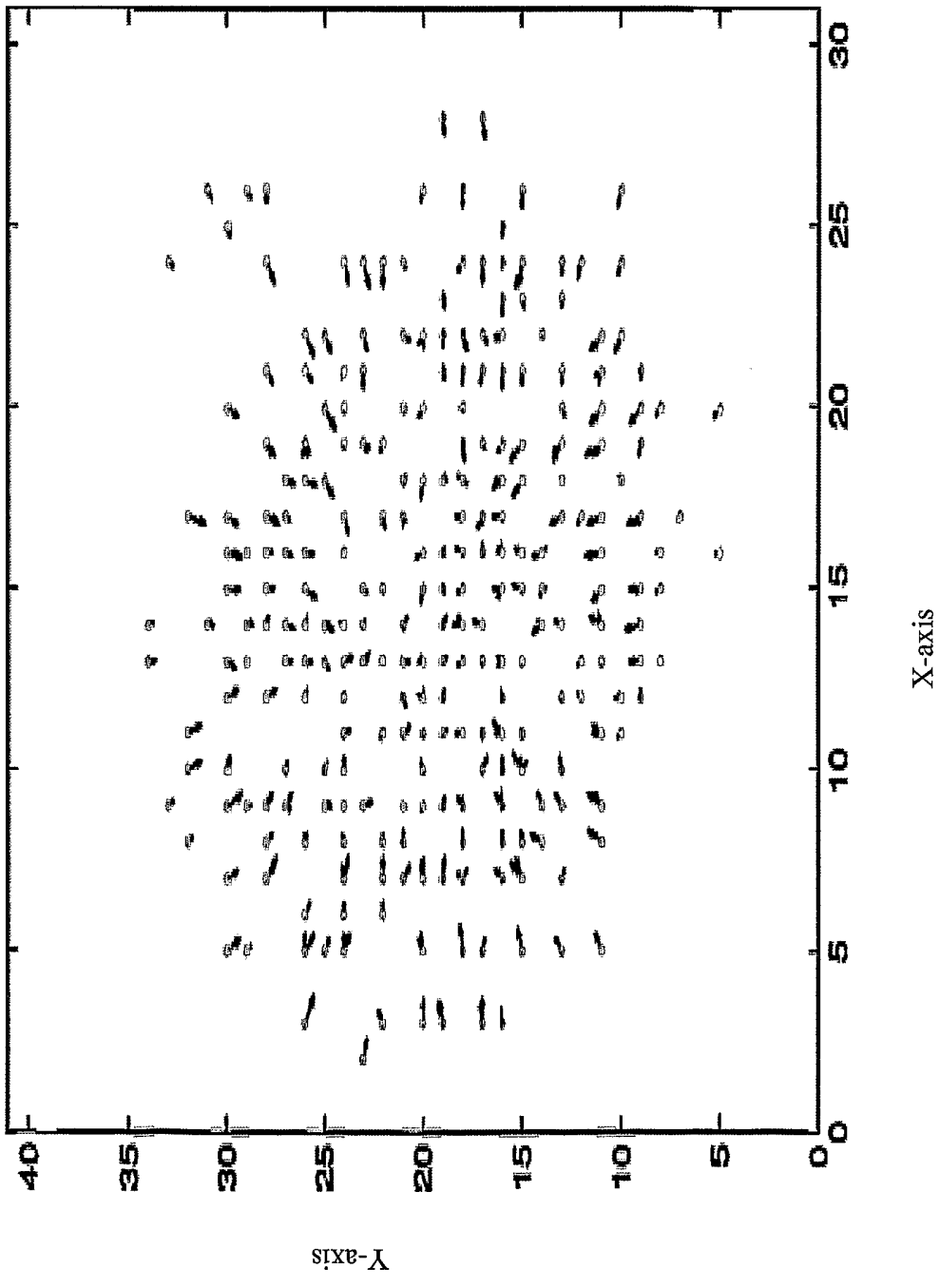

Figure 24

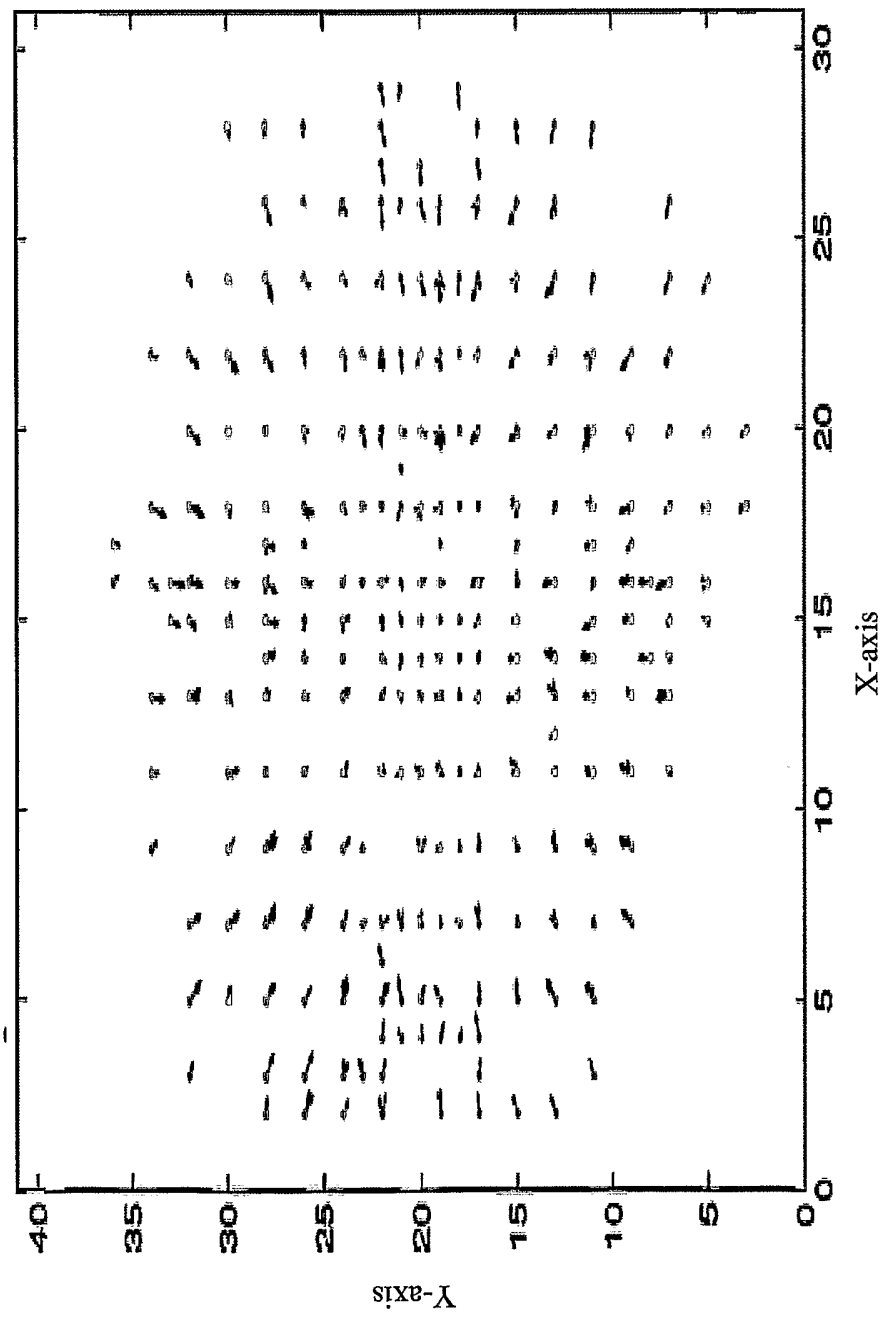

Figure 25

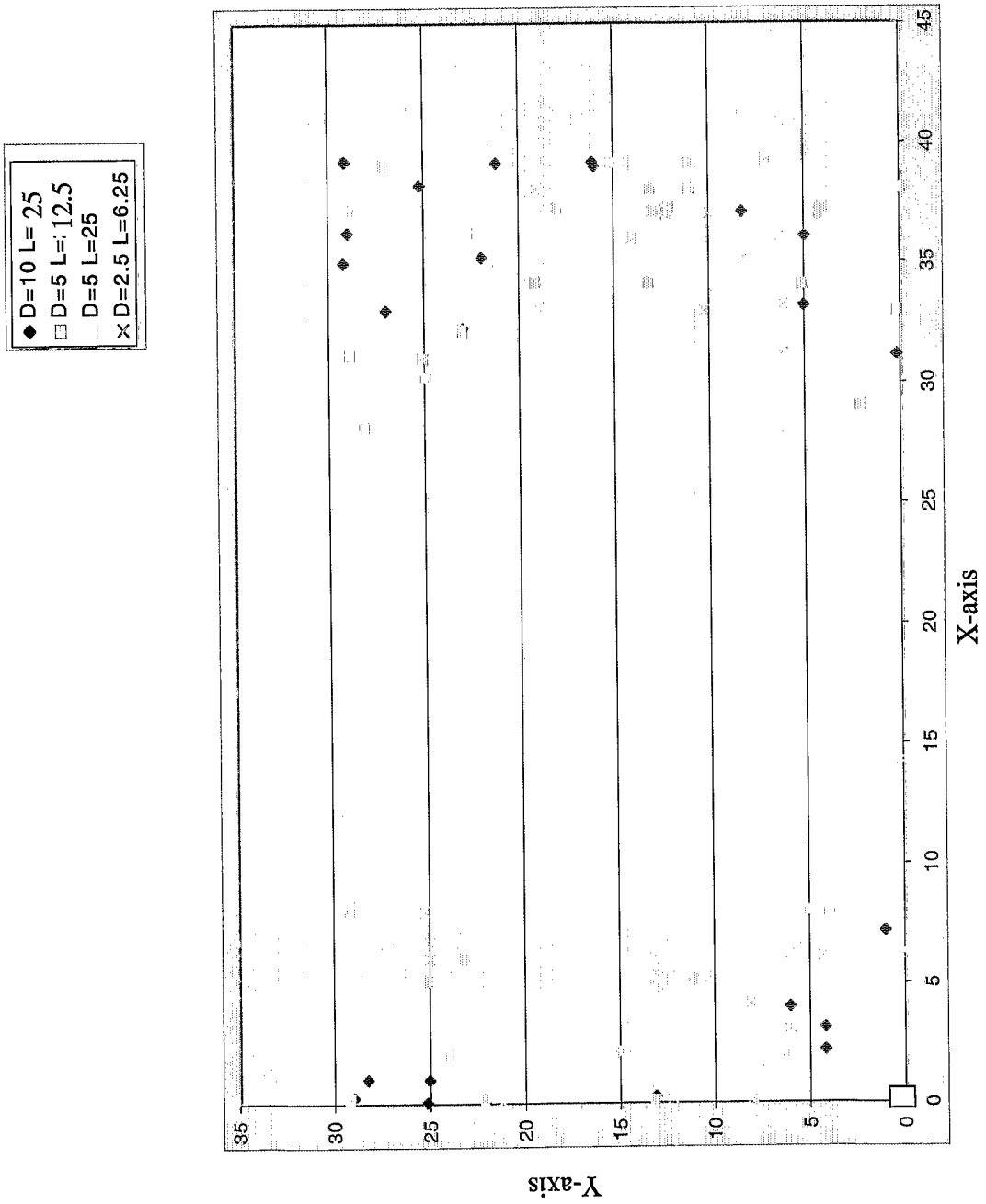
◆ D=10 L= 25
□ D=5 L=12.5
— D=5 L=25
× D=2.5 L=6.25
Y-axis
X-axis
0
5
10
15
20
25
30
35
40
45

Figure 26

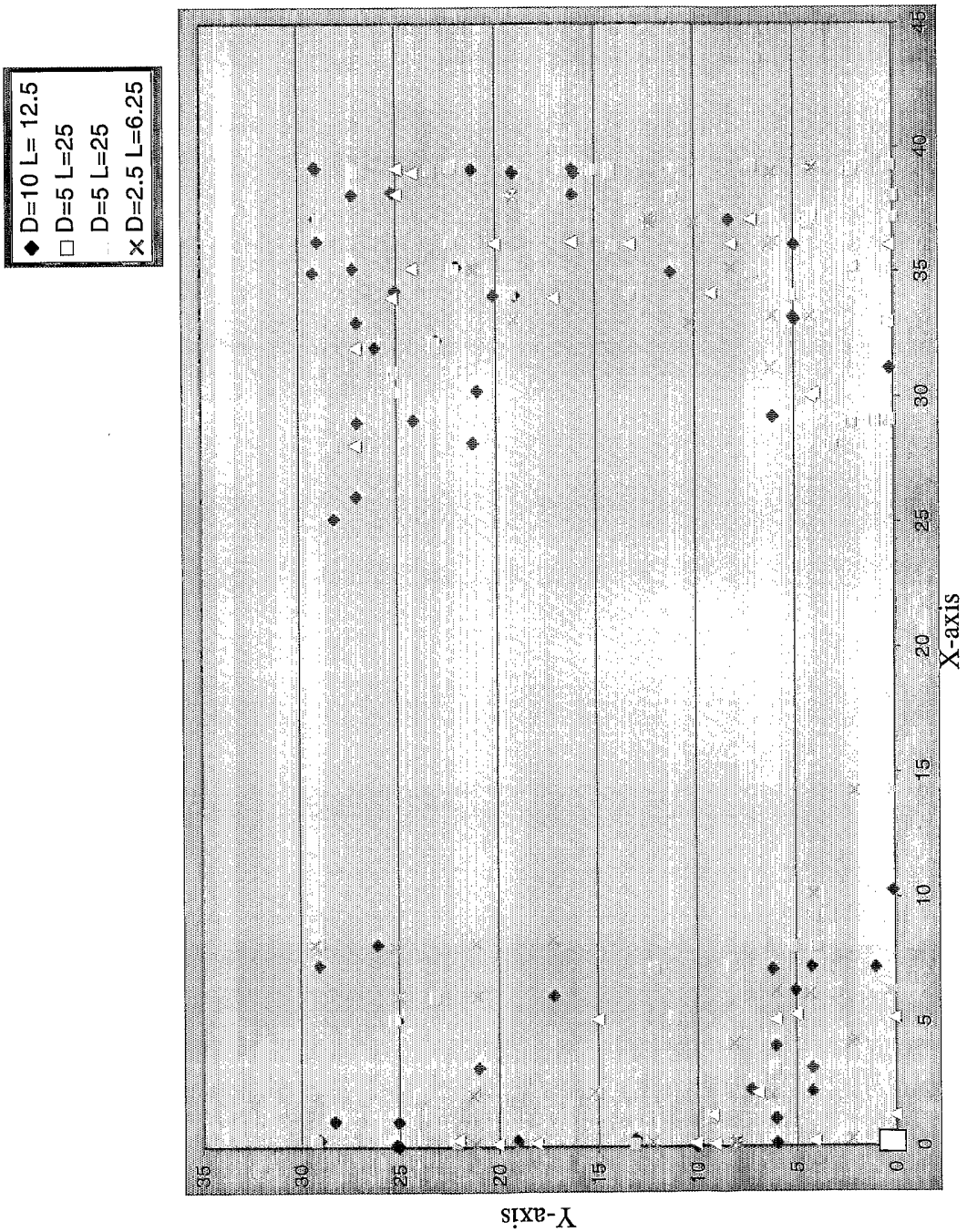
◆ D=10 L= 12.5
□ D=5 L=25
D=5 L=25
× D=2.5 L=6.25
Y-axis
X-axis
0
5
10
15
20
25
30
35
40
45

Figure 27

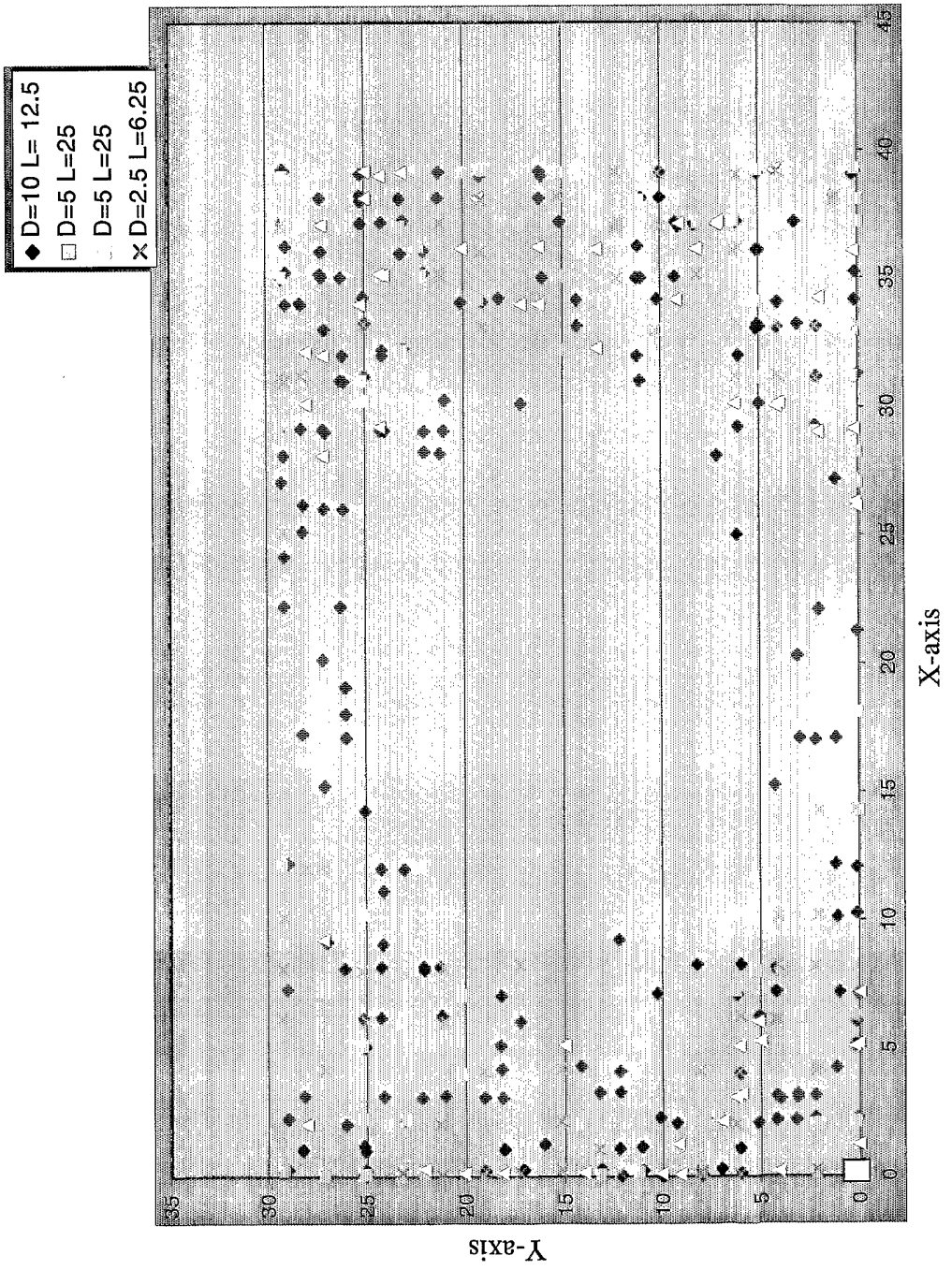
◆ D=10 L= 12.5
□ D=5 L=25
D=5 L=25
× D=2.5 L=6.25
Y-axis
X-axis
0
5
10
15
20
25
30
35
40
45

Figure 28

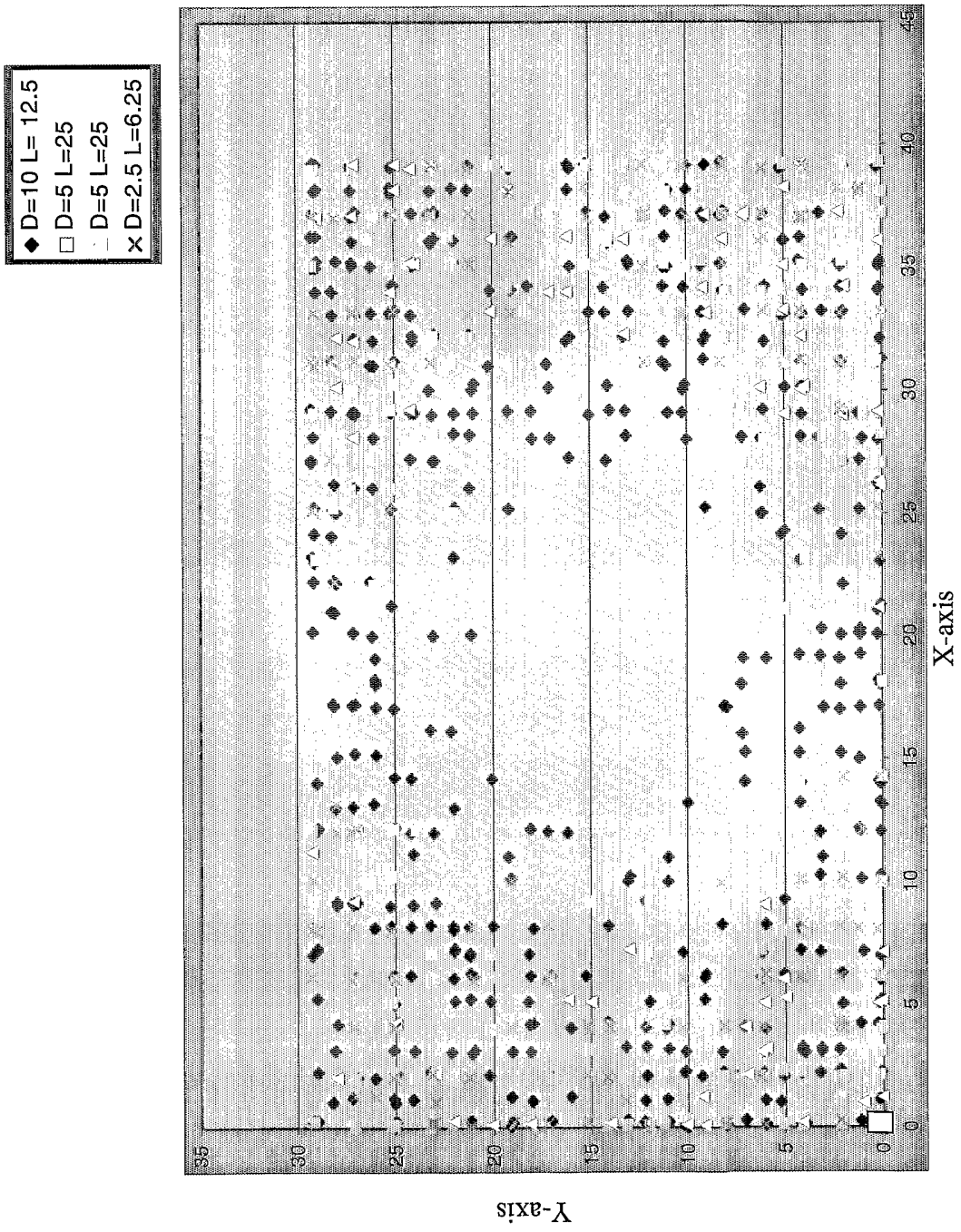
◆ D=10 L= 12.5
□ D=5 L=25
D=5 L=25
× D=2.5 L=6.25
0
5
10
15
20
25
30
35
40
45
X-axis
Y-axis

Figure 29

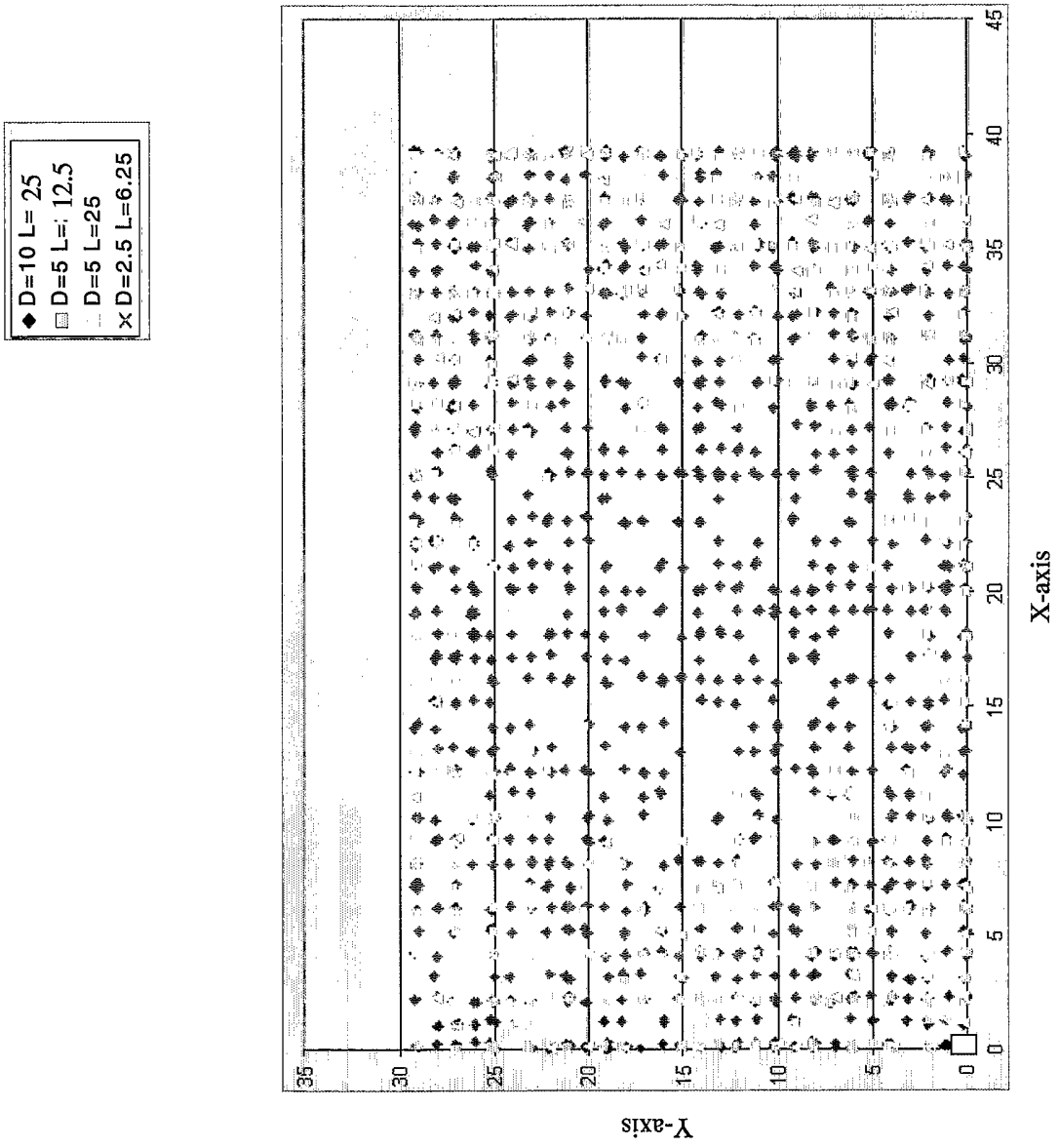
D=10 L= 25
D=5 L=; 12.5
D=5 L=25
D=2.5 L=6.25
Y-axis
X-axis
0
5
10
15
20
25
30
35
40
45

Figure 30

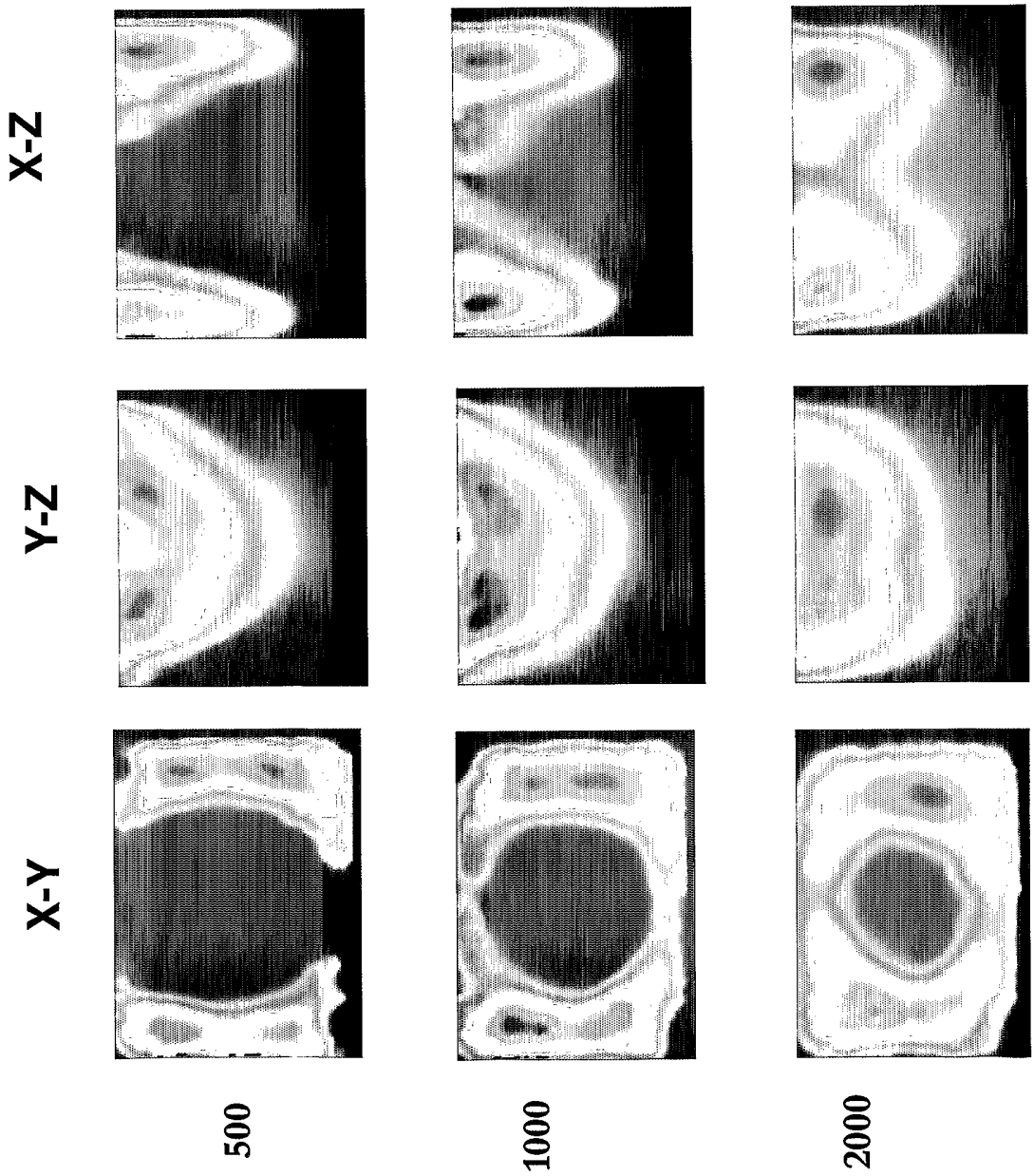

Figure 31

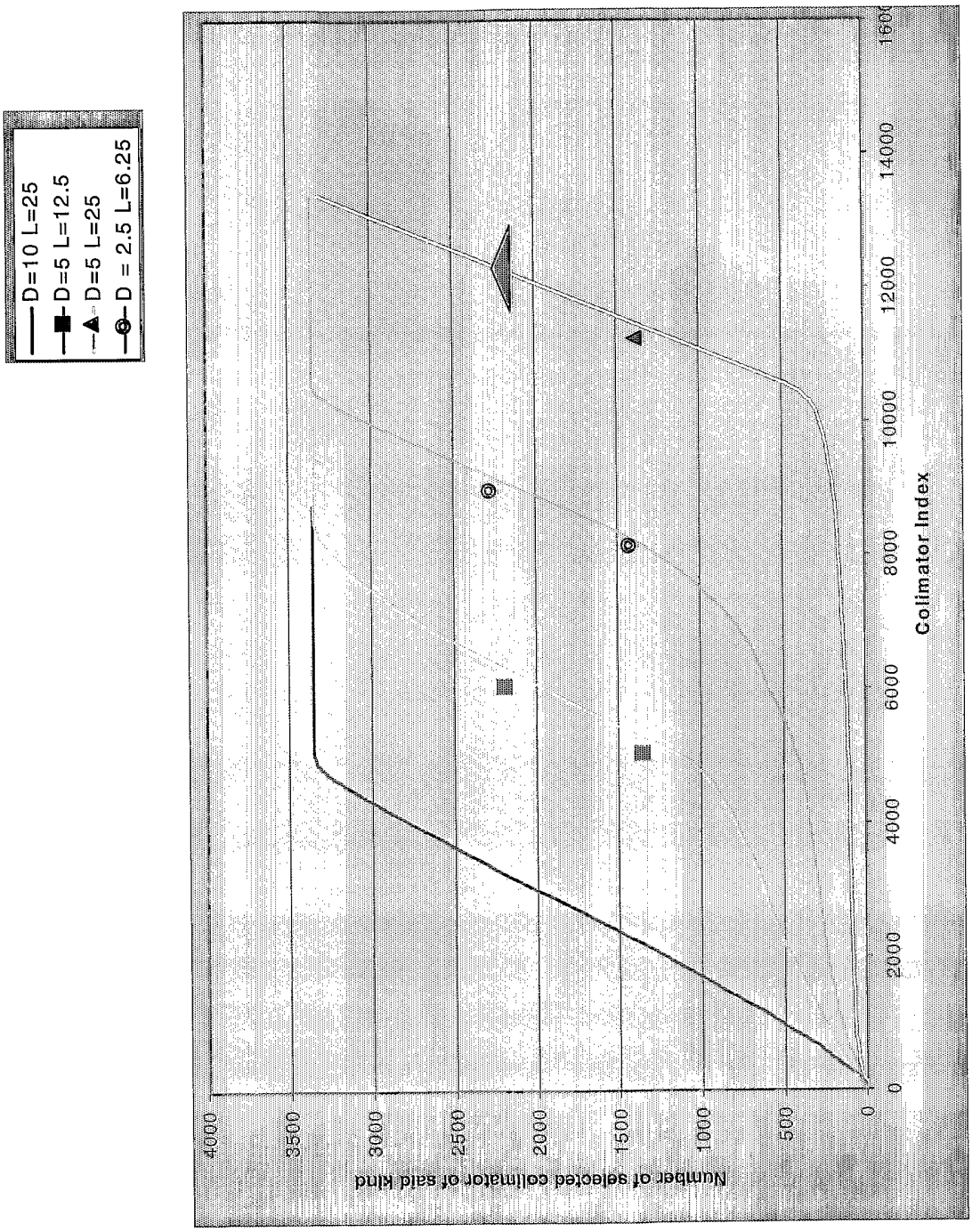
D=10 L=25
D=5 L=12.5
D=5 L=25
D = 2.5 L=6.25
Number of selected collimator of said kind
Collimator Index
0
500
1000
1500
2000
2500
3000
3500
4000
0
2000
4000
6000
8000
10000
12000
14000

Figure 32

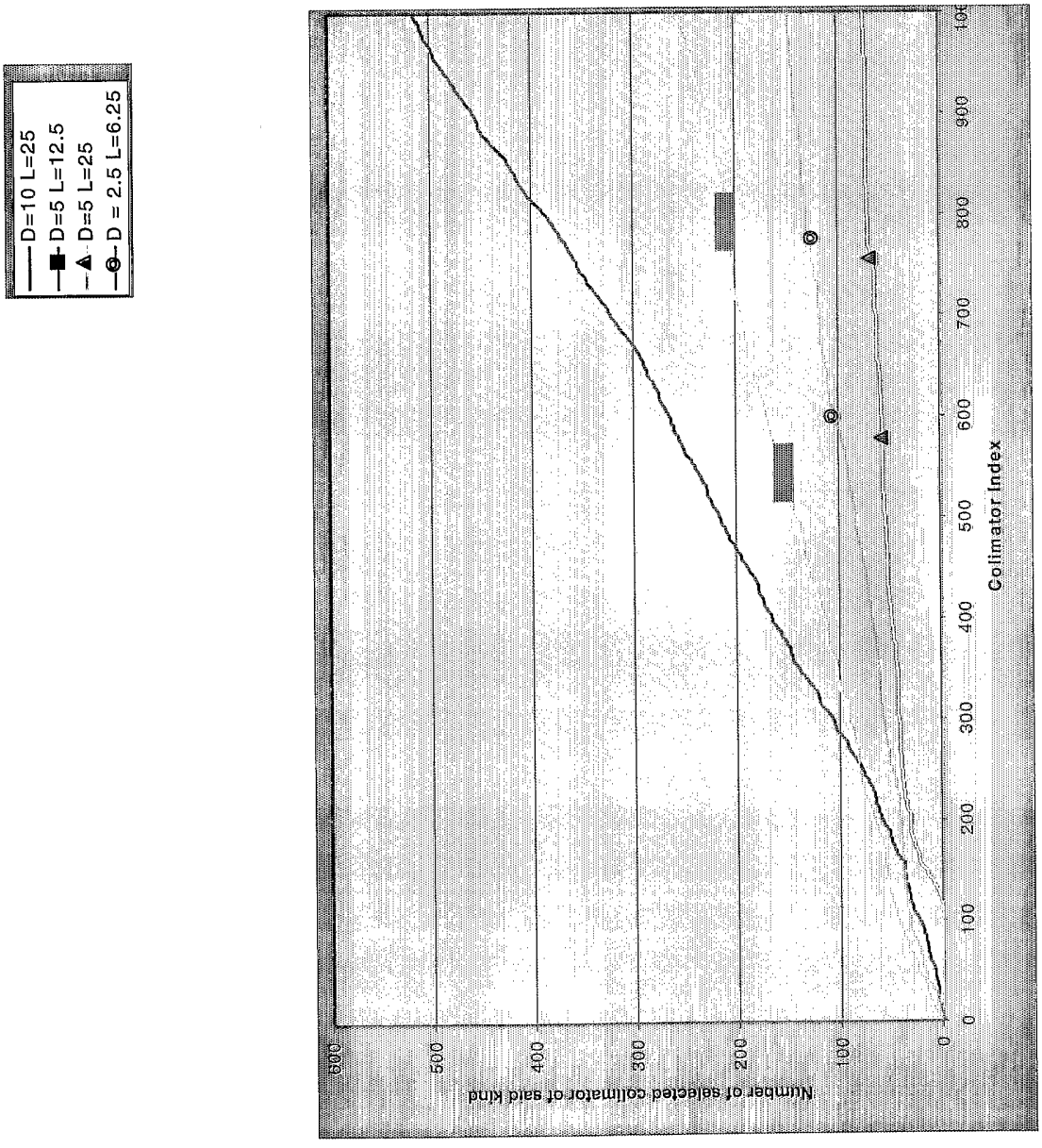
D=10 L=25
D=5 L=12.5
D=5 L=25
D = 2.5 L=6.25
Number of selected collimator of said kind
Colimator Index
0
100
200
300
400
500
600
700
800
900
100
600
500
400
300
200
100
0

Figure 33

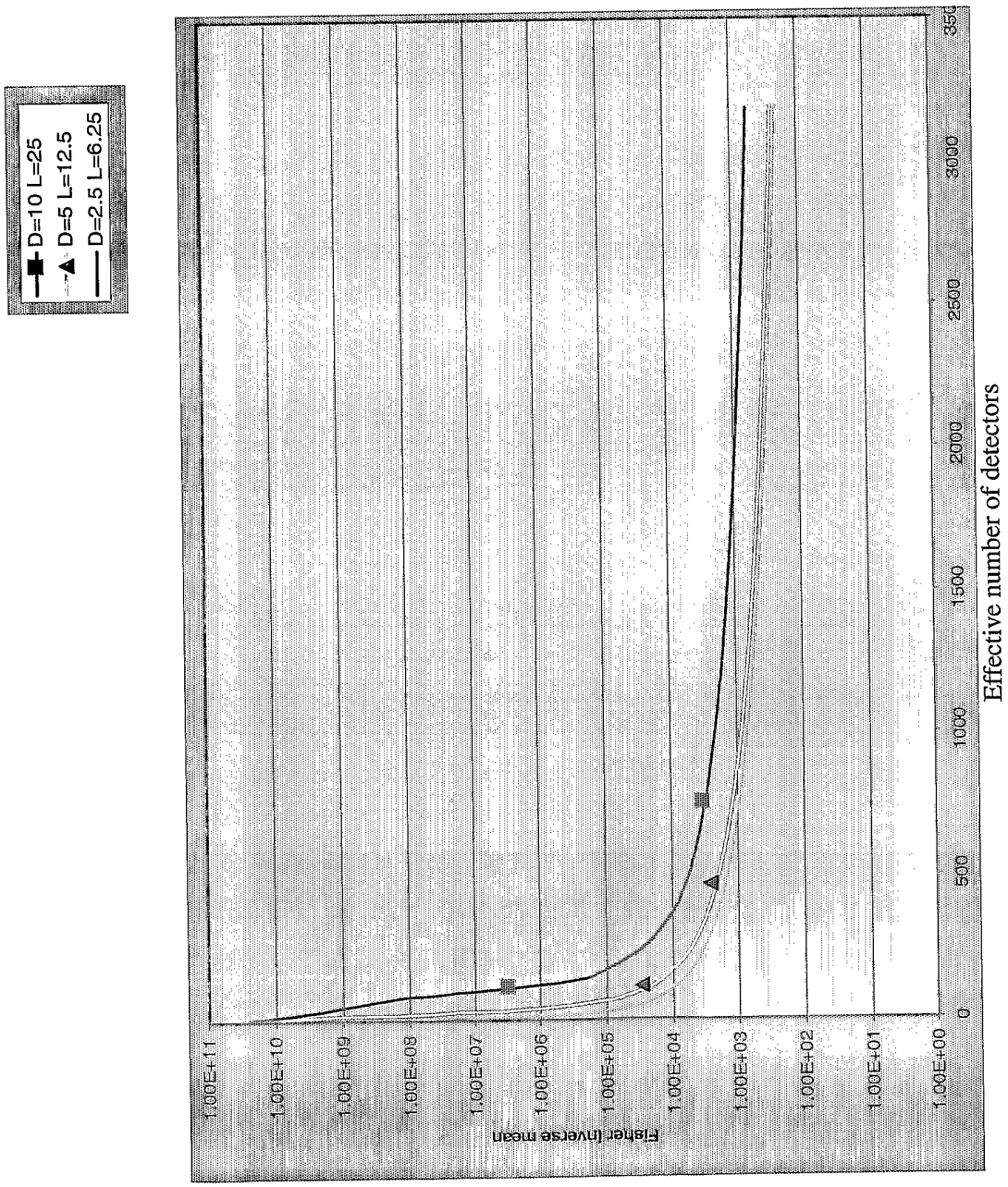
D=10 L=25
D=5 L=12.5
D=2.5 L=6.25
Fisher Inverse mean
1.00E+11
1.00E+10
1.00E+09
1.00E+08
1.00E+07
1.00E+06
1.00E+05
1.00E+04
1.00E+03
1.00E+02
1.00E+01
1.00E+00
0
500
1000
1500
2000
2500
3000
Effective number of detectors